Resonance oscillations of neutrinos in matter

S. P. Mikheev and A. Yu. Smirnov

Institute of Nuclear Research, Academy of Sciences of the USSR

Usp. Fiz. Nauk **153**, 3–58 (September 1987)

If the neutrino has mass and exhibits mixing, this must necessarily result in oscillations, i.e., periodic transformation of one type of neutrino into another and vice versa. In general, these oscillations depend on the properties of the medium in which the neutrinos propagate. The propagation of a neutrino through a medium of varying density is, in general, accompanied by a number of new oscillation phenomena that are resonant in character. These phenomena have analogs in different branches of physics, including mechanics, because the neutrino oscillations constitute an oscillatory process that is unrelated to the quantum nature of particles. This review discusses practically all the possible aspects of the effect of a medium on neutrino oscillations. The Introduction presents general ideas on neutrino oscillations and on the mechanism responsible for the effect of the medium on the oscillations. It also discusses the equations describing the evolution of neutrinos in matter. This is followed by an account of the theory of neutrino oscillations in media with different density distributions. Particular attention is devoted to the most interesting case of a slow variation in density (the adiabatic case). This theory is a direct generalization of the theory of vacuum oscillations, originally developed by B. M. Pontecorvo. The separation of wave packets and the absorption of neutrinos in the medium are taken into account in the next Section. The oscillations of three types of neutrino in the most general case of mass hierarchy are also discussed. The last Section examines possible manifestations of resonant oscillations during the passage of neutrinos through the Sun and the Earth.

CONTENTS

1. INTRODUCTION

If neutrinos are massive, it is quite likely that they mix. The mixing of quarks is an established fact and, because of quark-lepton symmetry or the correspondence between quarks and leptons, it is natural to assume that leptons exhibit mixing as well. An additional argument, in this sense, is provided by grand unification models, in which quarks and leptons are described in a unified manner. Another argument relies on the idea that only local symmetry can remain unbroken. The absence of mixing in the case of massive neutrinos would signify the existence of global symmetry, expressing the conservation of lepton numbers. Mixing means that ν_e, ν_μ, ν_τ,[1)] i.e., the states created in weak interactions, are different from the states ν_1, ν_2, ν_3 that have definite masses. The neutrinos ν_e, ν_μ, ν_τ are orthogonal combinations of $\nu_1, \nu_2, \ldots$, with different admixtures ν_i and different phases between them.

Mixing has as its consequence neutrino oscillations,[1] i.e., the process of periodic (complete or partial) transformation of neutrinos of one type into another, for example, $\nu_e \to \nu_s \to \nu_e \to \ldots$. This process was introduced in 1957 by B. M. Pontecorvo by analogy with K-meson oscillations. The components ν_i of a mixed neutrino have different masses and, hence, different phase velocities. It follows that the phase differences between the ν_i vary monotonically during the propagation process. This phase change leads to a change in the interactions of the mixed neutrino and manifests itself as neutrino oscillations.

The search for these oscillations has become a sensitive method of measuring neutrino masses and mixing. The fact that so far this has not produced a positive result has set an upper limit on $\Delta m^2 = m_1^2 - m_2^2$, i.e., on the difference between the squares of the masses of ν_1 and ν_2, and on the mixing angle θ (see Ref. 2). Oscillations can produce a sig-

 0038-5670/87/090759-32$01.80

nificant change in the properties of natural neutrino fluxes, e.g., fluxes of solar neutrinos, neutrinos originating in gravitational collapse, atmospheric neutrinos, and so on. In particular, Pontecorvo and Gribov[3] were the first to note that ν-oscillations could provide a solution to the problem of solar neutrinos, i.e., they could be the reason for the discrepancy between the Cl-Ar experiment of Davis and the predictions of the standard solar model.

Neutrino oscillations essentially constitute an oscillatory process that is unrelated to the quantum nature of particles. They have many analogs in different branches of physics, especially in mechanics. Mixed neutrinos (to be specific, ν_e and ν_μ) constitute a system of two weakly coupled oscillators. The oscillations of one of them correspond to the propagation of ν_e and those of the other to the propagation of ν_μ. The creation of the ν_e is equivalent to the excitation of the ν_e oscillator, and so on. Coupling between these oscillators produces a periodic transfer of oscillations from one of them to the other. The periodic transfer process constitutes the oscillations. When the natural frequencies of the oscillators are equal, the transfer of oscillations is complete, and this corresponds to oscillations of maximum depth. When the frequencies are different, the oscillations are only partially transferred. "Normal" oscillations are the propagation of ν-states with particular energies (masses in vacuum). The analogy can be continued to the case of neutrino oscillations in matter. It will be clear later that a system of coupled oscillators reproduces practically all the features of the oscillations when interactions are taken into account.

Because of interactions between neutrinos and the medium, the latter modifies the picture of the oscillations. This effect was examined in 1977 by Wolfenstein[4] by analogy with the physics of neutral K-mesons. As in the case of coherent regenration of the K_S, the effect of the medium is due to the difference between the elastic forward-scattering amplitudes of the mixed neutrinos, for example, ν_e and ν_μ. It reduces to the appearance of waves with different refractive indices. When combined with vacuum mixing, this ensures that the ν_{im} have energies and phase and group velocities in the medium that are different from those of the ν_i. Consequently, this alters mixing in the medium, and the ν_e and ν_μ "oscillate" relative to the new states ν_{im}. Moreover, a medium will also modify the length (period) of the oscillations. It can either suppress the oscillations or amplify their depth right up to the maximum value.[4,5]

The effect of the medium can also be described in terms of the potentials in which the neutrinos ν_e and ν_μ propagate. The interaction leads to a change in mixing and to the appearance of effective masses that are different from m_1 and m_2.[12,13]

In the mechanical analog, the effect of the medium is equivalent to a change in the natural frequencies of the oscillators, and this difference is different for the "ν_e" and "ν_μ". The depth and period of the oscillations and the character of the normal oscillations become different as a result of this (as compared with the "vacuum" quantities).

In 1977, Wolfenstein derived a set of differential equations for the motion of mixed neutrinos. The constant-density approximation was used to examine some of the consequences of oscillations in the Earth,[4,5,8] in the Sun,[4,6] and in collapsing stars.[6,7] However, the physical content of this theory, and also the most interesting and important effects from the point of view of applications, were not established until 1984–85. The influence of the medium on neutrino oscillations is resonant in character.[9,10] The dependence of the parameter $\sin^2 2\theta_m$ (θ_m is the mixing angle in the medium) on the density ρ of the medium or the energy of the neutrinos takes the form of a resonance peak, and maximum mixing occurs for certain definite resonance densities ρ_R and energies E_R for which the oscillations occur with maximum depth. At resonance, the vacuum oscillation length is equal to the refraction length, and the effective masses of the ν_e and ν_μ become equal, i.e., the natural frequencies of the weakly-coupled oscillators are equal. Qualitatively new effects arise[9–11] in media in which the density is not constant. The motion of the neutrinos is accompanied by a variation in the depth of the oscillations and in their average. Practically complete transformation of one type of neutrino into another is possible in a wide range of energy and for small mixing angles. In contrast to vacuum, in which complete oscillations transformations are realized only for the maximum mixing angle $\theta = 45°$, in a medium this is possible even for small angles θ. More than that, the degree of transformation increases with decreasing angle θ. We recall that mixing is small in the case of quarks. Again, in contrast to vacuum, and to a constant-density medium in which almost complete $\nu_e \to \nu_\mu$ transformations are achieved at a given distance only for definite discrete values of energy, strong transformations can occur in a variable-density medium in continuous energy ranges. In the limiting case, in which the initial density is much higher than the resonant value, a nonoscillatory transformation is found to occur[10] in which a neutrino of one type transforms, as the density varies, into a neutrino of another type with practically zero oscillation depth.

There are two conditions at the basis of strong oscillatory transformations in matter, namely, (1) the resonance condition[9,10] and (2) the adiabatic or weakly nonadiabatic condition.[9–11]

These conditions essentially determine the oscillation regime, and the magnitude and scale of the effects. The first condition establishes the resonance density for a neutrino of given energy, and strong transformations are realized when the neutrinos cross a resonance layer with $\rho = (\rho_R - \Delta\rho_R) - (\rho_R + \Delta\rho_R)$, where $2\Delta\rho_R$ is the width of the resonance. Most of the changes in the composition of the neutrino beam occur precisely in the resonance layer. Strong oscillatory transformations in the medium are therefore called resonance transformations (resonance oscillations). The second condition sets a limit on the rate of change of density, $d\rho/dr$. When ρ varies sufficiently slowly, the adiabatic regime is established, and the system (oscillating neutrinos) succeeds in following the changes in $\rho(r)$. In the mechanical example, propagation in a varying-density medium corresponds to a change in the natural frequencies of the oscillators (different for "ν_e" and "ν_μ"). When these frequencies are initially very different, and then their ratio inverts sufficiently slowly (adiabatically), so that $\omega_1 \gg \omega_2 \to \omega_1 \ll \omega_2$, the oscillations of an initially excited oscillator are transferred (practically completely and irreversibly) to another oscillator that was initially at rest. This is the analog of strong transformations of neutrinos in matter.[2)]

The influence of the medium becomes appreciable only when its thickness d is large, i.e., $d \gtrsim d_0 \simeq m_N/G_F \simeq 3.5 \times 10^9$

g/cm^2, where m_N is the nucleon mass and G_F the Fermi constant. Consequently, these effects have applications in neutrino geophysics, astrophysics, and cosmology. The conditions for strong transformations are satisfied in wide ranges of mixing angle, differences between squares of masses, and neutrino energies in the Sun, the Earth, and collapsing stars. The size of these intervals is determined by the density difference across the medium and by the rate of change of density, and can reach several orders of magnitude.

There is a range of values of Δm^2 and $\sin^2 2\theta$ in which resonance oscillations of solar neutrinos give rise to a 2–4-fold suppression of the rate of production of ^{37}Ar in the Cl-Ar experiment. This can explain David's results in terms of the standard solar model.[9] It produces a definite distortion of the shape of the neutrino energy spectrum, which also modifies the predictions for other solar neutrino experiments. The complete neutrino spectroscopy of the Sun for which radiochemical experiments with different thresholds and measurements of the shape of the spectrum by direct methods are the prerequisites, offers the prospect of establishing whether resonance neutrino transformations do actually occur on the Sun. If they do occur, then we will be able to determine Δm^2 and $\sin^2 2\theta$ as well. If they do not, a wide interval of values of Δm^2 and $\sin^2 2\theta$ will be excluded to the neutrinos.[9,10,12,13]

If the results of the Davis experiments are explainable in terms of resonance oscillations, then $\Delta m^2 \lesssim 10^{-4}$ eV^2 and, in the case of a mass hierarchy, it follows that $m(\nu_e) \ll 10^{-2}$ eV. This means that the mass of the electron neutrino lies well outside the range of existing methods of measurement (experiments with tritium and searches for neutrino-free 2β-decays and neutrino oscillations). This, in turn, means that the spectroscopy of solar neutrinos will be one of the more important sources of experimental information not only in astrophysics, but also in particle physics.

The significant point is that the Δm^2 resonance region on the Sun overlaps the probable region of the predicted seesaw mechanism that is capable of explaining the low value of the neutrino mass as compared with the masses of charged leptons in the corresponding generations.[73] The scale of lepton number conservation breaking (the scale of the Majorana masses of right-handed neutrino components) is then found to be at the level of the grand unification scales or supersymmetry breaking, or the scale of the invisible axion[74] (see also Refs. 75,76).

The conditions for strong transformations in the cores and shells of collapsing stars are satisfied in much wider intervals of Δm^2 and $\sin^2 2\theta$ than for the Sun. Resonance oscillations can lead to a significant change in the properties of neutrino fluxes from gravitational collapses, and this must be borne in mind in the interpretation of experimental data.[11] Measurements of the ν-signal can be used to set strict limits on the neutrino parameters and, if the oscillation effect becomes established, they should yield important information on stellar structure and the dynamics of collapse.

Strong resonance transformations can also occur in the Earth as it is crossed by neutrinos at relatively small zenith angles. This has led to discussions of effects in neutrino beams from accelerators as they cross the Earth,[20] the distortion of the flux of atmospheric neutrinos arriving from the lower hemisphere of the Earth,[16,78,79] the modulation of the solar neutrino flux,[16,47–49] and the variation in the ν-signal from gravitational collapses.[16]

One further application of resonance oscillations is to primordial neutrinos in the early Universe.[16,17]

This review is devoted to a systematic presentation of the theory of neutrino oscillations in matter and its applications, principally to solar neutrinos. In the case of the mixing of the two types of neutrino, a detailed discussion is given of the evolution equation (Sec. 2) and of the properties of oscillations under different conditions (Sec. 3). This is followed by a generalization of the theory to the case of three types of neutrino and by a discussion of the separation of wave packets and of neutrino-absorption effects (Sec. 4). Section 5 describes resonance oscillations in the Sun and the Earth, and summarizes the principal results of collapsing stars.

2. EVOLUTION EQUATIONS FOR NEUTRINOS IN MATTER

2.1. Wolfenstein equations[4]

2.1.1. Deviation. Consider a system of two mixed neutrinos with given flavors,[3] for example, ν_e and ν_μ: $\nu_f = (\nu_e, \nu_\mu)$. An arbitrary neutrino state $\nu(t)$ can be written as

$$|\nu(t)\rangle = \psi_e(t)\,|\nu_e\rangle + \psi_\mu(t)\,|\nu_\mu\rangle, \tag{2.1}$$

where ψ_e and ψ_μ and the ν_e and ν_μ wave functions. The evolution equations for $\psi_f = (\psi_e, \psi_\mu)$ in matter have the following form in the ultrarelativistic limit:

$$i\frac{d\psi_f}{dt} = \left(k\hat{I} + \frac{\hat{M}^2}{2k} + \hat{W}\right)\psi_f, \tag{2.2}$$

where k is the neutrino momentum, $\hat{I}$ the unit matrix, $\hat{M}^2$ the square of the neutrino mass matrix in vacuum, and $\hat{W}$ the matrix that represents the interaction of the neutrino with the medium and constitutes the potential energy due to this interaction. It is clear that (2.2) is a generalized Schrödinger equation for a single particle of mass m:

$$i\dot{\psi} = (E + W)\psi \approx [k + m^2(2k)^{-1} + W]\psi,$$

where ν_e and ν_μ are the weak-interaction eigenstates,[4] so that $\hat{W}$ is diagonal: $\hat{W} = \mathrm{diag}(W_e, W_\mu)$. The mixing in (2.2) is due to the fact that $\hat{M}^2$ is not diagonal. When the neutrino energies are not too high, so that $s \ll G_F^{-1}$ and the size of the layer of matter is less than the absorption length, the neutrino interactions reduce to elastic forward scattering at zero angle. The expressions for W_e and W_μ can then be readily obtained by considering the change in the wave function in a time dt. This change is due to the appearance of an additional wave that is the result of the addition of waves scattered by particles in a layer $dx \simeq dt$:

$$\begin{aligned} d\psi_\alpha &= -iW_\alpha\,dx\,\psi_\alpha, \\ W_\alpha &= \sum_i f_i^\alpha(0)\,N_i k^{-1} \qquad (\alpha = e,\ \mu); \end{aligned} \tag{2.3}$$

where $f_i^\alpha(0)$ is the amplitude for the scattering of ν_α by the ith component of the medium ($i = e, p, n$) and N_i is the concentration of this component. It is well-known that the elastic-scattering effect reduces to the appearance of a refractive index where, in accordance with (2.3),[4,28]

$$(n_\alpha - 1) = 2\pi k^{-1} W_\alpha. \tag{2.4}$$

Another derivation is based on the fact that W_α is an addition to the neutrino energy due to the interaction.[14,12] In

other words, $W_\alpha = \langle \Phi | \hat{H}_{\text{int}} | \Phi \rangle$, where $\hat{\mathrm{H}}_{\text{int}}$ is the interaction Hamiltonian and Φ is a state that includes one neutrino with momentum k and resting particles of the medium with concentrations N_i. Very simple manipulation then again leads to (2.3).

We note that physical consequences are unaffected by the addition of an arbitrary matrix proportional to the unit matrix, say $\xi(t)\hat{I}$, to the evolution matrix on the right-hand side of (2.2). (This is equivalent to the appearance of the phase factor

$$\exp\left(-i\int_0^t \mathrm{d}t'\,\xi(t')\right)$$

in all wave functions; we emphasize that the phase difference is significant for oscillations.) This property can be used to obtain a more convenient form of the evolution equations. (Henceforth, we shall therefore omit the first term in (2.2), which contains the neutrino momentum.) This means that physical consequences are determined by the difference between the diagonal elements of the matrices $\hat{M}^2$ and W, and, in particular, by the difference

$$W = W_{\mathrm{e}} - W_\mu = \sum_i \Delta f_i(0)\, N_i k^{-1}, \tag{2.5}$$

where $\Delta f_i(0) = f_i^{\mathrm{e}}(0) - f_i^{\mu}(0)$. If the interactions with ν_{e} and ν_μ were the same, the medium would have no effect on the oscillations. The medium must be asymmetric with respect to the oscillating components.

For $\nu_{\mathrm{e}} - \nu_\mu$ and $\nu_{\mathrm{e}} - \nu_\tau$ oscillations, W is due to the scattering of ν_{e} by electrons, as a consequence of charged currents.[4] Neither ν_μ nor ν_τ have such interactions:

$$\Delta f(0) = \sqrt{2} G_{\mathrm{F}} k,$$

and

$$W = \sqrt{2}\, G_{\mathrm{F}} N_{\mathrm{e}} = \sqrt{2}\, G_{\mathrm{F}} \rho m_{\mathrm{N}}^{-1} Y_{\mathrm{e}}, \tag{2.6}$$

where Y_{e} is the number of electrons per nucleon. The asymmetry of an ordinary medium with respect to ν_{e} and ν_μ is due to the fact that it contains electrons but not muons.

The other condition for the influence of the medium is its charge asymmetry. The amplitudes for scattering by particles and antiparticles have opposite signs, i.e., $f_{\nu \mathrm{e}}(0) = -f_{\nu \bar{\mathrm{e}}}(0)$, so that, if the number of particles and antiparticles is the same ($N_{\mathrm{e}} = N_{\bar{\mathrm{e}}}$), the resultant effect in (2.5) is zero.

In vacuum, $\hat{W} = 0$. The evolution matrix is proportional to the square of the mass matrix, and its eigenstates are identical with states of definite mass, $\boldsymbol{\nu} = (\nu_1, \nu_2)$.

The condition for the diagonalization of $\hat{M}^2$ yields

$$\boldsymbol{\nu}_f = \hat{S}_0(\theta)\, \boldsymbol{\nu}, \tag{2.7}$$

where

$$\hat{S}_0(\theta) = \begin{pmatrix} \cos\theta & \sin\theta \\ -\sin\theta & \cos\theta \end{pmatrix},$$

and

$$S^{+}(\theta)\, \hat{M}^2 S(\theta) = \hat{M}^{2\,\mathrm{diag}} = \mathrm{diag}\,(m_1^2,\ m_2^2); \tag{2.8}$$

in which m_1 and m_2 are the masses of ν_1 and ν_2. The angle θ in (2.7) relates states of specific flavor with states of specific mass, and is called the vacuum mixing angle.

The equations for the ν_i ($i = 1,2$) in vacuum are found to separate, $i\dot{\psi} = (M^{2\mathrm{diag}}/2k)\psi$, and their solution is $\psi_i = \psi_i(0)\exp(-i\varphi_i)$, where the phases are $\varphi_i(t) = (m_i^2/2k)t$. Because of the mass difference, the ν_i have different phase velocities. The distance $|l_\nu|$ for which the phase difference between the ν_i [$\Delta\varphi = (\Delta m^2/2k)t$] reaches 2π is called the vacuum oscillation length:

$$l_\nu = -4\pi k (\Delta m^2)^{-1}. \tag{2.9}$$

The square of the mass matrix can be expressed in terms of Δm^2 and θ:

$$\hat{M}^2 = \frac{\Delta m^2}{2} \begin{vmatrix} \cos 2\theta & -\sin 2\theta \\ -\sin 2\theta & -\cos 2\theta \end{vmatrix},$$

and the evolution equations (2.2) can be written in the form

$$i\frac{\mathrm{d}\psi_f}{\mathrm{d}t} = \hat{H}\psi_f, \tag{2.10}$$

where

$$\hat{H} = \begin{vmatrix} H_{\mathrm{e}} & \frac{1}{2}\overline{H} \\ \frac{1}{2}\overline{H} & H_\mu \end{vmatrix},$$

and

$$\overline{H} = -\Delta m^2 (2k)^{-1} \sin 2\theta,$$

$$H = H_{\mathrm{e}} - H_\mu = \Delta m^2 (2k)^{-1} \cos 2\theta + \sum_i \Delta f_i(0) N_i k^{-1}. \tag{2.11}$$

In a variable-density medium $N_i = N_i(x)$, so that (2.10) is a set of differential equations with variable coefficients ($t \simeq x/c \simeq x, c = 1$).

We note that the neutrino and antineutrino scattering amplitudes have different signs, $f_\nu(0) = -f_{\bar{\nu}}(0)$, so that the term in H that describes the influence of the medium changes sign when ν is replaced with $\bar{\nu}$. The evolution equations for $\bar{\nu}$ and ν in matter are different, and the oscillation picture is also different.

2.1.2. Refraction length.[4] The natural length in matter l_0 is defined by

$$l_0 = 2\pi W^{-1} = 2\pi \left(\sum_i \Delta f(0)\, N_i k^{-1}\right)^{-1}. \tag{2.12}$$

The additional phase difference $\Delta\varphi = 2\pi$ between the ν_{e} and ν_μ is acquired as a result of scattering within the path length l_0. This means that l_0 defines the scale over which the influence of the medium becomes significant. Since $\Delta f(0) \sim k$, l_0 is determined by the density of the medium and type of oscillation, but is independent of the neutrino energy. In this sense, l_0 is a parameter of the medium. For the $\nu_{\mathrm{e}} \to \nu_\mu$ oscillations, (2.6) shows that

$$l_0 = 2\pi m_{\mathrm{N}} \left(\sqrt{2}\, G_{\mathrm{F}} \rho Y_{\mathrm{e}}\right)^{-1} = \left(3 \cdot 10^7\ \mathrm{m}\,(\rho(\mathrm{g/cm^3}) \cdot 2Y_{\mathrm{e}})\right)^{-1}. \tag{2.13}$$

Hence, it follows that the thickness within which the effect of the medium becomes appreciable is

$$d_0 = \rho l_0 \sim 2\pi m_{\mathrm{N}} \left(\sqrt{2}\, G_{\mathrm{F}}\right)^{-1} \tag{2.14}$$

and is essentially determined by the Fermi constant alone.

The elements of the evolution matrix (2.11) can now be expressed in terms of l_0:

$$H = -2\pi l_\nu^{-1} (\cos 2\theta - l_\nu l_0^{-1}), \quad \overline{H} = 2\pi l_\nu^{-1} \sin 2\theta. \tag{2.15}$$

A large thickness is not sufficient for a strong change in the oscillation picture. According to (2.15), the size of the effect depends on the ratio of l_0 to l_ν. When $l_\nu \ll l_0$, there is little

change in the properties of the oscillations. The medium has a large effect when $l_\nu \gtrsim l_0$.

2.2. General properties of the evolution equations and their solutions

2.2.1. Amplitudes and probabilities of oscillatory transformations. For given initial conditions $|\nu(0)\rangle = \nu_\alpha$ ($\alpha = e, \mu$), the wave functions $\psi_e(t)$ and $\psi_\mu(t)$ determine the probability amplitudes for oscillatory transformations $\nu_\alpha \to \nu_e$, $\nu_\alpha \to \nu_\mu$ in time t. Let us denote them by $\psi_\beta^{(\alpha)}$. Using the most symmetric form of the evolution equations (2.10), for which $H_e = -H_\mu = H/2$, we can readily establish the following relationship between the amplitudes:

$$\psi_e^{(e)} = \psi_\mu^{(\mu)*}, \quad \psi_\mu^{(e)} = -\psi_e^{(\mu)*}. \tag{2.16}$$

Moreover, $\psi_\beta^{(\alpha)}$ must satisfy the normalization conditions

$$|\psi_e^{(\alpha)}|^2 + |\psi_\mu^{(\alpha)}|^2 = 1 \quad (\alpha = e, \mu). \tag{2.17}$$

It then follows from (2.16) and (2.17) that the transformation probabilities satisfy the conditions

$$P_{e\to e} = P_{\mu\to\mu}, \quad P_{e\to\mu} = P_{\mu\to e}, \quad P_{e\to e} + P_{e\to\mu} = 1, \tag{2.18}$$

where

$$P_{\alpha\to\beta} \equiv |\psi_\beta^{(\alpha)}|^2.$$

The significance of (2.18) is that, as they cross a given layer of the medium, the initial ν_e are transformed into ν_μ to the extent to which initial ν_μ are transformed into ν_e. If the oscillating neutrino fluxes in the generation region are equal, they remain equal after they leave the medium. Under these conditions, there is no observable effect.

2.2.2. Equations for the transformation probabilities.[9,10] In addition to $P \equiv |\psi_e|^2$, we now introduce $R = \mathrm{Re}(\psi_\mu^* \psi_e)$ and $I = \mathrm{Im}(\psi_\mu^* \psi_e)$. The equations for P, R, and I then follow[9] directly from (2.10)[5]:

$$\begin{aligned} \dot P &= -\overline{H} I, \\ \dot I &= -HR + \overline{H}\left(P - \frac{1}{2}\right), \\ \dot R &= HI. \end{aligned} \tag{2.19}$$

When electron neutrinos are created, the initial conditions are

$$P(0) = I, \quad R(0) = I(0) = 0. \tag{2.20}$$

In general, $|\nu(0)\rangle = a|\nu_e\rangle + b|\nu_\mu\rangle$ and

$$P(0) = |a|^2, \quad R(0) = \mathrm{Re}\, b^* a, \quad I(0) = \mathrm{Im}\, b^* a.$$

The functions P, R, and I satisfy the relation

$$P^2 + R^2 + I^2 = P,$$

which follows from their definition and the normalization condition (2.17).

We can write (2.19) in the more compact form

$$\frac{d\zeta}{dt} = [\mathbf{H} \times \zeta], \tag{2.21}$$

where

$$\zeta = \left\{R, I, P - \frac{1}{2}\right\}, \quad \mathbf{H} = \{-\overline{H}, 0, -H\}. \tag{2.22}$$

Eliminating R and I from (2.19), we obtain the following equation[11] for P:

$$\dddot P - \frac{\dot H}{H}\ddot P + H(H^2 + \overline{H}^2)\dot P - \overline{H}^2 \dot H\left(P - \frac{1}{2}\right) = 0. \tag{2.23}$$

with initial conditions $P(0) = 1$, $\dot P(0) = 0$, and $\ddot P(0) = -(1/2)\overline{H}^2$ when ν_e is created. Formulations in terms of the probabilities, given by (2.19), (2.21), and (2.23), are convenient for specific numerical calculations and for the analysis of the general properties of systems of mixed neutrinos.

2.2.3. Analogies. (a) The analogy between mixed neutrinos and a system of weakly-coupled oscillators was described in the Introduction and follows from (2.10). The wave function $\psi_e(t)$ corresponds to a combination of kinetic energy (E_{kin}) and potential energy (E_{pot}) of the oscillator ("ν_e"): $\psi_e(t) \to E_{kin}^{1/2} + iE_{pot}^{1/2}$ (and similarly for ψ_μ). The elements of the matrices $H_e/2$ and $H_\mu/2$ in the absence of mixing are identical with the eigenfrequencies of the oscillators. The off-diagonal elements determine the coupling between the oscillators.

The other analogy with a mechanical system of oscillators can be obtained by eliminating, say, ψ_μ from (2.10).[20]

(b) The vector equation (2.21) is a compact version of the equations for the probabilities, given by (2.29), and is identical with the equation for a spin in a magnetic field.[18,20] The components of ζ are the average components of the spin along the coordinate axes, and $\mathbf{H}$ is the magnetic field normalized so that the magnetic moment of the particle is $\mu = 1/2$. It is well-known that the solutions of (2.21) describe the precession of the spin (magnetic moment) about the direction of the field, with angular velocity $\mathbf{H}$. A change in the density of the medium is equivalent to a change in the component of the field $\mathbf{H}$. It is thus clear that the evolution of a system of mixed neutrinos in a medium with variable ρ is equivalent to the precession of a spin in a varying magnetic field. The probability of detecting a neutrino of the original type is determined by the mean projection of the spin along the z-axis: $P = \zeta_z + (1/2)$ [see (2.22)].

(c) The direct analog is the set of neutral K-mesons in a medium (with allowance for regeneration). (Of course, in contrast to the neutrinos, absorption is significant in the case of the K-mesons.) A set of K-mesons realizes a special case, i.e., maximum mixing in vacuum. By virtue of the CPT-theorem, $\theta = 45°$, and the oscillating components are the particle and the antiparticle. In the case of the neutrino, there is no such limitation, and mixing may turn out to be arbitrarily small. As will be shown later, it is precisely for small vacuum mixing that the most interesting effects are found to arise.

(d) The physical conditions incorporated in (2.10) can be reproduced for polarized light propagating in optically active media. The analogs of ν_e and ν_μ are then the two different polarizations of the wave.

Transitions between the eigenstates of the neutrino Hamiltonian in a medium are analogous to transitions between atomic levels under the influence of external perturbation (for example, the scattering of charged particles by atoms).[24]

We note that the effects described by the evolution equations (2.10) essentially constitute the physics of oscillations that is unrelated to the quantum nature of the neutrino. The common elements of all the analogies described so far are: (1) two or possibly more degrees of freedom, (2) coupling between them (mixing), and (3) a relative change in

their energies (eigenfrequencies). The only quantum-mechanical effect that influences the oscillations is due to the finite size of the neutrino wave packets and the separation of these packets due to the difference between the group velocities of ν_1 and ν_2 (their analogs in the medium). Of course, there are no analogs of such processes in mechanical systems.

The above analogies are used in the interpretation of the oscillation effects.

2.2.4. Flavor and mass oscillations. The equations for the wave functions of neutrinos with pure flavors are given by (2.10). They therefore determine flavor oscillations in a neutrino beam. If we use (2.7), we can deduce from (2.10) the equations for states with fixed ν_1 and ν_2 masses $(\psi = \psi_1, \psi_2)$[4]:

$$i\frac{d\psi}{dt} = \left(\frac{\hat{M}^{2\,\mathrm{diag}}}{2k} + \hat{S}^{+}(\theta)\,\hat{W}\hat{S}(\theta)\right)\psi$$

$$= \left[\frac{1}{2k}\begin{pmatrix} m_1^2 & 0 \\ 0 & m_2^2 \end{pmatrix} + \frac{W_e}{2}\begin{pmatrix} \cos 2\theta & \sin 2\theta \\ \sin 2\theta & -\cos 2\theta \end{pmatrix}\right]\psi. \quad (2.24)$$

According to (30), ν_1 and ν_2 will mix in a medium. Neutrino scattering leads to $\nu_1 \leftrightarrow \nu_2$ transitions. In addition to the flavor oscillations, there are also mass oscillations. This does not, of course, violate the law of conservation of energy: ν_1 and ν_2 in the medium are not the eigenstates of the Hamiltonian, and do not, therefore, have sharp energies.

Equations (2.20) and (2.24) have a similar structure. The corresponding evolution matrices can be written in the form

$$\hat{H} = A\begin{pmatrix} 1 & 0 \\ 0 & -1 \end{pmatrix} + B\begin{pmatrix} \cos 2\theta & -\sin 2\theta \\ -\sin 2\theta & -\cos 2\theta \end{pmatrix},$$

where

$$A = \frac{W_e}{2}, \quad B = \frac{\Delta m^2}{4k} \quad \text{for } \nu_e \text{ and } \nu_\mu,$$

and, conversely,

$$A = \frac{\Delta m^2}{4k}, \quad B = \frac{W_e}{2}, \quad \theta \to -\theta \quad \text{for } \nu_1 \text{ and } \nu_2.$$

When we pass from flavor oscillations to "mass oscillations," the medium and vacuum interchange their roles: $\Delta m^2/4k \leftrightarrow W_e/2$. In the former case, the medium is "diagonal" and mixing is due to the vacuum. The reverse situation occurs in the second case: the vacuum is diagonal and mixing is due to the medium.[29]

We note in this connection that vacuum (vacuum contribution to the evolution matrix) and matter can be regarded on an equal basis.[29] Vacuum can be imagined as a second medium with constant density $\rho \sim \Delta m^2/2k$. This is completely consistent with the Higgs mechanism for mass generation. The evolution of mixed neutrinos in a medium is then described as the propagation of ν_e and ν_μ in two media inserted into one another, and is asymmetric with respect to ν_e and ν_μ. In principle, the vacuum contribution can be replaced by the contribution of a real medium, assuming the neutrinos to be massless. However, this requires the introduction of nondiagonal neutral currents, which is unnatural from the point of view of gauge theories. Experimental limits on such currents are discussed in Ref. 32.

2.2.5. Limits of validity. The derivation of the evolution equations (2.10) was actually based on the following assumptions:

(1) inelastic-scattering and absorption effects are negligible

(2) the particles of the medium are at rest

(3) the scattering of neutrinos by the individual particles of the medium occurs independently, which corresponds to the limit of geometric optics.

Inelastic interactions and motion of the target particles, which are significant in the cores of collapsing stars and in the early Universe, will be examined in Section 4. Here, we confine our attention to assumption (3). For most particular applications, the condition for the validity of the geometric optics approximation, i.e., $\lambda\!\!\!^{-} \ll r$, is satisfied ($\lambda\!\!\!^{-}$ is the neutrino wavelength and r the separation between the scattering centers). The only exception may be the central regions of collapsing stars, where the density reaches nuclear values and $\lambda\!\!\!^{-}$ is of the order of r. However, even here, the corrections turn out to be small because the refractive index approaches unity. When $\lambda\!\!\!^{-} \gg r$, the collective effect reduces to the polarizability of the medium, and the refractive index is given by the Clausius-Mossotti formula $n - 1 = (n_0 - 1)[1 + (2/3)(n_0 - 1)]$, where n_0 is the refractive index without taking polarizability into account. According to (2.4) and (2.3), $n_0 - 1 \simeq 2\sqrt{2}\pi G_F \rho/km_N \simeq \lambda\!\!\!^{-}_\nu/l_0$, where l_0 is the refraction length (2.12), (2.14). For example, when $E_\nu = 1$ MeV and $\rho = 10^{12}$ g/cm^3, we have $n_0 - 1 = 10^{-9}$.

3. THEORY OF NEUTRINO OSCILLATIONS IN MATTER

In this Section, we present the formalism of neutrino oscillations in a medium in a form that is a generalization of the theory of oscillations in vacuum, and is best suited to the physics of the situation, since it enables us to describe the effects of wave packet separation and allows a generalization to an arbitrary number of neutrinos.

3.1. Mixing of neutrinos in matter

3.1.1. Eigenstates of neutrinos and the mixing angle. In vacuum, the mixing $\nu_f = (\nu_e, \nu_\mu)$ is determined relative to states of fixed mass, $\nu = (\nu_1, \nu_2)$, i.e., relative to the eigenstates of the Hamiltonian or, in other words, states that diagonalize the evolution matrix in vacuum. Similarly, in a medium, the mixing of ν_e and ν_μ is determined relative to $\nu_m = (\nu_{1m}, \nu_{2m})$, i.e., the eigenstates of the Hamiltonian in the medium. The ν_{im} diagonalize the evolution matrix $\hat{H}$ with allowance for the interactions (2.10). If we define $\hat{S}(\theta_m)$ so that

$$\nu_f = \hat{S}_m(\theta_m)\nu_m, \quad \hat{S}_m(\theta_m) = \begin{pmatrix} \cos\theta_m & \sin\theta_m \\ -\sin\theta_m & \cos\theta_m \end{pmatrix}, \quad (3.1)$$

we can write the diagonalization condition in the form

$$\hat{S}_m^{+}(\theta_m)\hat{H}\hat{S}_m(\theta_m) = \hat{H}_m^{\mathrm{diag}} = \mathrm{diag}\,(H_1^d,\ H_2^d). \quad (3.2)$$

The angle θ_m establishes, according to (3.1), the connection between eigenstates of the medium and states with particular flavors. It is called the mixing angle in matter (Fig. 1). The elements H_i^d of $\hat{H}^{\mathrm{diag}}$ are the eigenvalues of the Hamiltonian, i.e., energy levels of the neutrino system. It follows from (3.2) and (2.10) that

$$\sin 2\theta_m = \overline{H}\,(H^2 + \overline{H}^2)^{-1/2}, \quad (3.3)$$

$$H_{1,2}^d = \frac{1}{2}\left[H_e + H_\mu \pm (H^2 + \overline{H}^2)^{1/2}\right]. \quad (3.4)$$

The energies H_i^d enable us to introduce the effective masses

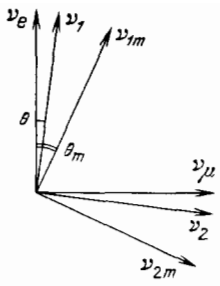

FIG. 1. Graphical representation of mixing in vacuum and in matter.

of the ν_{im}: $M^2 = 2kH_i^d$. The quantities ν_{im}, θ_m, and M_i^2 are the analogs of ν_i, θ, and M_i^2 in the medium. The evolution matrix in matter is different from that in vacuum, so that $\nu_{im} \neq \nu_i$, $\theta_m \neq \theta$, and $M_i^2 \neq m_i^2$. When interactions are taken into account, mixing is found to change (Fig. 1). H and, hence, ν_{im}, θ_m, and M_i^2, depend on the density of the medium and the neutrino energy. The transformations $\nu_{im} \to \nu_i, \theta_m \to \theta$, and $M_i^2 \to m_i^2$ occur as the density of the medium tends to zero.

The most important properties of the system of mixed neutrinos are: resonance, absence of level crossing, and the change in the flavors of eigenstates with varying density.

3.1.2. Resonance.[9,10] The dependence of mixing parameters $\sin^2 2\theta_m$ on neutrino energy or the density of the medium is found to exhibit a resonance. From (3.3) and the expressions for $\overline{H}$ and H, given by (2.15), it follows that

$$\sin^2 2\theta_m = \sin^2 2\theta \cdot R(l_\nu l_0^{-1}, \theta), \tag{3.5}$$

where

$$R = [(\cos 2\theta - l_\nu l_0^{-1})^2 + \sin^2 2\theta]^{-1} \tag{3.6}$$

will be referred to as the resonance factor (Fig. 2). We recall that $l_\nu / l_0 \sim \rho E$. When

$$l_\nu l_0^{-1} = \cos 2\theta \tag{3.7}$$

R reaches a maximum: $R_\nu = \sin^{-2} 2\theta$ and $\sin^2 2\theta_m = 1$. Condition (3.7), for which mixing in the medium reaches its maximum ($\theta = 45°$), is called the resonance condition. The half-width at half-height of the resonance is determined by the vacuum mixing angle

$$\Delta(l_\nu l_0^{-1}) = (l_\nu l_0^{-1})_R \tan 2\theta = \sin 2\theta. \tag{3.8}$$

The resonance peak becomes narrower as vacuum mixing is reduced. As $l_\nu / l_0 \to 0$, which corresponds, for example, to

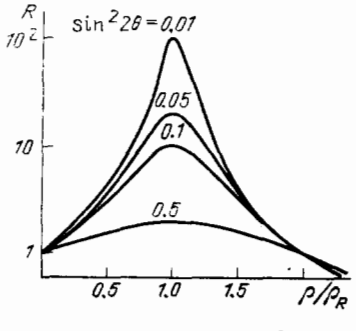

FIG. 2. Resonance factor as a function of the density of matter for different mixing angles in vacuum.

$\rho \to 0$, we find that $\sin^2 2\theta_m$ tends to the vacuum value $\sin^2 2\theta (R \to 1)$. When $|l_\nu / l_0| \to \infty$, the factor R is strongly suppressed: $R \simeq (l_\nu / l_0)^{-2} \ll 1$, and the mixing parameter in the medium is much smaller than the vacuum value: $\sin^2 2\theta_m = \sin^2 2\theta (l_0 / l_\nu)^2$.

The density of the medium that satisfies the resonance condition is called the resonance density. According to (3.7), (2.9), and (2.14),

$$\rho_R = -m_N \Delta m^2 \cdot \cos 2\theta (2\sqrt{2} G_F E)^{-1}; \tag{3.9}$$

where $\rho_R = \rho^{eff} = \rho Y_e$. We emphasize that ρ_R is inversely proportional to the neutrino energy and is a slowly-varying function of θ when there is little vacuum mixing. The resonance energy is defined similarly. In terms of ρ_R, the resonance dependence (3.5), (3.6) assumes the form

$$\sin^2 2\theta_m = \tan^2 2\theta \cdot [(1 - \rho \rho_R^{-1})^2 + \tan^2 2\theta]^{-1}. \tag{3.10}$$

Along the ρ scale, the half-width of the resonance is

$$\Delta \rho_R = \rho_R \tan 2\theta. \tag{3.11}$$

When a neutrino transforms into an antineutrino, $\Delta f(0)$ and, hence, l_ν / l_0 change sign. Consequently, in a given medium, the resonance occurs either for the neutrino or the antineutrino, depending on the relative signs of $\cos 2\theta$, Δm^2, and $\Delta f(0)$. We shall consider that ν_e consists preferentially of ν_1, i.e., $\theta < 45°$ and $\cos 2\theta > 0$, so that the resonance condition is satisfied for $-\Delta m^2 / \Delta f(0) > 0$. For the $\nu_e \to \nu_\mu$ and $\nu_\mu \to \nu_e$ oscillations, $\Delta f(0) = \sqrt{2} G_F k > 0$ (the correct sign of Δf was established by Langacker[14]), so that resonance in the ν_e-channels occurs for $m_2^2 - m_1^2 > 0$, where ν_e consists mainly of the lighter neutrino. This result is important for the interpretation of solar neutrino experiments.

The resonance is due to the fact that mixed neutrinos constitute a system of weakly-coupled oscillators. The oscillator eigenfrequencies are equal at resonance: $H = 0$ or $H_e = H_\mu$. For a homogeneous medium ($\rho = \text{const}$), $\sin^2 2\theta_m$ determines the oscillation depth (Sec. 3). At resonance, $\sin^2 2\theta_m = 1$, and the depth is a maximum. This corresponds to the fact that, when the eigenfrequencies are equal, the oscillations of one of the oscillators are completely transferred to another. There is also a different interpretation. When there is little mixing (and resonance occurs), the resonance condition has the form $l_\nu = l_0$, i.e., the eigenfrequency of the system, $1/l_\nu$, is equal to the frequency characterizing the ambient medium, $1/l_0$ (Refs. 9 and 10).

Specific manifestations of resonance depend on the density distribution in the medium, the initial conditions, and so on.

3.1.3. Level crossing. In the absence of mixing, the diagonal elements of the evolution matrix H_e and H_μ are the energy levels of ν_e and ν_μ. In a medium, H_e and H_μ are linear functions of ρ. They cross at the point $\rho \simeq \rho_R$ ($H_e \simeq H_\mu$), i.e., at the resonance density[12,13] (Fig. 3). This picture is radically altered when mixing is introduced. The states ν_{1m} and ν_{2m}, which are different from ν_e and ν_μ, have sharp energies H_1^d and H_2^d. The trajectories $H_1^d(\rho)$ and $H_2^d(\rho)$ do not cross (Fig. 3): mixing removes level crossing. The energy difference is then

$$H^d = H_2^d - H_1^d = (H^2 + \overline{H}^2)^{1/2} = \Delta H_0 R^{1/2},$$

where the vacuum splitting $\Delta H_0 = \Delta M^2 / 2k$ is a minimum at

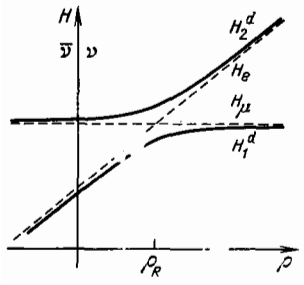

FIG. 3. Energy levels of two neutrinos plotted against density in the absence of mixing (broken lines) and with mixing taken into account (solid lines).

resonance. We note that, as the density increases, $H_1^d(\rho)$ transfers from the H_e trajectory to the H_μ trajectory, whereas H_2^d shows the reverse behavior, and the transition occurs mostly in the resonance region.

3.1.4. Variation in the flavors of neutrino eigenstates in a medium.[9,10] Equation (3.1) can be "inverted":

$$\nu_m = \hat{S}_m^+(\theta_m)\nu_f. \tag{3.12}$$

This means that the mixing angle θ_m in a medium determines the flavor, i.e., ν_e, ν_μ constitute the composition of the eigenstates ν_{im}. The angle θ_m depends on the density, so that the flavor of the ν_{im} varies with ρ. According to (3.3), $\tan 2\theta_m = \tan 2\theta[1 - (\rho/\rho_R)]^{-1}$. When $\rho \ll \rho_R$, we have $\theta_m \simeq \theta$; θ_m increases monotonically with increasing density, passing the value $\theta_m = 45°$ at $\rho = \rho_R$. When $\rho \gg \rho_R$, the angle θ_m approaches $\pi/2$: $[(\pi/2) - \theta_m] \simeq \tan 2\theta(\rho_R/2\rho)$. Thus, as the density varies from $\rho \ll \rho_R$ to $\rho \gg \rho_R$, the mixing angle in matter varies from θ to $\pi/2$ (Ref. 16) (Fig. 4). For small θ, this means that the flavor of the eigenstates ν_{im} changes almost completely as ρ varies from 0 to $\rho \gg \rho_R$. When a state ν_{im} has mostly the e-flavor for $\rho \simeq 0$, it will be dominated by the muon flavor for $\rho \gg \rho_R$ ($\nu_{im} \simeq \nu_\mu$). The variation in the flavor of the ν_{im} can also be followed by considering the dependence of energy levels on ρ (see Fig. 3).

The above properties of mixing are consequences of the density dependence of the Hamiltonian, and can be described[19] directly in terms of changes in the matrix $\hat{H}(\rho)$.

3.2. General properties of neutrino oscillations in matter

3.2.1. Definitions. Mixing angle.[27,29] An arbitrary neutrino state $|\nu(t)\rangle$ can be expanded in terms of the neutrino eigenfunctions in matter as follows:

$$|\nu(t)\rangle = \cos\theta_a |\nu_{1m}\rangle + \sin\theta_a e^{-i\varphi} |\nu_{2m}\rangle; \tag{3.13}$$

where $\theta_a(t)$ is the angle defining the fraction of eigenstates ν_{im} in a given state $\nu(t)$, and $\varphi \equiv \varphi_2 - \varphi_1$ is the phase difference between the components ν_{1m} and ν_{2m}. The common factor $\exp(-i\varphi_1)$, which has no effect on physical consequences, is omitted from (3.13). The coefficients in front of $|\nu_{im}\rangle$, i.e.,

$$\psi_{1m} = \cos\theta_a, \quad \psi_{2m} = \sin\theta_a e^{-i\varphi} \tag{3.14}$$

are the wave functions of ν_{im}, normalized so that $|\psi_{1m}|^2 + |\psi_{2m}|^2 = 1$.

As in vacuum, the monotonic increase in the phase difference φ with t leads to oscillations in the flavor of $|\nu\rangle$. Actually, in view of (3.12), the probability amplitude that ν_e will be found in $|\nu(t)\rangle$ is

$$\langle \nu_e | \nu(t) \rangle = \cos\theta_a \cdot \cos\theta_m + \sin\theta_a \cdot \sin\theta_m e^{-i\varphi}. \tag{3.15}$$

Hence, the probability of finding ν_e is

$$P(t) = \overline{P}(t) + \frac{1}{2} A_P(t)\cos\varphi, \tag{3.16}$$

where the average (over the period) probability is

$$\overline{P}(t) = \cos^2\theta_a \cdot \cos^2\theta_m + \sin^2\theta_a \cdot \sin^2\theta_m, \tag{3.17}$$

the oscillation depth is

$$A_P = \sin 2\theta_a \cdot \sin 2\theta_m \tag{3.18}$$

and the quasiperiod is

$$T_m = l_m = 2\pi\dot{\varphi}^{-1}. \tag{3.19}$$

Vacuum oscillations are a special case of (3.15)–(3.19), in which: (1) the impurity angle does not depend on time and is equal to the mixing angle in vacuum $\theta_a = \theta$, and (2) the flavors of the eigenstates $\nu_{im} = \nu_i$ do not depend on time and are also determined by the angle θ. We note that $\theta_a = \theta$ is a consequence of the fact that states with pure flavors, ν_e or ν_μ, are created in weak interactions.

The general case realized in a medium with variable ρ corresponds to the fact that the admixture of eigenstates (θ_a) in $\nu(t)$ and the flavors of the eigenstates themselves are also functions of time. This means that both the mean probability and the oscillation depth will vary in the medium.

The most complete description of oscillations is given in terms of θ_m, θ_a, and φ. θ_a and φ relate a given state ν to ν_{im}; θ_m, in turn, relates ν_{im} to ν_e and ν_μ:

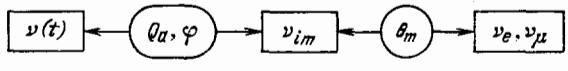

In (3.15)–(3.19), θ_m is a known function of density, so that $\theta_a(t)$ and $\varphi(t)$ must be determined before we can describe the oscillations.

3.2.2. Graphical representation of ν-oscillations.[16,21,22,27,30] A graphical representation of the above relationships provides not only an informative picture of ν-oscillations, but also enables us to reproduce the results of the analytic solution.

With the eigenstates ν_{im} we can associate an orthonormal basis $\{\nu_m\} = \{\nu_{1m}, \nu_{2m}^R, \nu_{2m}^I\}$ in which ν_{2m}^R and ν_{2m}^I correspond to the real and imaginary parts of the wave function ν_{2m}. In this basis, the state $|\nu(t)\rangle$ in (3.13) is described by the unit vector $\nu = \{\cos\theta_a, \sin\theta_a \cdot \cos\varphi, \sin\theta_a \sin\varphi\}$. A monotonic variation in φ is equivalent to the rotation of ν around ν_{1m} or, more precisely, to the motion of ν over the surface of a cone with axis along ν_{1m} and cone angle θ_a (Fig.

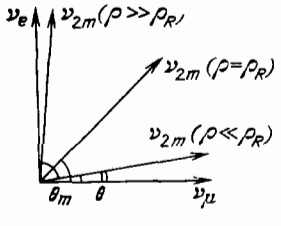

FIG. 4. Flavor of the eigenstate ν_{2m} as a function of density.

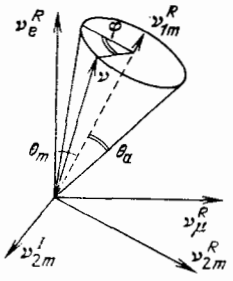

FIG. 5. Graphical representation of neutrino oscillations.

5). The quasiperiod of this rotation is $l_m = 2\pi/\dot{\varphi}$. The states ν_e and ν_μ are associated with the flavor basis $\{\nu_f\} = \{\nu_e^R, \nu_\mu^R, \nu_\mu^I\}$, rotated relative to $\{\nu_m\}$ so that, in $\{\nu_m\}$, $\nu_e^R = \{\cos\theta_m, \sin\theta_m, 0\}$, $\nu_\mu^R = \{-\sin\theta_m, \cos\theta_m, 0\}$, $\nu_e^I = \{0,0,i\sin\theta_m\}$. The imaginary part of the wave function of ν_m corresponds to the vector $\nu_\mu^I = \{0,0,i\cos\theta\}$. The component of ν along a given axis ν_x is equal to the probability amplitude of finding ν_x in $\nu(t)$. In most cases, it is sufficient to consider the components of ν along the real plane.

In a varying-density medium, the evolution of a ν-state consists of two rotations, namely, rotation of ν around ν_{1m} (motion on a cone) with angular velocity $\dot{\varphi}$, where the angle of the cone may vary with time, and rotation of the cone itself in the flavor basis. The position of the axis of the cone (ν_{1m}) in $\{\nu_f\}$ is determined by the mixing angle θ_m which, in turn, depends on the density of the medium.

The graphical representation that we have described is not unique. Another possibility is to use the analogy between the oscillations and the motion of a spin in a magnetic field[18,20] (see Section 2.5). A neutrino state is described by the vector ζ that rotates around $\mathbf{H}$ on the surface of a cone or angle $2\theta_a$. The vector $\mathbf{H}$ is at an angle $2\theta_m$ to the z-axis. The component ζ_z determines directly the transition probability: $P = \zeta_z + (1/2)$.

3.2.3. Evolution of the neutrino eigenstates in matter.[19,22,23] *The equations for θ_a and φ.* According to (3.1), the wave functions of states with particular flavors, ψ_f, can be expressed in terms of the wave functions of the eigenstates as follows: $\psi_f = \hat{S}_m(\theta)\psi_m, \psi_m = (\psi_{1m}, \psi_{2m})$. Substituting these in (2.10), and recalling (3.2), we obtain the evolution equation for ν_{im}:

$$i\frac{d\psi_m}{dt} = \hat{H}_m\psi_m,$$

$$\hat{H}_m = \left(\hat{H}^{diag} - i\hat{S}_m^{+}\frac{d\hat{S}}{dt}\right) = \begin{vmatrix} H_1^d & -i\dot{\theta}_m \\ +i\dot{\theta}_m & H_2^d \end{vmatrix}. \tag{3.20}$$

The off-diagonal terms $-i\dot{\theta}_m$ are proportional to the rate of change of density:

$$\frac{d\theta_m}{dt} = \sin^2 2\theta\cdot\frac{R}{2\Delta\rho_R}\frac{d\rho}{dt} = \frac{\sin^2 2\theta_m}{2\Delta\rho_R}\frac{d\rho}{dt}. \tag{3.21}$$

The transitions $\nu_{1m} \leftrightarrow \nu_{2m}$ occur in an inhomogeneous medium ($d\rho/dt \neq 0$), $\dot{\theta}_m \neq 0$, and the set of equations for the eigenstates does not separate.

Substituting the expressions for the wave functions (3.14) in (3.20), we obtain the equation for the angle θ_a and the phase φ (Ref. 30):

$$\dot{\theta}_a = \dot{\theta}_m\cos\varphi, \tag{3.22}$$

$$\dot{\varphi} = \dot{\varphi}^d - 2\dot{\theta}_m\sin\varphi\cdot\operatorname{ctg}2\theta_a, \tag{3.23}$$

where

$$\dot{\varphi}^d = H_2^d - H_1^d = 2\pi l_m^{-1} = 2\pi(l_\nu R^{1/2})^{-1}. \tag{3.24}$$

The initial conditions for (3.22), (3.23) are determined by the fact that the impurities ν_{im} at the time of neutrino generation are specified by the mixing angle θ_m at that time. When $\nu(0) = \nu_e$, we have $\nu(0) = \cos\theta_m(0)\cdot\nu_{1m} + \sin\theta_m(0)\cdot\nu_{2m}$. Comparing this expression with (3.13), we find that

$$\theta_a^0 = \theta_m^0, \quad \varphi^0 = 0. \tag{3.25}$$

Equations (3.22) and (3.23) have a simple geometric interpretation, and can be deduced graphically. Infinitesimal changes $d\theta_a$ occur only as a result of rotation of the cone axis (ν_{1m}). Rotation of ν over the surface of the cone does not contribute to $d\theta_a$. Both rotations participate in the phase change: the first term on the right-hand side of (3.23) is the contribution of the rotation of ν over the cone, and the second is the result of the rotation of the cone axis, i.e., ν_{1m} in flavor space.

3.3. Neutrino oscillations under different conditions

The properties of oscillations are determined by the nature of the density variation in the medium. A number of situations can be distinguished, depending on the rate of change of density with distance ($d\rho/dt \simeq d\rho/dx$): (1) constant density, (2) adiabatic regime (slow density variation), (3) departure from adiabaticity in a resonance layer, and (4) strong departure from adiabaticity and, as a limiting case, a density discontinuity. In addition, we shall consider oscillations for particular density distributions.

3.3.1. Constant density. The mixing angle in matter is a constant. Substituting $\theta_m = 0$ in (3.22) and (3.23), we obtain

$$\dot{\theta}_a = 0 \quad \text{or} \quad \theta_a = \theta_a^0, \qquad \dot{\varphi} = \dot{\varphi}^d = H^d. \tag{3.26}$$

Hence, it follows that: (1) the impurities ν_{im} in a given state $\nu(t)$ are determined at the initial time and remain constant throughout subsequent evolution. In other words: for $\dot{\theta}_m = 0$, the set of equations for ν_{im} given by (3.20) separates, ν_{im} evolve independently, and there are no $\nu_{1m} \leftrightarrow \nu_{2m}$ transitions; (2) since $\theta_m = \text{const}$, the flavors of the eigenstates do not vary.

Conservation of the impurities ν_{im} and of their flavors means that the picture of the oscillations in the constant-density medium is the same as in vacuum, and only the parameter values undergo a change. If the initial state $\nu(0)$ is the electron neutrino, then, according to (3.26) and (3.25), $\theta_a = \theta_a^0 = \theta_m^0 = \theta_m$. Substituting this and $\dot{\varphi}$ from (3.26) into the general relations given by (3.16)–(3.19), we find the parameters of the ν-oscillations:

$$\bar{P} = 1 - \frac{1}{2}\sin^2 2\theta_m, \quad A_p = \sin^2 2\theta_m = \sin^2 2\theta\cdot R,$$
$$l_m = 2\pi(H^d)^{-1} = l_\nu R^{1/2}. \tag{3.27}$$

These reproduce Wolfenstein's results.[4] We note that $\bar{P}$, A_p, l_m are constants, and the expressions for them are the same as the vacuum expressions when θ_m is replaced with θ.

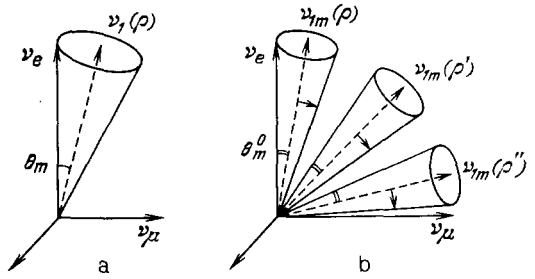

FIG. 6. Graphical representation of neutrino oscillations in constant-density matter (a) and in the adiabatic regime (b).

In the graphical representation of evolution, ν is described by the rotation of the vector ν around ν_{im} with constant cone angle and frequency. The position of ν_{1m} remains constant (Fig. 6).

The manifestations of resonance are as follows. According to (3.27), the oscillation depth is $\sin^2 2\theta_m$, i.e., it has a resonance dependence on the density of the medium and on neutrino energy. When $\rho = \rho_R$ ($\theta_m = 45°$), we have $A_p = 1$, and the depth is a maximum for arbitrarily small degree of vacuum mixing.

When a medium of density ρ intercepts a neutrino beam with a continuous energy spectrum, the neutrino oscillations will be resonance-enhanced for energies $E \simeq E_R(\rho)$, where E_R is the resonance energy. When $E = E_R$, the density is a maximum. In the energy interval $(E_R - \Delta E_R)$—$(E_R + \Delta E_R)$, where $\Delta E_R = E_R \tan 2\theta$, we have $A_p \geqslant 1/2$. At exit from a layer of thickness d, the probability $P(E)$ of finding a neutrino of the initial type is an oscillating function of energy with frequency determined by d (Fig. 7). The envelope of $P(E)$ is the same as the resonance curve $P_{env}(E) = \sin^2 2\theta_m(E)$.

3.3.2. Adiabatic regime. Integrating with respect to φ in (3.22), and using (3.23), we obtain the following expression for the impurity angle[30]:

$$\theta_a = \theta_a^0 + \int_0^\varphi \frac{\dot\theta_m}{\dot\varphi^d}\left(1 - \frac{\dot\theta_m}{\dot\varphi^d}\cdot 2\sin\varphi'\cdot\cot 2\theta_a\right)^{-1}\cos\varphi'\,d\varphi'. \tag{3.28}$$

Hence, when $\dot\theta_m/\dot\varphi^d$ is small, we have $\theta_a = \theta_a^0 + O(\dot\theta_m/\dot\varphi^d)$. Similarly, it follows from (3.23) that $\dot\varphi = \dot\varphi^d + O(\dot\theta_m/\dot\varphi^d)$.

In the case of constant density [see (3.21)], $\dot\theta_m \sim d\rho/dx$, $\theta_m \neq$ const. However, if the density varies slowly, so that

$$\dot\theta_m \ll \dot\varphi^d, \tag{3.29}$$

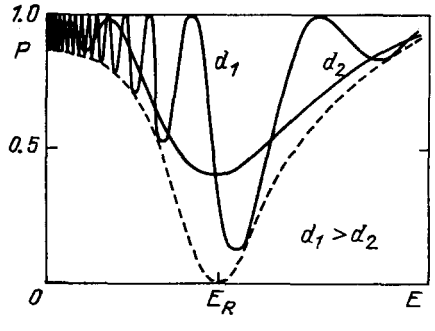

FIG. 7. The ν_e-ν_e transformation probability as a function of energy in a layer of constant-density matter of thickness d.

we may assume in the first (adiabatic) approximation that

$$\theta_a \approx \theta_a^0, \quad \dot\varphi = \dot\varphi^d \tag{3.30}$$

[see also (3.23)]. The dynamics of the oscillations in the adiabatic regime, determined by (3.30), is as follows.

(1) The impurities ν_{im} in a given state ν are determined at the initial time and are conserved throughout the evolution process. In other words, condition (3.29) signifies that the off-diagonal elements of the evolution matrix for ν_{im} (3.20) and, hence, the $\nu_{1m} \leftrightarrow \nu_{2m}$ transitions can be neglected, and the ν_{im} evolve independently. As in (3.20), this is analogous to the situation in a constant-density medium.

(2) The flavors of the eigenstates ν_{im} determined by θ_m vary in accordance with the density variation. This is the basic difference as compared with a constant-density medium.

The adiabatic condition is given by (3.29). It is particularly critical in a resonance layer[9] for $\rho = \rho_R$. Actually, the derivative $\dot\theta_m$, which is proportional to the factor R in (3.21), is a maximum at resonance:

$$\dot\theta_m^R = \frac{1}{2\Delta\rho_R}\frac{d\rho}{dt} = \frac{1}{2\Delta r_R}; \tag{3.31}$$

where

$$\Delta r_R = \left(\frac{d\rho}{dr}\right)_R^{-1}\Delta\rho_R \tag{3.32}$$

is the spatial half-width of the resonance layer. On the other hand, the quantity $\dot\varphi^d = 2\pi/l_m$ is inversely proportional to $R^{1/2}$, and the oscillation length l_m is a maximum at resonance. Substituting for $\dot\varphi_R^d$ and $\dot\theta_m^R$ from (3.31) in (3.29), we find that $2\Delta r_R \ll l_m^R/2\pi$. Consequently, when

$$\Delta r_R \geqslant l_m^R \tag{3.33}$$

the parameter $\dot\theta_m/\dot\varphi^d$, characterizing the precision of the adiabatic approximation, is of the order of 0.1. The adiabatic condition in the form given by (3.33)[9,10] signifies that at least one oscillation length fits into the resonance layer. This is a most important condition because most of the changes in the ν-beam occur in the resonance layer.

The adiabatic condition (3.29) has a simple geometric interpretation: the rotation of the vector ν around ν_{1m} on the surface of the cone should occur more rapidly than the rotation of the vector ν_{1m} (i.e., of the cone itself) in flavor space.

Conservation of the impurities ν_{im} when the flavors of the ν_{im} themselves change determines the properties of the oscillations under adiabatic conditions. If the initial state is the electron neutrino, then, account to (3.30) and (3.25),

$$\theta_a = \theta_a^0 = \theta_m^0, \tag{3.34}$$
$$\varphi = \int_0^t H^d\,dt'.$$

Substituting for θ_a from (3.34) into the general formulas of Section 3.2, we obtain

$$\bar P = \cos^2\theta_m^0\cdot\cos^2\theta_m + \sin^2\theta_m^0\cdot\sin^2\theta_m, \tag{3.35}$$
$$A_p = \sin 2\theta_m^0\cdot\sin 2\theta_m.$$

These results can also be obtained graphically.[11,16,22,33] Solution in the adiabatic regime constitutes (1) rotation of ν over the surface of the cone with constant cone angle θ_m^0 and

(2) rotation of the cone itself, determined by the angle θ_m (Fig. 6).

The adiabatic solution (3.35) has the following properties.[11,16,22,23]

(a) Universality. The angle $\theta_m(t)$ is determined by the density $\rho(t)$ at time t. Hence, in accordance with (3.35), the average probability $\overline{P}(t)$ and the oscillation depth $A_p(t)$ are determined by the instantaneous values of the density at the initial (t_0) and running (t) instants of time, and do not depend on the density distribution. $\overline{P}$ and A_p do not depend on the frequency or phase of the oscillations. The dependence of $\overline{P}$ and A_p on time is confined to ρ:

$$\overline{P}(t) = \overline{P}(\rho(t)), \quad A_p(t) = A_p(\rho(t)).$$

Universality can also be formulated in terms of the dimensionless variable[11,16] (see also Ref. 23)

$$n = (\rho - \rho_R)(\Delta\rho_R)^{-1}, \tag{3.36}$$

i.e., the distance from the point ρ_R on the density scale (in units of $\Delta\rho_R$). Using the definition given by (3.36), we have

$$\begin{aligned} n &= -(\tan 2\theta)^{-1}, & \rho &= 0, \\ &= 0, & \rho &= \rho_R, \\ &= +\infty, & \rho &\to \infty. \end{aligned} \tag{3.37}$$

In terms of n,

$$\sin 2\theta_m = (n^2+1)^{-1/2} \tag{3.38}$$

and the oscillation parameters (3.35) assume the form (Fig. 8)

$$\begin{aligned} \overline{P}(n, n_0) &= \frac{1}{2}\{1 + n n_0 [(n_0^2+1)(n^2+1)]^{-1/2}\}, \\ A_p(n, n_0) &= [(n_0^2+1)(n^2+1)]^{-1/2}. \end{aligned} \tag{3.39}$$

(b) Monotonic variation of $\overline{P}$ with density. There is a single-valued relationship between $\overline{P}$ and ρ. When the neutrinos are created in a layer with initial density ρ_0 and then enter regions with lower ρ, $\overline{P}$ decreases monotonically for $\rho_0 > \rho_R$ and increases monotonically for $\rho_0 < \rho_R$ with decreasing ρ. When the neutrinos are created in vacuum, and propagate in a medium with increasing density, $\overline{P}$ decreases from its vacuum value $1 - \sin^2 2\theta/2$ to $\sin^2\theta$ as $\rho \to \infty$.

(c) Nonoscillatory transition.[11,16,33] As the initial density increases ($n_0 \to \infty$), the oscillation depth tends to zero: $A_p \sim n_0^{-1}$ and $\overline{P}(n)$ approaches the asymptotic relation:

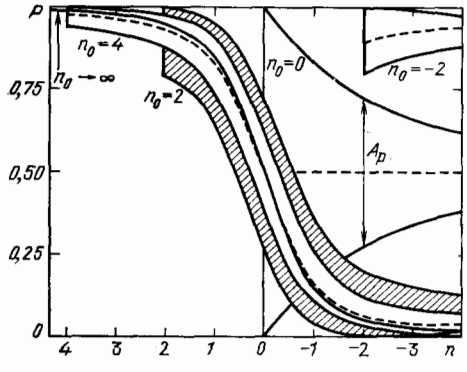

FIG. 8. Mean probability $\overline{P}$ (broken lines) and oscillation depth A_p (solid lines) as functions of n for different initial conditions (n_0) in the adiabatic regime.

$$P_{as} = \frac{1}{2}[1 + n(n^2+1)^{-1/2}] \tag{3.40}$$

(Fig. 8). This can be explained as follows. When $n_0 \simeq \rho_0/\rho_R \to \infty$, the initial mixing angle θ_m^0 is close to $\pi/2$ (Fig. 4), i.e., $\nu(0)$ is practically identical with one of the eigenstates $\nu(0) \simeq \nu_e \simeq \nu_{2m}$, and adiabaticity ensures that $\nu(t) \simeq \nu_{2m}(t)$ throughout subsequent evolution. There are then no oscillations in $P(t)$, which are a measure of the noncoincidence between ν and ν_{im}. The changes in the ν-beam described by (3.40) are due to the change in the flavor of ν_{2m}. On the level diagram (Fig. 3), a nonoscillatory transition corresponds to motion over a particular trajectory: $H_1^d(\rho)$ or $H_2^d(\rho)$. The cone angle θ_a is equal to 0 or $\pi/2$.

(d) Effect at exit. If the neutrinos are created in a dense layer and leave the object for $\rho_f = 0$, then, at exit, $n = -1/\tan 2\theta$ and the oscillation parameters are given by

$$\overline{P}_f = \frac{1}{2}[1 - n_0 \cos 2\theta \cdot (n_0^2+1)^{1/2}], \quad A_p = \sin 2\theta \cdot (n_0^2+1)^{-1/2}. \tag{3.41}$$

When there is little mixing in vacuum, and the initial densities are high, we have $\overline{P}_f \simeq \sin^2\theta + (1/4n_0^2)$. In the nonoscillatory limit ($n_0 \gg 1/4\sin^2\theta$), we have $\overline{P}_f = \sin^2\theta$ (Ref. 9). The final neutrino state then coincides with a ν_2-state with a particular mass. The smaller the vacuum angle and the greater the density ρ_0, the greater is the suppression of the flux of the neutrinos of the original kind that can be attained.

(e) Manifestations of resonance. For a fixed initial value n_0, the oscillation depth reaches its maximum at resonance (for $\rho = \rho_R$):

$$A_p(n=0, n_0) = (n_0^2+1)^{-1/2} > A_p \quad (n \neq 0, n_0).$$

The oscillation depth is a maximum ($A_p = 1$) only in the resonance layer, and only when the neutrino is generated for $\rho = \rho_R$ ($n_0 = 0$). In all other cases, A_p ($n = 0$) < 1 and, moreover, A_p is close to zero for a nonoscillatory transition. This is a significant difference as compared with oscillations in a homogeneous medium, and is due to the fact that the oscillation depth is determined not only by the mixing angle θ_m, but also by the impurity angle θ_a, while, in a medium with varying density, $\theta_a \neq \theta_m$. At resonance, $\overline{P} = 1/2$ independently of n_0. It is precisely in the resonance layer ($n = -1 - +1$) that the largest changes occur in the properties of the ν-beam: $\Delta\overline{P} = \overline{P}(-1, n_0) - \overline{P}(1, n_0) = n_0[2(n_0^2+1)]^{-1/2}$, and this value of $\Delta\overline{P}$ increases from $1/2$ to $1/\sqrt{2}$ as n_0 rises from 1 to $n_0 \to \infty$.

The above results correspond to strict conservation of impurities ν_{im}, i.e., $\theta_a = \theta_a^0$. The first correction in $\dot{\theta}_m/\dot{\varphi} \simeq \dot{\theta}_m/\dot{H}^d$ to the adiabatic approximation can be written in the following form in view of (3.28):

$$\theta_a - \theta_a^0 = \int_0^{\varphi} \frac{\dot{\theta}_m}{H^d} \cos\varphi' \, d\varphi'. \tag{3.42}$$

When the density variation in monotonic and sufficiently slow, the oscillating factor under the integral sign ensures that the correction increases with time and, for arbitrary φ, can be estimated from $|\Delta\theta_a| < |\dot{\theta}_m/H^d|_{max} = |\dot{\theta}_m/H^d|_R$[6]).

3.3.3. Departure from adiabaticity. When (3.29) is not satisfied, then $\nu_{1m} \leftrightarrow \nu_{2m}$ transitions become significant. The impurities ν_{im} in a given neutrino state ν are not conserved:

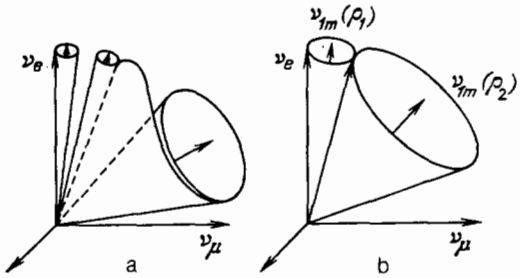

FIG. 9. Graphical representation of neutrino oscillations: a—departure from adiabaticity in the resonance layer, b—density jump.

the impurity angle θ_a changes, and this change depends on the phase of the oscillations (Fig. 9). The phase itself is determined not only by the difference between the energy levels H_i^d, but also by variations in the impurities ν_{im}.

The set of equations given by (3.22) and (3.23) is conveniently analyzed by transforming from time as the variable to θ_m:

$$\frac{d\theta_a}{d\theta_m} = \cos\varphi, \tag{3.43}$$

$$\frac{d\varphi}{d\theta_m} = -\frac{4\pi\varkappa}{\sin^3 2\theta_m} - 2\sin\varphi\cdot\cot 2\theta_a, \tag{3.44}$$

where

$$\varkappa = \left(\frac{d\rho}{dr}\right)^{-1}\frac{\Delta\rho_R}{l_m^R}.$$

The first term on the right-hand side of (3.44), namely, $\xi \equiv 4\pi\varkappa \sin^{-3} 2\theta_m$, is equal to $H^d/\dot\theta_m \simeq \dot\varphi^d/\dot\theta_m$, i.e., according to (3.29), it is a measure of the degree of departure from the adiabatic state. If the derivative $d\rho/dr$ does not vary with r too rapidly, ξ decreases as resonance is approached ($|\sin 2\theta_m| \to 1$). At resonance, $\xi = 4\pi\varkappa_R$, where

$$\varkappa_R = \Delta r_R (l_m^R)^{-1}. \tag{3.45}$$

When the density variation is slow, the term ξ is dominant. It corresponds to the first correction (3.42) and, when it is taken into account, the phase change that accompanies passage through the layer of the medium in which θ_m varies from $\theta_m^0 = \theta_m(\rho_0)$ to $\theta_m = \theta_m(\rho)$ is given by

$$\Delta\varphi(\theta_m) = \varphi - \varphi_0 = -4\pi\int_{\theta_m^0}^{\theta_m}\frac{\varkappa(\theta_m)\,d\theta_m}{\sin^3 2\theta_m}, \tag{3.46}$$

where φ_0 is the initial phase. Substituting for φ in (3.43), we obtain the change in the cone angle:

$$\Delta\theta_a = \theta_a - \theta_a^0 = \int_{\theta_m^0}^{\theta_m}\cos(\varphi_0 + \Delta\varphi(\theta_m'))\,d\theta_m'. \tag{3.47}$$

If an average is taken over φ_0, then, according to (3.47), the correction $\overline{\Delta\theta}_a$ is zero. This is so because $\Delta\varphi$ in (3.46) does not depend on θ_a.

The adiabatic condition is particularly critical at resonance, so that, as the density rate of change $d\rho/dr$ varies, the departure from the adiabatic conditions occurs first in the resonance layer. One can then use the linear approximation for the distribution $\rho(r)$. Actually, for small mixing angles θ, the width of the resonance layer is small ($\Delta\rho \sim \rho\tan 2\theta$), and virtually any function $\rho = \rho(r)$ can be replaced in it with a linear function. Since it is precisely in the resonance layer that the strongest transformations occur in ν-beams, the deviation of $\rho(r)$ from the linear form outside this layer has no significant effect on the final results. In the case of a linear density variation, the solution of the above system of equations for the wave functions ψ_e and ψ_μ can be found in analytic form.[24,25,37,49,80] Eliminating the wave function ψ_μ from (2.10), we obtain a second-order differential equation for ψ_e, which can be reduced to the Weber equation. The solution of this takes the form of parabolic cylinder functions.

Certain important conclusions follow directly from the general form of (3.43) and (3.44), and from the known results for the analogs of mixed neutrinos. In the case of a linear density variation $d\rho/dr = (d\rho/dr)_R = \text{const}$, the parameter $\varkappa$ in (3.44) is found to be a constant, $\varkappa = \varkappa_R$, and this defines the limit of adiabaticity in the resonance layer (3.45). When the initial density is high, $\rho_0 \gg \rho_R$, and the final density is low, $\rho_f \ll \rho_R$, then, for small mixing angles, the limits of integration in (3.43) and (3.44) have the fixed values $\theta_m^0 \simeq \pi/2$ and $\theta_m^f = 0$. The solution (θ_a at exit) then depends on the single parameter $\varkappa_R$:

$$\theta_a^f = \theta_a(\varkappa_R) = \theta_a\left[\rho\left(\frac{d\rho}{dr}\right)_R^{-1}\frac{\tan 2\theta}{l_m^R}\right]. \tag{3.48}$$

When the density varies exponentially, so that $\rho(d\rho/dr)^{-1} = H = \text{const}$, and $H \gg \Delta r_R$ (the condition for the validity of the linear approximation), it follows from (3.48) that θ_a and, hence, P, depend on θ, Δm^2, and E in the following combination: $\tan 2\theta/l_m^R \simeq \sin^2 2\theta(E/\Delta m^2)^{-1}$ (this result was obtained by A. Messiah in a different form[19]). This peculiar scaling is realized in the outer layers of the Sun.

Departure from adiabaticity in the resonance layer means that, at resonance, the $\nu_{2m} \leftrightarrow \nu_{1m}$ transformations take place, i.e., there are transitions between the energy levels H_1^d, H_2^d. In this respect, the neutrino problem is analogous to the quantum-mechanical problem of transitions in atoms in which an external perturbation produces level crossing. Landau[36] and Zener[37] have obtained a solution for a perturbation that is a linear function of time. The probability of the $2 \to 1$ transition is $P_{LZ} = \exp[-(\pi/2)\Delta H/i\overline{H}]$, where ΔH and $\overline{H}$ are, respectively, the energy level difference and the matrix element describing the $2 \to 1$ transition at the crossing point, i.e., at resonance. In the case of the neutrino, (3.20) shows that $i\overline{H} = 2\dot\theta_m$, $\Delta H = (H_2^d - H_1^d)_R = H_R^d$ and $(\Delta H/i\overline{H})_R = H^d/2\dot\theta_m = 2\rho\varkappa_R$, i.e., the $\nu_{2m} \to \nu_{1m}$ transition probability is

$$P_{LZ} = \exp(-\pi^2\varkappa_R). \tag{3.49}$$

The correspondence with the neutrino problem is achieved when the neutrinos are created far enough in density from ρ_R [$(\rho - \rho_R)/\Delta\rho_R \gg 1$]. When this is so, $\theta_m^0 = \pi/2$, the cone angle is $\theta_a = \pi/2$ ($\cos\theta_a \simeq 0$), and $\nu(0) = \nu_e \simeq \nu_{2m}$. This means that the system occupies a particular level H_2^d. The probability of finding ν_1 and ν_2 at exit is $\cos^2\theta_a = P_{LZ}$ and $\sin^2\theta_a = 1 - P_{LZ}$, respectively. Substituting these in (3.17), we obtain the average probability of the transition $\nu_e \to \nu_e$ from the region of large ρ to the region with $\rho = 0$ (Refs. 24, 25):

$$\overline{P} = P_{LZ}\cos^2\theta + (1 - P_{LZ})\sin^2\theta = \sin^2\theta + P_{LZ}\cos 2\theta. \tag{3.50}$$

In the adiabatic case ($\varkappa_R \gtrsim 1$), we have $P_{LZ} \ll 1$ and (3.50) reproduces the result of the nonoscillatory transition: $\overline{P} \simeq \sin^2\theta$. As $\varkappa_R$ decreases, the probability of the $\nu_{2m} \to \nu_{1m}$ transition increases and so does $\overline{P}$. Departure from adiabaticity reduces the depth of the resonance transformation.

The expressions given by (3.49) and (3.50) reflect the asymptotic behavior. Whe ν_e is created near resonance, it contains appreciable impurities, and ν_{2m} and ν_{1m} occupy both levels. In that case, we must take into account not only the $\nu_{2m} \to \nu_{1m}$, ν_{2m} transitions, but also the $\nu_{1m} \to \nu_{2m}$, ν_{1m} transitions, i.e., interference between the corresponding matrix elements.[45] Moreover, the probability $P_{1\to 2}$ is then no longer equal to P_{LZ} (3.49).

3.3.4. *Strong departure from adiabaticity. Density jump.* If the density and, hence, θ_m very rapidly, so that $\dot{\theta}_m \gg \dot{\varphi}^d$ ($\varkappa \ll 1$), the first term on the right-hand side of (3.44) can be neglected. Dividing (3.43) by (3.44), we obtain

$$\frac{d\theta_a}{d\varphi} = -\frac{\tan 2\theta_a}{2\tan\varphi},$$

which provides us with a direct and unambiguous connection between changes in the cone angle and changes in the phase. Integration of this with the initial values φ_0 and θ_a^0 yields

$$\sin\varphi = \sin\varphi_0 \cdot \sin 2\theta_a^0 (\sin 2\theta_a)^{-1}. \tag{3.51}$$

Substituting this expression in (3.43), and integrating between θ_m^0 and $\theta_m(t)$, we obtain

$$\cos 2\theta_a = \cos 2\theta_a^0 \cdot \cos 2(\theta_m - \theta_m^0) - \cos\varphi_0 \cdot \sin 2\theta_a^0 \cdot \sin 2(\theta_m - \theta_m^0), \tag{3.52}$$

where φ and θ_a do not explicitly depend on time, and the result of the evolution process is determined exclusively by the change in the mixing angle $(\theta_m - \theta_m^0)$. Essentially, (3.51) and (3.52) describe the behavior of the neutrino state for a jump-like change in the density at some time t^0. When $\varphi_0 = 0$ or π, (3.51) and (3.52) show that $\varphi = 0$, $\theta_a(0) = \theta_a^0 + (\theta_m - \theta_m^0)$ or $\theta_a(\pi) = -\theta_a^0 + (\theta_m - \theta_m^0)$ (Fig. 9).

In the graphical representation, this corresponds to an instantaneous rotation of the axes $\{\nu_m\}$ in the flavor basis. There is also a discontinuous change in the components of ν, which also rotates around the new position ν_{1m}. When $\varphi_0 = 0$ or π, the jump leaves ν unaltered in flavor space. However, it is more convenient to consider the graphical representation in terms of probability. Here, the vector ξ corresponding to ν remains unchanged at the time of the jump for any initial condition.

4. GENERALIZATION OF THE THEORY OF NEUTRINO OSCILLATIONS

In this Section, we present a generalization of the theory due to 1) allowance for the finite length of wave packets, 2) the inclusion of a third type of neutrino, and 3) allowance for absorption effects and motion of target particles. Oscillations to sterile states are discussed.

4.1. Separation of wave packets[22,27,33]

A rigorous description of oscillations must be based on an examination of wave packets. In vacuum, a mixed neutrino state is a set of two (or more) such packets that correspond to states with particular mass. In a medium, the mixed neutrino is described by wave packets of eigenstates ν_{im}. It is precisely these ν_{im} that have the particular phase and group velocities.

The length of a packet ($c\tau_p$) depends on the conditions under which the neutrinos are generated. If a neutrino is created in the decay of a particle, τ_p is equal to the smallest of the following three quantities: 1) the decay time τ, 2) the time between two inelastic collisions τ_{col}, and 3) $1/kT$ (T is the temperature of the medium) if $\tau \gg \tau_{col}$. When the neutrino is created in collisions, τ_p is determined by the time of flight and the length of the packets representing the colliding particles.

The wave packets in a mixed ν-state have 1) different phase velocities v_{ph} and 2) different group velocities. The former leads to oscillations, and the latter results in a separation of the wave packets in space. The packets separate from one another, their overlap decreases, and this changes the picture of the neutrino oscillations.[7)] The "point" description of oscillations, discussed above, remains valid if the separation of the wave packets in space can be neglected.

The group velocities of the eigenstates in the medium are given by

$$v_{im} = \frac{dE_i}{dk} \approx 1 + \frac{dH_i^d}{dk}.$$

Using the explicit form of H_i^d, and introducing the dimensionless parameter n, we find from this that

$$\Delta v_m = v_{1m} - v_{2m} = \Delta v_v \cos 2\theta \cdot (-n + \operatorname{tg} 2\theta)(n^2+1)^{-1/2}, \tag{4.1}$$

where $\Delta v_v = v_1 - v_2 = -\Delta m^2/2k^2$ is the group velocity difference in vacuum. The dependence of Δv_m on density has the following properties (Fig. 10). As ρ increases, the difference Δv_m decreases monotonically. At resonance, $\Delta v_m = v_v \sin 2\theta$, and, at $\rho_R' = \rho_R/\cos^2 2\theta$, the difference Δv_m vanishes and then changes sign. The density ρ_R', for which the group velocities v_{1m} and v_{2m} are equal, is equal to the resonance density for the mass oscillations ($\nu_1 \leftrightarrow \nu_2$). For $\rho \gg \rho_R$, $\Delta v_m \simeq -\Delta v_v \cos 2\theta$, and, if the angle θ is small, we have $\Delta v_m \simeq -\Delta v_v$, i.e., the separation of the packets is opposite to that in vacuum. In the resonance channel, the medium suppresses the separation for any ρ: $|\Delta v_m| \leqslant |\Delta v_v|$.

In a medium with constant or slowly-varying density (under adiabatic conditions), the states ν_{im} evolve independently, and the separation of wave packets over a path length L is

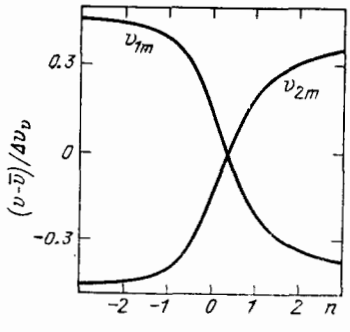

FIG. 10. Group velocity of neutrino eigenstates as a function of n: $\bar{v} = (v_{1m} + v_{2m})/2$; $\tan 2\theta = 0.4$.

$$D(L)=\int_0^L \Delta v_m(\rho(r))\,dr. \tag{4.2}$$

Separation effects can be neglected when $D(L)\ll\tau_p$. Because of the superposition principle, separation does not affect average probabilities. Actually, if, in the neutrino state, the fraction of ν_{1m} at a particular time is $\cos^2\theta_a$ and the fraction of ν_{2m} is $\sin^2\theta_a$, the probability of finding ν_e in the packets ν_{1m} and ν_{2m} is $P_1=\cos^2\theta_a\cos^2\theta_m$ and $P_2=\sin^2\theta_a\sin^2\theta_m$, respectively. Hence, it follows that $P_s\equiv P_1+P_2=\overline{P}$, i.e., the total probability of finding ν_e, summed over the packets, is equal to the average probability in the case where the packets overlap completely.

The separation of packets changes the oscillation depth, which is proportional to the degree of overlap of the packets. If the time dependence of a packet is described by $\exp(-t/\tau_p)$, then

$$A_p=A_p^0\exp(-|D|\tau_p^{-1}), \tag{4.3}$$

where A_p^0 is the oscillation depth in the case of complete overlap.

We note that, according to (4.1), the separation of packets in media with $\rho>\rho'_R$ and $\rho<\rho'_R$ has different signs. When the neutrino crosses the resonance layer, separation effects before and after resonance cancel one another out, and this may lead to a restoration of packet overlap.

4.2. Oscillations of three neutrinos in matter

Let us now consider the oscillations of ν_e, ν_μ, and ν_τ on the assumption that $m_1\ll m_2\ll m_3$ and that the degree of mixing is small. This case is the most natural from the point of view of quark-lepton symmetry (unification of quarks and leptons) and the seesaw mechanism of neutrino mass generation.[73]

4.2.1. *Mixing and resonances in a system of three neutrinos.* The oscillation dynamics is now described by (2.2), in which $\psi_f=(\psi_e,\psi_\mu,\psi_\tau)$, $\hat{M}^2$ is a 3×3 matrix of the squares of the masses, and $\hat{W}=\mathrm{diag}(\hat{W}_e,\hat{W}_\mu,\hat{W}_\tau)$. The neutrino eigenstates in the medium, ν_{im} $(i=1,2,3)$, and the mixing are determined as in the case of two neutrinos. The 3×3 mixing matrix S that relates the eigenstate ν_{im} to the states with definite flavor ($\nu_f=\hat{S}\nu_m$) depends on three angles[8] and satisfies the diagonalization condition

$$\hat{S}^+\hat{H}\hat{S}=\hat{H}^{\mathrm{diag}}=\mathrm{diag}(H_1^d,\ H_2^d,\ H_3^d),$$

where H_i^d $(i=1,2,3)$ are the energy levels in the three-neutrino system. It is convenient to parametrize $\hat{S}$ with the aid of the Gell-Mann matrices[39,40] $\hat{U}_\alpha$: $\hat{S}=\hat{U}_7(\psi_m)\hat{U}_5(\varphi_m)\hat{U}_2(\omega_m)$, where $\Phi_m=\{\psi_m,\varphi_m,\omega_m\}$ are the mixing angles in the medium. When $\rho=0$, the ν_{im} transform into the ν_i-states with masses m_i $(i=1,2,3)$, and $\hat{S}$ becomes identical with $\hat{S}_0=\hat{U}_7(\psi)\hat{U}_5(\varphi)\hat{U}_2(\omega)$, i.e., the vacuum mixing matrix.

In the lowest-order perturbation theory, elastic interactions of ν_μ and ν_τ in an ordinary medium are identical, i.e., $W_\mu=W_\tau$. The difference $W_\tau-W_e=W_\mu-W_e$ arises from scattering of ν_e by electrons, due to charged currents [see (3.26)], so that $\hat{W}=\mathrm{diag}(W,0,0)$.

In higher orders, there is a difference between W_μ and W_τ due to the difference between the muon and τ-lepton masses.[41] For an electrically neutral medium

$$W_\mu-W_\tau\approx-\frac{G_F}{\sqrt{2}}\frac{3\alpha}{2\pi\sin^2\theta_W}\frac{m_\tau^2}{m_W^2}\times\left[(N_p+N_n)\ln\frac{m_W^2}{m_\tau^2}-\left(N_p+\frac{2}{3}N_n\right)\right], \tag{4.4}$$

where $\alpha=1/137$, θ_W is the Weinberg angle, m_τ and m_W are the τ-lepton and W-boson masses, and N_p and N_n are the proton and neutron concentrations, respectively (see, however, Ref. 41). Comparison with (2.6) yields $W_\mu-W_\tau=5\times10^{-5}\,W$. Hence, it follows that, first, the refraction length for the $\mu-\tau$ channel, $l_0^{\mu\tau}$, is greater than $l_0^{e\mu}$ by four orders of magnitude, so that the thickness of the medium within which interactions appreciably modify $\nu_\mu-\nu_\tau$ oscillations is greater by four orders of magnitude than $d_0\simeq m_N/G_F$. Second, $W_\mu-W_\tau$ and W_e-W_μ have opposite signs. Consequently, in the case of direct mass hierarchy, $m_3>m_2$, resonance will occur in the antineutrino channel $\bar{\nu}_\mu-\bar{\nu}_\tau$.

The diagonal elements of $\hat{H},H_\alpha=(M_\alpha^2/2k)+W_\alpha(\rho)$ are linear functions of ρ, and, when the degree of mixing Φ is small, their crossing (Fig. 11) determines the resonances in the three-neutrino system:

$$H_e(\rho_R^l)=H_\mu(\rho_R^l),\quad H_e(\rho_R^h)=H_\tau(\rho_R^h),\quad H_\mu(\rho_R^{\mu\tau})=H_\tau(\rho_R^{\mu\tau}), \tag{4.5}$$

where ρ_R^l, ρ_R^h, and $\rho_R^{\mu\tau}$ (the corresponding resonance densities) are called the lower, higher, and $\mu\tau$-resonance densities.

There are three resonances in the 3ν-system.[9] The $H_\alpha(\rho)$ are the asymptotes for the energy levels H_i^d as $|\rho|\to\infty$.

For the mass hierarchy $M_e^2\ll M_\mu^2\ll M_\tau^2$, the resonances (4.5) are separated:

$$\rho_R^l:\rho_R^h:|\rho_R^{\mu\tau}|\approx M_\mu^2:M_\tau^2:W_cM_\tau^2(W_\tau-W_\mu)^{-1}\approx m_2^2:m_3^2:2\cdot10^4m_3^2. \tag{4.6}$$

The l- and h-resonances lie in the neutrino half-plane (Fig. 11) and the $\mu\tau$-resonance in the antineutrino plane. (When $W_\mu-W_\tau>0$, all three crossings occur for $\rho>0$.)

Let us now introduce the intermediate densities $\tilde{\rho}$ and ρ' so that $\rho_R^l\ll\tilde{\rho}\ll\rho_R^h\ll\rho'\ll\rho_R^{\mu\tau}$, assuming, for example, that $\tilde{\rho}=(\rho_R^l\rho_R^h)^{1/2}$ and $\rho'=(\rho_R^h|\rho_R^{\mu\tau}|)^{1/2}$. The density intervals $0-\tilde{\rho},\tilde{\rho}-\rho'$, and $\rho>\rho'$ are called the lower, higher, and $\mu\tau$-resonance regions.

The mixing angles Φ_m depend on the density and, as ρ varies, the eigenstate basis rotates in flavor space. General expressions for $\Phi_m(\rho)$ are obtained in Ref. 5. They become

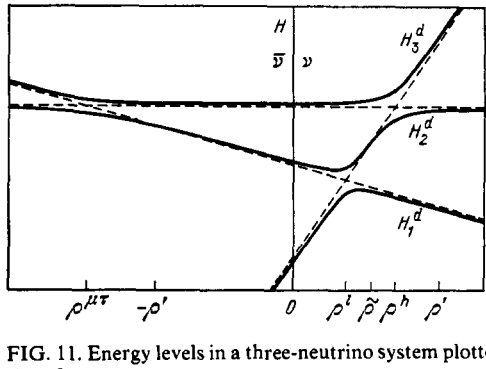

FIG. 11. Energy levels in a three-neutrino system plotted against the density of matter.

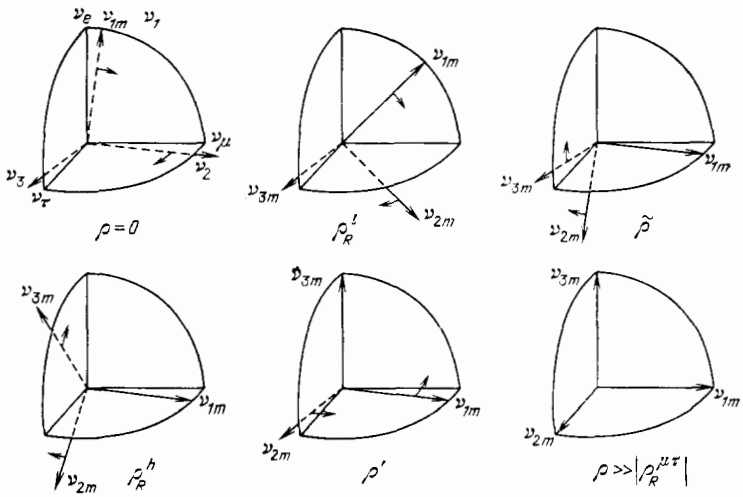

FIG. 12. Mixing in a three-neutrino system as a function of the density of matter.

significantly simpler near resonances[39] and in the first order in the sines of the vacuum mixing angles.[40,42] Figure 12 illustrates qualitatively the rotation of the basis $\{\nu_{im}\}$ for small vacuum mixing.[43] As ρ increases from 0, $\{\nu_m\}$ rotates first in a plane near (ν_e,ν_μ) (the region of the l-resonance), then in (ν_e,ν_τ) (the region of the h-resonance) and, finally, in (ν_μ,ν_τ). For densities much greater than all the resonance values, the eigenstates ν_{im} have pure flavors and mixing is suppressed.

4.2.2. ν-oscillations in the adiabatic regime. In the case of mass hierarchy, the adiabatic condition splits into the following three conditions for each of the resonances separately: $\dot{\omega}_m |H_1^d - H_2^d|^{-1} \ll 1$, $\dot{\psi}_m |H_2^d - H_3^d|^{-1} \ll 1$, $\dot{\varphi}_m |H_1^d - H_3^d|^{-1} \ll 1$. As in the 2ν-case, the ν_{im} propagate independently, there are no $\nu_{im} \leftrightarrow \nu_{jm}$ $(i \neq j)$ transformations, and the ν_{im} impurities in $\nu(t)$ are conserved. The expressions for the oscillators transformation probabilities $(P_{\alpha\beta})$ are direct generalizations of the corresponding expressions in the 2ν case:

$$P_{\alpha\beta} = \bar{P}_{\alpha\beta} + \frac{1}{2} \sum_{i>j} A_{pij}^{(\alpha\beta)} \cos(\varphi_i - \varphi_j),$$

where the average probability is

$$\bar{P}_{\alpha\beta} = \sum_i |S_m(\rho_0)_{\alpha i} S_m(\rho_t)_{\beta i}|^2,$$

the oscillation depths are

$$A_{pij}^{(\alpha\beta)} = S_m(\rho_0)_{\alpha i} S_m(\rho_0)_{\alpha j} S_m^+(\rho_t)_{i\beta} S_m^+(\rho_t)_{j\beta},$$

and the phases are

$$\varphi_i = \int_0^t H_i^d(t)\, dt'.$$

$\bar{P}$ and A_p are functions of the instantaneous values of density at the beginning (ρ_0) and at the end (ρ_t) of the evolution process, and do not depend on the density distribution at intermediate times. It follows that dynamics reduces to "geomerty," i.e., to the determination of mixing for $\rho = \rho_0$ and $\rho = \rho_t$. The characteristics of the oscillations can be obtained graphically.[43,44] The initial state $\nu(0)$ fixes in the basis $\{\nu_{im}\}$ the positions ν_R of the vector $\nu(t)$ for which it crosses the "real" volume (Fig. 13). The components of $\nu(t)$ in this volume at an arbitrary time lie within the tetragonal pyramid formed by the ν_R. The shape of the pyramid remains unaltered in the course of neutrino evolution, but the pyramid rotates in flavor space together with the basis $\{\nu_m\}$. The motion of $\nu(t)$ is "frozen into" the basis $\{\nu_m\}$. When the initial state is identical with one of the eigenstates ν_{im}, the pyramid degenerates into a unit segment. This is accompanied by a nonoscillatory transformation, in accordance with the change in the flavor of the particular eigenstate. The system remains in a particular energy level H_i^d during the evolution process. The graphical representation can be used to draw the following conclusions.[42,43,44]

A) During successive crossing of the two resonance regions, the maximum suppression of neutrinos of the original type is proportional to the square of the sine of the mixing angle in vacuum, $P \sim \sin^2\Phi$, and not to the fourth power of this quantity, as one would expect[10,39] on the assumption of factorization (i.e., $P = P_{e\to e}^h P_{e\to e}^l \sim \sin^2 w \sin^2 \varphi = \sin^4 \Phi$). Actually, if ν_e is created at $\rho_0 = \rho'$, then in accordance with Fig. 12, $\nu(0) = \nu_e \sim \nu_{3m}(\rho_0)$ and, in the final state corresponding to $\rho = 0$, $\nu_f \simeq \nu_{3m}(0) = \nu_3 \simeq \nu_\tau + s_\psi \nu_\mu + s_\varphi \nu_e$, i.e., ν_e is transformed mostly into ν_τ, and the probability of its remaining in the original state is $P_{e-e} \simeq s_\varphi^2$.

B) The type of transition (final-state flavor) depends on the initial density: ν_e created in the layer with $\rho_0 = \rho'$ transform mostly into ν_τ, ν_e, whereas ν_e created at $\rho_0 = \tilde{\rho}$ transform into ν_μ.

C) The type of transition depends on the direction of the change in density. ν_e transform into ν_τ if the density varies from ρ' to 0, and ν_e transform into ν_μ if the density varies in the reverse direction (from 0 to ρ') (see also Refs. 42, 82, 83).

4.2.3. Reduction of the three-particle to the two-particle problem.[10,39,43,44] The problem becomes much more compli-

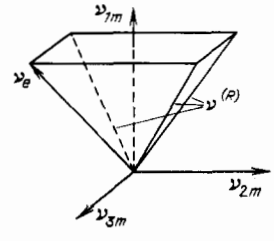

FIG. 13. Graphical determination of the parameters of ν-oscillations of the three-neutrino system in the adiabatic regime.

cated in the general case, which includes departure from adiabaticity. However, if the neutrino mass spectrum has a hierarchy, then evolution in the 3ν-system can be reduced to evolution in the 2ν-system in certain particular density intervals. Accordingly, the 3ν-transition can be expressed in terms of the probabilities discussed above for 2ν-transitions.

Reduction of the 3ν-problem to the 2ν-problem in a given density interval $\Delta\rho$ means that, in this particular interval, we can introduce neutrino states $\nu^{\Delta\rho}$ (combinations of the original ν_f) such that

$$\nu_f = \hat{O}\nu^{\Delta\rho}, \tag{4.7}$$

and the system of three equations can be separated relative to these states. Two equations for two of the $\nu^{\Delta\rho}$ remain coupled, but the equation for the third $\nu^{\Delta\rho}$ turns out to be independent.

Strict decoupling of the system does not occur in a varying-density medium. The original evolution matrix $\hat{H}$ can be reduced to $(2\times 2+1)$ blocks $\hat{H}\to\hat{H}_b$ using ρ-dependent $\hat{O}^{\Delta\rho}$, i.e., $\hat{O}^{\Delta\rho}=\hat{O}^{\Delta\rho}[\rho(t)]$: $\hat{H}_b^{\Delta\rho}=\hat{O}^{+}\hat{H}\hat{O}$. However, the set of equations for $\nu^{\Delta\rho}$ then acquires the additional term $-\hat{O}^{+}\mathrm{d}\hat{O}/\mathrm{d}t$, which prevents decoupling:

$$i\dot{\nu}^{\Delta\rho}=\left(\hat{H}_b^{\Delta\rho}-i\hat{O}^{+}\frac{\mathrm{d}\hat{O}}{\mathrm{d}i}\right)\nu^{\Delta\rho}.$$

Hence, the condition for the approximate decoupling of $\nu_\alpha^{\Delta\rho}$ is

$$\left(\hat{O}^{+}\frac{\mathrm{d}\hat{O}}{\mathrm{d}t}\right)_{\alpha\beta}\ll(\hat{H}_b^{\Delta\rho})_{\alpha\alpha}-(\hat{H}_b^{\Delta\rho})_{\beta\beta},\quad \beta\neq\alpha,$$

where $(\hat{H}_b^{\Delta\rho})_{\alpha\alpha}$ are the diagonal elements of the matrix H_b. This condition is obviously identical with the adiabatic condition for the $\nu_\alpha^{\Delta\rho}$. We note in this connection that complete decoupling of the system occurs in the adiabatic regime, and $\nu_i^{\Delta\rho}=\nu_{im}$. Since the adiabatic condition is particulary critical at resonance, and becomes weaker with distance from the resonance, there will be a decoupling from the neutrino for which resonances lie outside the interval $\Delta\rho$ and far enough from it. Clearly, this situation occurs in the case of mass hierarchy when $\rho_R^l\ll\rho_R^h\ll|\rho_R^{\mu\tau}|$.

If, for a given ν_α, the resonances lie far outside the interval $\Delta\rho$, the variation of $\hat{O}^{\Delta\rho}(\rho)$ with ρ within $\Delta\rho$ will be small, and $\hat{O}^{\Delta\rho}$ can be regarded as a constant. The terms $i\hat{O}^{+}\mathrm{d}\hat{O}/\mathrm{d}t$ are then absent, but the $2\times 2+1$ block structure of $\hat{H}^{\Delta\rho}$ is reached only for a single value of ρ, while, at other points in $\Delta\rho$, it will be modified. The decoupling condition is then that the modification in $\Delta\rho$ must be small.

In the region of the lower resonance ($\rho=0-\tilde{\rho}$), the degree of freedom associated mostly with the heaviest neutrino (ν_3) is decoupled:

$$\hat{O}^l=\hat{U}_7(\psi)\hat{U}_5(\varphi), \tag{4.8}$$

where ψ and φ are the vacuum mixing angles. Using the explicit form of the evolution matrix for $\nu^l=\hat{O}^{l-1}\nu_f$, i.e., $\hat{H}^l=\hat{O}^{l+}\hat{H}\hat{O}^l$, we find[39,33,44] that ν_e^l and ν_μ^l form a 2ν-system with the mixing angle, the difference between mass squared, and the interaction matrix, respectively given by

$$\theta=\omega,\quad \Delta m^2\approx m_2^2,\quad \hat{W}^l=\mathrm{diag}\,(W\cos^2\varphi,\ 0), \tag{4.9}$$

and the state ν_τ^l is decoupled.

In the region of the higher resonance ($\tilde{\rho}-\rho'$), the degree of freedom associated preferentially with ν_2 is "frozen":

$$\hat{O}^h=\hat{U}_7(\psi). \tag{4.10}$$

The states $\nu_e^h=\nu_e$ and ν_τ^h ($\nu^h=\hat{O}^{h-1}\nu_f$) from a 2ν-system with the parameters

$$\theta=\varphi,\quad \Delta m^2\approx m_3^2,\quad \hat{W}^h=\mathrm{diag}\,(W,\ 0), \tag{4.11}$$

and the state ν_μ^h is decoupled.

The strongest modification of the $2\times 2+1$ structure in both cases occurs on the boundary between the regions for $\rho=\tilde{\rho}$ (Refs. 43 and 44). It can be characterized by additional angles of rotation $\Delta\hat{O}^l(\tilde{\rho})$, $\Delta\hat{O}^h(\tilde{\rho})$, which restore the $2\times 2+1$ form of the matrix $\hat{H}^{\Delta\rho}$:

$$\sin 2\Delta\varphi\approx\sin 2\varphi\cdot\tilde{\rho}\,(\rho_R^h)^{-1}\approx\sin 2\varphi\cdot m_2m_3^{-1}, \tag{4.12}$$

$$\sin 2\Delta\omega\approx\sin 2\omega\cdot\rho_R^l\tilde{\rho}^{-1}\approx\sin 2\omega\cdot m_2m_3^{-1}. \tag{4.13}$$

The parameters $\sin 2\Delta\varphi$ and $\sin 2\Delta\omega$ are the uncertainties in the transition amplitudes due to the reduction of the 3ν problem to the 2ν problem. In the case of mass hierarchy ($m_2\ll m_3$), $\Delta\varphi$, $\Delta\omega$, the block structure modification, and, hence, the above uncertainties, are all small, even for large vacuum mixing angles.

We note in conclusion that the $\mu\tau$-resonance lies in the $\bar{\nu}$-channel, and has practically no effect on the above l- and h-resonances.

4.2.4. Probabilities of oscillatory transformations in the 3ν-system. The probability amplitude for the oscillatory transformation $\nu_\alpha-\nu_\beta$ as the neutrino beam crosses the upper ($\rho_0\sim\tilde{\rho}$) and then the lower ($\tilde{\rho}-\rho_f$) resonances is

$$A_{\alpha\beta}=\langle\nu_\beta\mid\hat{H}\mid\nu_\alpha\rangle$$

$$=\mathrm{V}_\beta^{\mathrm{T}}\hat{U}_7\hat{U}_5[\hat{A}^l(\rho_f,\ \tilde{\rho})]^{\mathrm{T}}\hat{U}_5^{\mathrm{T}}[\hat{A}^h(\tilde{\rho},\ \rho_0)]^{\mathrm{T}}\hat{U}_7^{\mathrm{T}}\mathrm{V}_\alpha, \tag{4.14}$$

where V_α and V_β are the vectors in flavor space $\{\nu_e,\nu_\mu,\nu_\tau\}$ that determine the initial and final states: for ν_e, for example, $V_e=(1,0,0)$, and so on. The structure of (4.14) is as follows.

A) The matrix $\hat{U}_7^{\mathrm{T}}$ performs the decomposition of the initial state into the ν_α^h-states that decouple the system in the region of the h-resonance (4.10).

B) $\hat{A}^h(\tilde{\rho},\rho_0)$ is the transformation matrix for the region of the h-resonance:

$$\hat{A}^h=\begin{vmatrix} A_e^{h(e)} & 0 & A_\tau^{h(e)}\\ 0 & A_\mu^{h(\mu)} & 0\\ A_e^{h(\tau)} & 0 & A_\tau^{h(\tau)}\end{vmatrix}, \tag{4.15}$$

where $A_\beta^{h(\alpha)}(\rho_0,\tilde{\rho})$ is the $\nu_\alpha^h\to\nu_\beta^h$ transformation amplitude for propagation between ρ_0 and $\tilde{\rho}$; the elements $A_\beta^{h(\alpha)}$ ($\alpha,\beta=e,\tau$) are determined by the dynamics of the 2ν-oscillations, and satisfy (2.16).

C) The matrix $\hat{U}_5^{\mathrm{T}}$ gives the decomposition of the ν-state on the boundary between the h- and l-resonances into the states ν_α^l that decouples the set of equations in the region of the lower resonance [actually, it follows from (4.8) and (4.10) that $\nu^l=\hat{U}_5^{\mathrm{T}}\nu^h$].

D) $\hat{A}^l(\rho_f,\tilde{\rho})$ is the transformation matrix in the region of the lower resonance:

$$\hat{A}^l=\begin{vmatrix} A_e^{l(e)} & A_\mu^{l(e)} & 0\\ A_e^{l(\mu)} & A_\mu^{l(\mu)} & 0\\ 0 & 0 & A_\tau^{l(\tau)}\end{vmatrix}, \tag{4.16}$$

where $A_\beta^{l(\alpha)}$ ($\alpha, \beta = e, \mu$) satisfy (2.16).

E) The matrix $\hat{U}_7 \cdot \hat{U}_5$ performs the decomposition of the ν-state at exit into the basis of states with definite flavors.

When the neutrino is created and propagates only in the region of the lower (higher) resonance, we must substitute $\hat{A}^h = \hat{1}$ ($\hat{A}^e = \hat{1}$) in (4.14). When the neutrino propagates in the direction of increasing density, the matrix between V_α and V_β in (4.14) must be transposed.

In accordance with (4.14), the amplitude for the transformation $\nu_e \to \nu_e$ is

$$A_{e-e} = A_e^{l(e)}(c_\varphi^2 A_e^{h(e)} - s_\varphi c_\varphi A_\tau^{h(e)}) + A_\tau^{l(\tau)}(s_\varphi^2 A_e^{h(e)} + s_\varphi c_\varphi A_\tau^{h(e)}) \tag{4.17}$$

($s_\varphi \equiv \sin\varphi$, $c_\varphi \equiv \cos\varphi$, and so on). Hence, the probability averaged over the period is $\overline{P} = P^l P^h + K$, and

$$K = P^l P^h(-3s_\varphi^2 + 2s_\varphi^4) + s_\varphi^2 c_\varphi^2 + s_\varphi^2 c_\varphi^2 P^l - (s_\varphi^2 c_\varphi^2 - s_\varphi^4) P^h - 2s_\varphi c_\varphi^3 P^l R^h + 2s_\varphi^3 c_\varphi R^h, \tag{4.18}$$

where, for small φ,

$$K = s_\varphi^2(1 + P^l - P^h - 3P^l P^h - 2P^l R^h(s_\varphi^{-1})); \tag{4.19}$$

and $P^l = |A_e^{l(e)}|$ and $P^h = |A_e^{h(e)}|^2$ are the probabilities of 2ν-transformations in the region of the l- and h-resonances; $R^h = \mathrm{Re}(A_e^{h(e)*} A_\tau^{h(e)})$ is the interference term that can be expressed in terms of P^h with the aid of the equations for the probabilities: $R^h = \{\dot{P}^h/\overline{H}) + \overline{H}[P^h - (1/2)]\}/H$ (2.19). In the adiabatic regime: $R^h = -n_0(n_0^2+1)^{-1/2}(n^2+1)^{-1/2}$. When $n \gg 1$, this yields $R^h = -\tan 2\varphi(1-2P^h)/2$. We also have the estimate $|R^h| \leqslant [P^h(1-P^h)]^{1/2}$. The factorized term in (4.18), (4.19), i.e., $P^l P^h$, corresponds to successive $\nu_e \to \nu_e$ transformations in the region of the higher and lower resonances. The term that upsets the factorization of K is due to the fact that the states that decouple the set of equations are not the same as the states with definite flavors. The complete $\nu_e \to \nu_e$ transformation is accomplished not only through ν_e at $\rho = \bar{\rho}$, but also through ν_τ: $\nu_e \to \nu_\tau \to \nu_e$. K contains the factor $\sin^2\varphi$. When P^l and P^h are appreciably greater than $\sin^2\varphi$, the factorized term reproduces the total probability with sufficient precision. When P^l and/or P^h are at the level of maximum suppression, K is of the order of $P^l P^h$. When both factors P^l and P^h are small, K provides the dominant contribution: $P \simeq \sin^2\varphi$.

Similarly, we can obtain the probabilities of $\nu_\mu \to \nu_e$ and $\nu_\tau \to \nu_e$ transformations: $P_{\mu\to e} = (1-P^l) + O(s_\Phi^2)$, $P_{\tau\to e} = P^l(1-P^h) + O(s_\Phi^2)$.[43]

4.3. Oscillations into sterile states

The picture of the oscillations $\nu_f \leftrightarrow \nu_s$ ($f = e, \mu, \tau$) is the same as in the case of oscillations in flavors. The difference between them reduces to a change in the refraction length l_0. In general,

$$l_0 = 2\pi m_N(\sqrt{2}G_F\rho\sum_i A_i Y_i)^{-1}, \tag{4.20}$$

where A_i is the difference between the scattering amplitudes of the oscillating neutrinos in an i-component medium (in units of $\sqrt{2}G_F k$) and Y_i is the number of particles of type i per nucleon. The length l_0 is determined by the sum $\Sigma_i A_i Y_i$. For the $\nu_e - \nu_\mu$ oscillations, $A_e = 1$ and $\Sigma_i A_i Y_i = Y_e$. A sterile neutrino has no weak interactions, so that the difference $\Delta\Sigma_i [f_i(0) N_i]$ arises from the scattering of the ν_f by all the components of the medium, which is due to both charged and neutral currents. For the $\nu_e \leftrightarrow \nu_s$ oscillations in an electrically neutral medium ($Y_e = Y_p$),[16] we have

$$\sum_i A_i Y_i = Y_p - \frac{1}{2} Y_n. \tag{4.21}$$

Hence, for a medium consisting mostly of hydrogen ($Y_n \ll Y_p$), we have $\Sigma_i A_i Y_i = Y_p = Y_e$, so that the $\nu_e - \nu_s$ and $\nu_e - \nu_\mu$ refraction lengths are equal ($l_0^{es} = l_0^{\mu e}$). In an isotopically neutral medium ($Y_n = Y_p$), we have $\Sigma_i A_i Y_i = Y_e/2$, and $l_0^{es} = 2l_0^{\mu e}$. For a medium consisting mostly of neutrons, the sum $\Sigma_i A_i Y_i = -Y_n/2$ changes sign, and l_0^{es} may be much smaller than $l_0^{\mu e}$.

The differences between the interactions of ν_μ (ν_τ) and ν_s in an electrically neutral medium are due to ν-scattering by neutrons and are such that $\Sigma_i A_i Y_i = -Y_n/2$. The contributions of neutrons and protons then cancel out.

Let us now introduce the effective density

$$\rho^{eff} = \rho\sum_i A_i Y_i,$$

so that $l_0 = 2\pi m_N(\sqrt{2}G_F\rho^{eff})^{-1}$. The analysis given above for the $\nu_e \to \nu_\mu$ oscillations can be extended to other channels in terms of ρ^{eff} without change. The specificity of particular channels is then represented by ρ^{eff}.

4.4. Effect of inelastic neutrino scattering and absorption on oscillations[44]

The effects of inelastic interactions and of absorption in the direct wave are described by the imaginary part of the scattering amplitude Im $f(0)$. Correspondingly, the diagonal elements of the evolution matrix acquire imaginary parts:

$$H_\alpha = H_\alpha^R + iH_\alpha^I = M_\alpha^2(2k)^{-1} + W_\alpha^R + iW_\alpha^I \quad (\alpha = e, \mu);$$

where $W_\alpha^I = \Sigma_i \mathrm{Im} f_i^\alpha(0) N_i k^{-1}$ and W_α^R is equal to the quantity W_α, discussed earlier in (2.11). Using the optical theorem, we obtain

$$W_\alpha^I(W_\alpha^R)^{-1} \approx G_F s\cdot(2\pi)^{-2}, \tag{4.22}$$

where s is the square of the total energy in the center-of-mass system. The difference $W_e^R - W_\mu^R$ between the real parts and the imaginary parts W_α^I determine the refraction length l_0 and the mean free path l_a, respectively, and, since $W_e^R - W_\mu^R \simeq W_e^R$, we find from (4.22) that $l_0/l_a \simeq W^I/W^R \simeq G_F s/4\pi^2$. Hence, it follows that the ratio of l_0 to l_a is determined by the neutrino energy, and is independent of the density of the medium, where, for low energies $s \ll G_F^{-1}$, the refraction length is much smaller than the mean free path ($l_0 \ll l_a$). Since $W_e^I \neq W_\mu^I$, absorption not only reduces the intensity of the ν_e and ν_μ waves, but also modifies the oscillation picture. When absorption is taken into account, $\hat{H}$ is diagonalized by the matrix $\hat{S}(\theta_{ab})$ which has complex diagonal elements: $\cos\theta_m$ in $\hat{S}(\theta_m)$ must be replaced with $\cos\theta_{ab}\exp(i\varphi)$. We then have $\tan 2\theta_{ab} = \tan 2\theta_m \cdot \cos\varphi$, and $\sin\varphi = -(W_e^I - W_\mu^I)\sin 2\theta_m/\overline{H}$. According to (4.22), φ is small at low energies: $\sin\varphi \simeq Gs/4\pi^2$. In the lowest order in φ, the parameters of adiabatic oscillations are $\overline{P} = e^{-\lambda}(e^{-\Delta\lambda}\cos^2\theta_m^0\cos^2\theta_m + e^{\Delta\lambda}\sin^2\theta_m^0 \times \sin^2\theta_m)$, $A_p = e^{-\lambda}\sin 2\theta_m^0 \cdot \sin 2\theta_m$, where

$$\lambda = -\int_0^t (W_e^I + W_\mu^I)\,dt', \quad \Delta\lambda = -\int_0^t (W_e^I - W_\mu^I)\cos 2\theta_m\,dt'$$

[cf. (3.35)]. The average probability is thus a combination of two exponentials, the oscillation depth decreases with time more rapidly than A_p, and universality is lost.

In specific applications (cores of collapsing stars or early Universe), the oscillatory transformations must be taken into account both in the incident and scattered waves. For small s, when $l_m \sim l_0 \ll l_a$, we use the following picture: 1) the oscillatory transformations occur between two successive inelastic collisions and 2) the coherence of the ν-state is disturbed in each such collision, and noncoherent neutrino fluxes with fixed flavors, that were present in ν at the point of collision, begin to oscillate. The resultant oscillation effect is determined by the ratio of the mean free path l_a the width of the resonance layer $\Delta r_R = \rho(d\rho/dr)^{-1}\tan 2\theta$, and the dimensions of the object itself. (We shall assume that the adiabatic condition is satisfied: $l_m^R < \Delta r_R$.) When $\Delta r_R \ll l_a$ and $R \gtrsim l_\alpha$, strong oscillatory transformations occur in the ν-beam in the region of the resonance, and a small number of collisions ($R \gtrsim l_a$) will not lead to averaging.

When $\Delta r_R \gtrsim l_a$ (the density changes little over one mean free path), strong oscillatory transformations will not occur.

When $R \gg l_a$, a large number of purely inelastic collisions will lead to the averaging of the probability, $\bar{P} \to 1/2$, even for small mixing, and $\Delta r_R \ll l_a$.

Suppose that a neutrino passing through a layer of matter undergoes k inelastic collisions, in which case the probability of an oscillatory transition in the layer is[44]

$$P_k = \frac{1}{2}\left(1 + \tilde{n}_0\tilde{n}_f\prod_{i=1}^{k}\tilde{n}_i^2\right), \tag{4.23}$$

where $\tilde{n} \equiv n(n^2+1)^{-1/2}$, $n = (\rho - \rho_R)/\Delta\rho_R$, and $\tilde{n}_0, \tilde{n}_f$, and $\tilde{n}_i$ are the values of $\tilde{n}$ at the point of creation of the neutrino, at exit from the layer, and at the point of the ith collision, respectively.[10] We note that $\tilde{n}_i^2 < 1$, so that $P_k \to 1/2$ as $k \to \infty$. If at least one of these collisions occurs in the resonance layer, we have $\tilde{n} = 0$ and $P_k = 1/2$. The product in (4.23) can be estimated as follows. Consider a layer near the resonance layer of width $r_a < l_a$. The probability of a collision in this layer is $P_{col} < 1$, i.e., neutrinos pass through without collision. On the boundary of the layer, we have $n = n_a \simeq \mu_a/\rho_R\Delta r_R$, where $\mu_a = \rho_R l_a$. Since $\tilde{n}$ increases with distance from resonance (we are assuming that the density varies monotonically with r), we can write

$$\prod_{i=1}^{k}\tilde{n}_i^2 \geqslant (\tilde{n}_a^2)^k = (1 + n_a^{-2})^{-k} = [1 + (\rho_R\Delta r_R)^2\mu_a^{-2}]^{-k}. \tag{4.24}$$

Hence, the effect of inelastic collisions is small if the number of collisions is

$$k \ll \mu_a^2(\rho_R\Delta r_R)^{-2} \approx l_a^2(\Delta r_R)^{-2}. \tag{4.25}$$

Since $\Delta r_R \sim \tan 2\theta$, (4.27) yields the upper bound for the vacuum mixing angle. Averaging occurs for $k > (\mu_a/\rho_R\Delta r_R)^2$ and $\bar{P} \simeq 1/2$.

4.5. Medium containing relativistic particles[44]

This situation occurs in the cores of collapsing stars and in the early Universe. The effect of the medium is determined by the product $(f/k)N$, where N is the particle number density. Transforming to the reference frame in which the target particles are at rest, and using the Lorentz invariance of the phase acquired by the waves along the path between two given points (or the invariance of the oscillation depth), it may be shown that

$$\langle\langle N f k^{-1}\rangle\rangle = N f k^{-1}(1 + v\cos\theta), \tag{4.26}$$

where v is the velocity, $n(v)$ is the target-particle density, and θ is the angle between the direction of motion and the neutrino momentum ($\mathbf{k}$). The ratio f/k then has the same form as for a target at rest. For an isotropic distribution of target particles, the second term in (4.26) vanishes after integration with respect to θ and "Nf"$/k$ is found to be the same as for $v = 0$. The quantity N in the resulting expression is the total particle-number density in the target in the laboratory frame.

5. APPLICATIONS OF NEUTRINO OSCILLATIONS IN MATTER

Strong oscillatory neutrino transformations in matter[11] occur when the following conditions are satisfied.

1) The resonance conditions: the neutrino must cross the resonance layer.

2) The adiabaticity conditions, or the conditions for weak departure from adiabaticity. Here, the density must vary sufficiently slowly with distance.

In addition:

3) The thickness of the medium must be large enough.

4) The medium must be asymmetric with respect to the oscillating components; the particle and antiparticle number densities must be different.

5) The initial fluxes of oscillating neutrinos must be different.

6) The number of inelastic collisions must be small.

In this type of medium, resonance and, hence, strong transformations, occur either for the neutrino or the antineutrino.

The conditions enumerated above are satisfied for particular values of neutrino parameters (Δm^2, $\sin^2 2\theta$) in the Sun, the Earth, the cores and envelopes of collapsing stars, and the early Universe.

5.1. Oscillation suppression factors in the Sun

5.1.1. Physical conditions. The picture of ν-oscillations depends on 1) the density distribution in the medium, 2) the distribution of neutrino sources, and 3) the conditions governing neutrino generation, i.e., the type of nuclear interaction and the parameters of the medium at the point at which the neutrinos are created. We shall use these parameters in accordance with the standard solar model (SSM)[46] (Fig. 14).

The maximum (central) density ρ_c determines the upper boundary of the resonance region on the $\Delta m^2/E \equiv 1/y$, $\sin^2 2\theta$ diagram [see (3.7)]:

$$\left(\frac{\Delta m^2}{E}\right)_c = \frac{1}{y_c} \equiv \rho_c^{eff}\,\frac{\sqrt{2}\,G_F}{m_N\cos 2\theta} \approx \frac{2\cdot 10^{-5}}{\cos 2\theta}\,\frac{eV^2}{MeV}. \tag{5.1}$$

When θ is small, this boundary is practically independent of $\sin^2 2\theta$ (Fig. 15). For a neutrino with $\Delta m^2/E > (\Delta m^2/E)_0$, there is no resonance. When $\Delta m^2/E = (\Delta m^2/E)_0$, there is a resonance at the center of the Sun. As $\Delta m^2/E$ decreases, the resonance layer shifts from the center toward the surface.

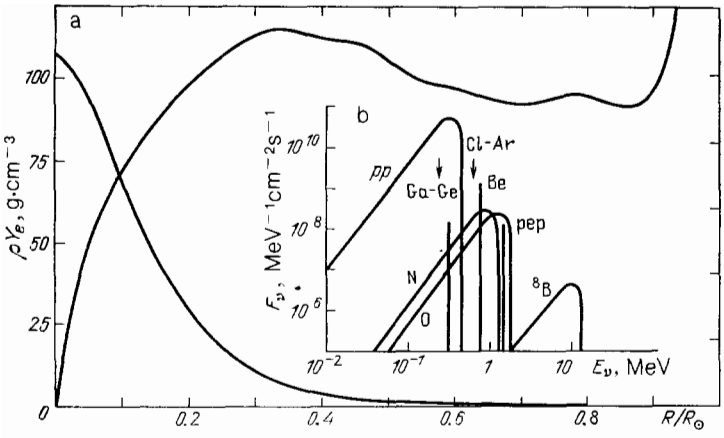

FIG. 14. a—Distribution of density ρ and of its gradient $d\rho/dr$ in the Sun, b—spectrum of solar neutrinos.

The boundary of the adiabatic region on the $\Delta m^2/E$, $\sin^2 2\theta$ diagram follows from (3.34), (3.32), and (3.33):

$$\frac{\sin^2 2\theta}{\cos 2\theta} = 2\pi \left(\frac{1}{\rho}\frac{d\rho}{dr}\right)_{\rho=\rho_R} \frac{1}{\Delta m^2/E}, \qquad (5.2)$$

where $\rho_R = \rho_R(\Delta m^2/E, \cos 2\theta)$ (Fig. 15). In the wide range $\rho = 0.02$–90 g/cm^3, the distribution $\rho(r)$ is exponential, $\rho(d\rho/dr)^{-1} = h = \text{const}$, and (5.2) assumes the simpler form

$$\sin^2 2\theta = \frac{2\pi}{h\Delta m^2/E} = \frac{1.8\cdot 10^{-8}}{(\Delta m^2/E)(\text{eV}^2/\text{MeV})}. \qquad (5.3)$$

Equations (5.2) and (5.3) determine the lower boundary of the adiabatic region. As $\Delta m^2/E$ decreases (for fixed θ), the spatial width of the resonance layer, $\Delta r_R \simeq h \tan 2\theta$, remains practically constant and the resonance oscillation length increases, $l_m^R \sim E/\Delta m^2$, so that (3.34) ceases to be valid.

In the region on the $\Delta m^2/E$, $\sin^2 2\theta$ diagram below the boundary (5.3), the conditions for the validity of the Landau-Zener result (3.49) and (3.50) are satisfied for $\sin^2 2\theta < 0.1$ and $\Delta m^2/E \lesssim (\Delta m^2/E)_0/2$: the width of the resonance layer is $\Delta r_R \simeq h \tan 2\theta \ll h$ and we can use a linear approximation for $\rho(r)$. The transition probabilities now depend on the combination $(\Delta m^2/E)\sin^2 2\theta$ and increase with distance from the boundary (5.3). The "triangle" formed by (5.1), (5.3), and $\sin^2 2\theta = 0.1$–0.2 is the region of strongest oscillatory transitions in the Sun.

The separation between the wave packets can be estimated as follows: $D(R_\odot) \leqslant |\Delta v_v| R_\odot = (\Delta m^2/2E^2) R_\odot$ [see (4.1)]. Its effects are small when $D(R_\odot)$ is much less than the length τ_ρ of the neutrino packet, for example, $D(R_\odot) \leqslant 10^{-1}\tau_p$. Hence, the upper boundary of the region on the diagram of Fig. 15 in which the separation can be neglected is

$$\frac{\Delta m^2}{E} = \frac{1}{5} E \frac{\tau_p}{R_\odot}. \qquad (5.4)$$

The pp-neutrinos have τ_p of the order of the length of the packets of colliding protons, $\tau_p^{pp} \simeq \tau_p^p$; τ_p^p is, in turn, determined by the time between collisions: $\tau_p^p \simeq v_p \tau_p \simeq 1/\sigma_p n_p$, where n_p is the charged-particle density and σ_p the electromagnetic interaction cross section. Estimates[12] yield $\tau_p^{pp} \simeq 10^{-9}$–$10^{-8}$ cm. For boron neutrinos: $\tau_p^B \simeq c\tau_B$, where τ_B is the time between two collisions with the ^{8}B nucleus: $\tau_p^B \simeq 3\times 10^{-9}$–$3\times 10^{-8}$ cm. The same result is obtained when τ_p is estimated from the temperature dependence: $\tau_p \sim 1/kT \simeq 2\times 10^{-8}$ cm (Fig. 15).

The effects of wave-packet separation increase with increasing $\Delta m^2/E$. Let us determine the boundary of the Δm^2, $\sin^2 2\theta$ region in which complete separation occurs by demanding that the wave-packet overlap vanishes *before* the resonance layer: $D^R(L_R) = \tau_p$, where $L_R(\Delta m^2/E, \sin^2 2\theta)$ is the distance between the center of the Sun and the layer with $\rho = \rho_R$ and D is defined by (4.2) and (4.1) (Fig. 15). According to Fig. 15, wave-packet separation is either complete or partial on most of the region in which there is a strong resonance effect on the Sun, and the separation is greater for pp-neutrinos than for boron neutrinos.[22]

5.1.2. Suppression factors. The oscillatory suppression factor $P_S(E, \Delta m^2, \sin^2 2\theta)$ is defined by

$$F(E) = P_S(E) F^0(E), \qquad (5.5)$$

where F^0 and F are the ν_e fluxes at exit from the Sun, without and with oscillations, respectively. Because of differences between source distributions in space, the factors $P_S^\alpha(E)$ are different for $\nu_e^{(\alpha)}$ neutrinos from different reactions (α = pp, Be, B, ...). The finite size of the region in which the neutrinos are generated and the finite energy resolution of equipment lead to the averaging of the oscillations over their period, and $P_S(E)$ in (4.1) represents the average oscillatory effect.

For a point source of ν_e at the center of the Sun, the suppression factor is equal to the average probability of finding ν_e at exit (see Section 3): $P_S = \bar{P}_{e\to e}(E/\Delta m^2, \sin^2 2\theta)$. Conditions (5.2) and (5.3) for fixed θ then determine the boundary of the adiabatic region in $y = E/\Delta m^2$:

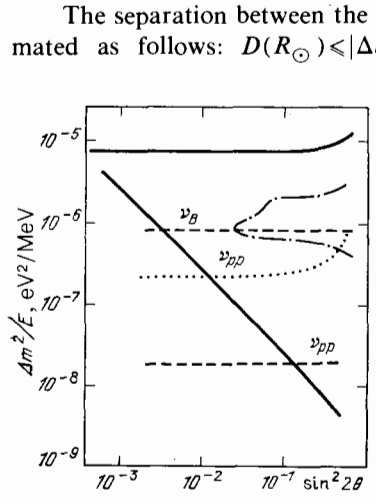

FIG. 15. Boundaries of resonance regions in the Sun, adiabaticity regions (solid lines), and regions of partial (broken lines) and complete (dotted line) separation of wave packets. The figure also shows the resonance region in the Earth (dot-dash line).

$$y_a = \sin^2 2\theta_a \cdot h \cdot (2\pi)^{-1}. \quad (5.6)$$

The adiabatic approximation is valid for $y < y_a$ and it follows from (3.41)[33] that

$$P_S(y, y_0, \theta) \approx \frac{1}{2}\left\{1 - \left(\frac{y}{y_0} - 1\right) \times \cos 2\theta \left[\left(\frac{y}{y_0} - 1\right)^2 + \tan^2 2\theta\right]^{-1}\right\}; \quad (5.7)$$

where y_0 [see (5.1)] is equal to the quantity $E/\Delta m^2$ for which the resonance condition is satisfied at the point of creation of the neutrinos (in this case, at the center of the Sun). For $y > y_a$, the adiabatic condition is violated and, for small mixing angles [$\sin^2 2\theta \simeq (3\times 10^{-3} - 10^{-1})$], we can use the Landau-Zener result.[24,25] In accordance with (3.50) and (3.47),

$$P_S \approx \sin^2\theta + \cos 2\theta \cdot \exp\left(-\frac{\pi}{4}\frac{\sin^2 2\theta}{\cos 2\theta}\frac{h}{y}\right), \quad (5.8)$$

where $h = \rho(d\rho/dr)^{-1}$. This formula is not valid at very small angles such that $\sin^2 2\theta \leqslant 10^{-3}$ and for $y_a \simeq y_0$ for which the creation of the neutrinos occurs near resonance.

The dependence of the suppression factor (5.7), (5.8) on y has the bath-tub shape (Fig. 16a), and the entire interval of y corresponding to a strong effect can be divided into three parts.

A. The region in which the resonance is turned on (adiabatic edge of the bath-tub). When $y \ll y_0$, the resonance density $\rho_R(y)$ is much greater than the central density ρ_c, the effect of the medium is negligible, the oscillation picture is identical with the vacuum picture, and $P = 1 - \sin^2 2\theta/2$ (Fig. 16b). As y approaches y_0, $\rho_R \to \rho_0$, and the medium begins to amplify the oscillations, so that their depth increases and P at exit falls. $y = y_0$ is the point at which resonance is turned on: $\rho_R = \rho_0$ corresponds to the generation of the neutrinos at resonance, the oscillations in the resonance layer occur with maximum depth, and $P(y_0) = 1/2$ (Fig. 16c). For $y > y_0$, $\rho_R < \rho_0$ corresponds to the crossing of the resonance layer by the neutrinos. As y increases, this layer shifts toward the surface of the Sun, the oscillation depth decreases, and P also decreases (Fig. 16d). The width of region A is proportional to $\sin 2\theta$.

B. Region of maximum of suppression (bottom of the bath-tub). For values of y for which $4n_0^2[\rho_R(y)] \gg \sin^{-2}\theta$, the conditions for nonoscillatory transition are satisfied, and $P(y) \simeq \sin^2\theta - [4n_0^2(y)]^{-1} \simeq \sin^2\theta$ (Fig. 16e).

C. The region of departure from adiabaticity ($y > y_a$). The oscillations are now irregular (Fig. 16f) and $P(y)$ increases in accordance with (5.8).

At the vacuum mixing angle decreases, the left-hand edge of the bath-tub does not change its position, but becomes steeper. The bottom descends and the right-hand edge shifts toward lower y: $y_a \sim \sin^2 2\theta$, so that the bath-tubs become narrower. The shape of the right-hand edge does not change between wide limits of $\sin^2 2\theta$ (Fig. 17).

Averaging of the suppression factors over the spatial distribution of neutrino sources reduces the slope of the left-hand (adiabatic) edge of the bath-tub, and the region in which the resonance is turned on expands (see Fig. 17). The reduced slope of the edge is due to the fact that, for given

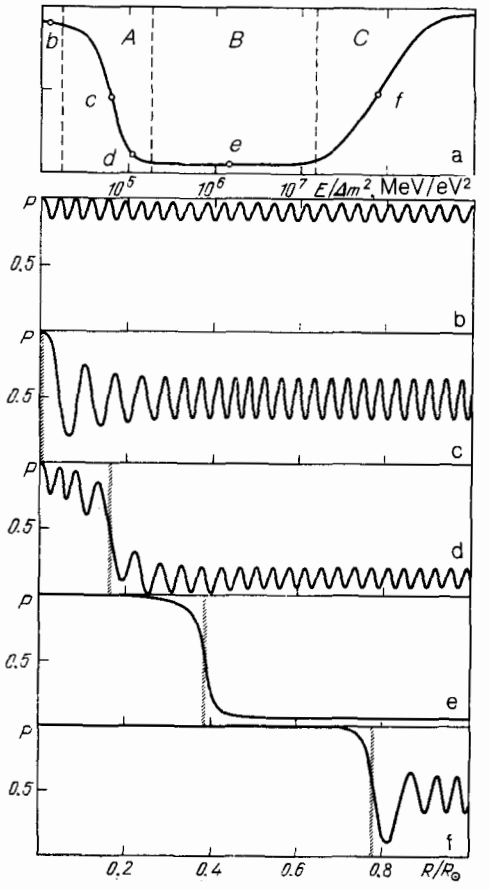

FIG. 16. a—Suppression factor for the ν_e flux in the Sun as a function of $E/\Delta m^2$; b–f—neutrino oscillations with different $E/\Delta m^2$ (the separation of packets is not taken into account and the oscillation period has been increased for the sake of clarity).

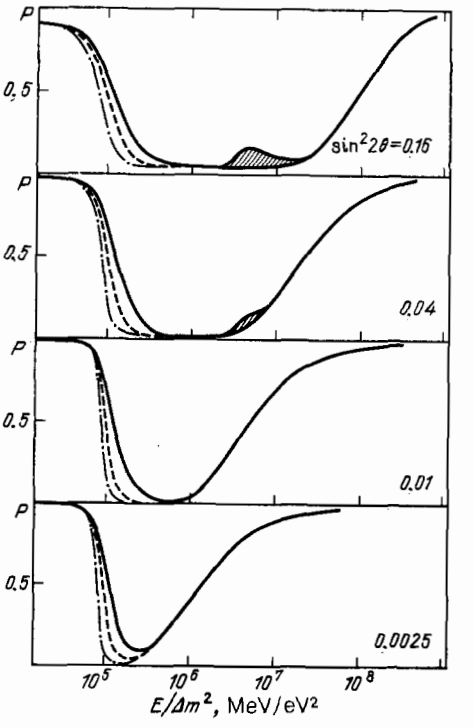

FIG. 17. Suppression factor P in the Sun as a function of $E/\Delta m^2$ for different mixing angles in vacuum with allowance for the finite dimensions of the neutrino sources: pp—solid lines, ^{7}Be—broken lines, ^{8}B—dot-dash lines. The shaded region shows ν_e regeneration in the Earth, averaged over one year.

$y = E/\Delta m^2$, the adiabatic suppression is weaker for ν_e generated for $\rho < \rho_c$ as compared with ν_e created at the center ($\rho = \rho_c$): $P_S[y, y_0(\rho)] > P_S[y, y_0(\rho_c)]$. The maximum averaging effect occurs for the pp-neutrinos for which the dimensions of the generation region are a maximum. The shape of the right-hand edge of the bath-tub for $\sin^2 2\theta > 3 \times 10^{-3}$ remains practically constant. At smaller angles, for which the resonance layer lies near the center, double nonadiabatic crossing of the resonance layer must be taken into account.[25]

5.1.3. Suppression factors in the case of three-neutrino oscillations. When the mass spectrum has a hierarchy, the suppression factors for the 3ν-transitions can be expressed in terms of P^l and P^h, i.e., the suppression factors for 2ν-transitions over the upper and lower resonance regions (4.18), (4.19). P^h and P^l are practicaly equal to the 2ν-factors $P[(E/\Delta m^2), \sin^2 2\theta]$ discussed above. The difference between P^h, P^l and P is due to the presence of the boundary $\tilde{\rho}$ between the resonances, and is negligible in the case of a mass hierarchy.[43,44] According to (4.9) and (4.1),

$$P^l = P(E\cos^2\varphi \cdot m_2^{-2},\ \sin^2 2\omega),$$
$$P^h = P(Em_3^{-2},\ \sin^2 2\varphi) \quad E > \tilde{E},$$

where $\tilde{E}$ is defined by the condition $\tilde{\rho}(\tilde{E}) = \rho_c$. When $E < \tilde{E}$, the upper resonance region is absent, so that $P^h = 1$.

The total suppression factor is a superposition of P^l and P^h. The "bath-tub" $P^h(E)$ is shifted relative to the "bath-tub" $P^l(E)$ to the right, so that its left-hand edge lies at an energy greater by the factor $m_3^2\cos^2\varphi/m_2^2$ than the left edge of P^l (Ref. 10). Depending on the magnitude of $m_3^2\cos^2\varphi/m_2^2$, there are two qualitatively different mutual dispositions of P^l and P^h. They are determined by the ratio of the energy at which the h-resonance is turned on ($E_0^h = y_0 m_3^2$) and the energy E_a^l corresponding to adiabaticity at l-resonance. 1) $E_a^l > E_0^h$. The bath-tub P^h is inscribed[13] into P^l or significantly overlaps P^l. 2) $E_a^l < E_0^h$. The bath-tubs are completely separated and the bottom of P^h does not overlap the bottom of P^l (see Fig. 18b).

In accordance with the general analysis given in Sec. 4.2, the maximum difference between P^3 (4.18), (4.19) and $P^l P^h$ occurs in the region of maximum suppression of both

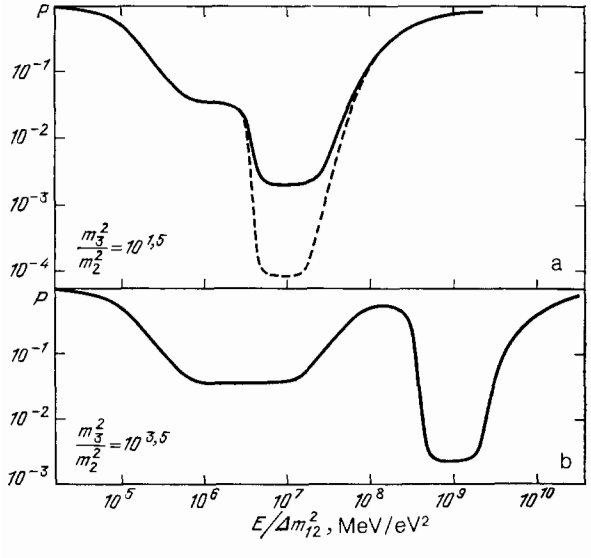

FIG. 18. Suppression factors in the case of three-neutrino oscillations (broken line: $P^l P^h$).

P-factors (Fig. 18a). The product $P^l P^h$ satisfactorily reproduces P^3 whenever P^l and P^h are much greater than their minimal values $\sin^2\omega$ and $\sin^2\varphi$. When $E_a^l \ll E_0^h$, there is practically no overlap between the bath-tubs, and P^3 is equal to either P^l or P^h in the corresponding energy intervals.

5.1.4. Oscillations into sterile neutrinos. The ratio of effective densities ρ^{es} and $\rho^{e\mu}$ is determined by M_{He}, i.e., by the mass abundance of ^{4}He:

$$\frac{\rho^{es}}{\rho^{e\mu}} \approx \frac{Y_e - (Y_n/2)}{Y_e} \approx 1 - \frac{M_{He}}{2(2 - M_{He})}.$$

At the center of the Sun, $M_{He} \simeq 0.65$, so that $\rho^{es}/\rho^{e\mu} \simeq 0.76$. The distribution $\rho^{es}(d\rho^{es}/dr)^{-1}$ is practically the same as the corresponding distribution for the e-μ oscillations. It follows that the only difference between the suppression bath-tubs for $\nu_e - \nu_s$ transitions and the $\nu_e - \nu_\mu$ bath-tubs is that their left-hand edges (determined by the density at the center) are shifted toward higher energies by the factor $\rho_c^{e\mu}/\rho_c^{es} \simeq 1.24$.

5.2. Neutrino oscillations in the Earth [4,8,20,16]

5.2.1. Physical conditions. The density distribution consists of several layers with relatively slow variations of density ρ, separated by a discontinuity (Fig. 19). In the first approximation, there are two intervals: 1) $\rho = 3$–6 g/cm^3 (the mantle) and 2) $\rho = 9$–12 g/cm^3 or (depending on the model) 9–19 g/cm^3 (the core).

The material of the Earth can be regarded, with good precision, as isotopically neutral, so that $Y_e = 1/2$ and the effective density for the ν_e–ν_μ and $\nu_e - \nu_\tau$ oscillations is $\rho_{eff}^{e\mu} = \rho/2$. In accordance with this distribution (see Fig. 19), the region in which the resonance effect occurs [see (5.1)] is $(\Delta m^2/E)_{res} \simeq 2 \times 10^{-7}$–$10^{-6}$ eV^2/MeV. This is much narrower than for the Sun and, in contrast to the Sun, it has a lower limit and lies inside the solar resonance region (Fig. 16). When $\sin^2 2\theta < 0.2$, resonances in the core and mantle of the Earth are found to be separated: $\Delta\rho_R^{core} \leqslant \rho_{min}^{core} - \rho_{min}^{m}$.

The thickness of the material of the Earth is of the order of m_N/G_F, so that the dimensions of the layers limit the regions Δm^2, $\sin^2 2\theta$ of the strong effect. For the mean density of the core $\bar{\rho} = 11$g/cm^3, the resonance oscillation length is $l_m^R = 3.5 \times 10^3$ km/sin 2θ. When sin $2\theta \leqslant 0.25$, half this length becomes greater than the diameter of the core and oscillations with maximum depth do not succeed in developing. There is an approximately similar limitation on sin 2θ for resonance in the mantle.[14] Since $l_m^R \sim R_\delta$, and the di-

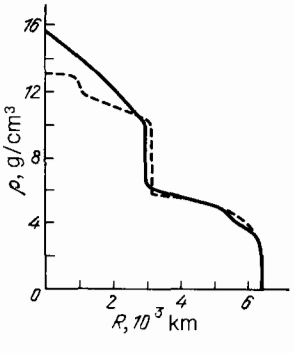

FIG. 19. Density distribution in the Earth for two different models.

mensions of the neutrino sources (atmosphere, etc.) are relatively small, averaging over the oscillation period does not occur in the Earth. The strong oscillation effect is due to the fact that, in this case, about half the resonance length l_m^R fits into the thickness of the Earth. The effect is sensitive to the density distribution.[20]

5.2.2. Suppression factors in the Earth. [16] The basic properties of the graphs of $P_{e-e}(E/\Delta m^2, \sin^2 2\theta) = P_{\mu-\mu}(E/\Delta m^2, \sin^2 2\theta)$ are as follows (Fig. 20):

A) The suppression factors have two well-defined peaks that correspond to resonances in the mantle and core. The density distribution can be represented very approximately by a set of constant-density layers. The resultant suppression fact is then the superposition of two resonance envelopes, into which the oscillating curves are inscribed (see Section 3.3.1). The large width of the left-hand peak is due to the considerable density spread in the core.

B) As the mixing angle decreases, the oscillation lengths increase and, when $\sin^2 2\theta < 0.06$, oscillations of maximum depth do not succeed in developing, i.e., P does not reach 0.

C) As the zenith angle ψ increases, the thickness of the medium traversed in the core by the neutrinos decreases rapidly and vanishes for $\cos\psi \leqslant 0.84$. In the mantle, this thickness initially increases, reaching its maximum for $\cos\psi \simeq 0.84$, and then decreases. Accordingly, as ψ increases (fixed θ), the peak corresponding to the core initially disappears, and then the peak corresponding to the mantle disappears.

For cosmic neutrinos (solar neutrinos or neutrinos from gravitational collapses), a significant separation of the wave packets is found to occur, so that states of definite mass fall on the Earth and evolve independently within it. The ν_e, ν_μ (ν_s) fluxes are determined by the $\nu_2 \to \nu_e$ transition probability: P_{2e} (for $\nu_1 \to \nu_e$; $P_{1e} = 1 - P_{2e}$). The differences between P_{2e} and $P_{\mu-e}$ can be followed by considering the example of constant density (see also Ref. 48). The oscillation depth is equal to the difference between $A_p^{max} = \sin^2(2\theta_m - \theta)$ and $A_p^{max} = \sin^2\theta$, where, for $\nu_e \leftrightarrow \nu_\mu$, the corresponding quantities are $\sin^2 2\theta$ and 0 (Fig. 7). The maximum depth $A_p^{max} = 1$ is reached for $\theta^{max} = (\pi/4) + (\theta/2)$, and the maximum $A_p^{max}(E)$ is shifted relative to the resonance energy of the $\nu_e \leftrightarrow \nu_\mu$ channel: $E_{max} = E_R(1 + \tan\theta \cdot \tan 2\theta)$. For both $E \ll E_R$ and $E \gg E_R$, we have $A_p^{max} \simeq \sin^2\theta$, i.e., the oscillation depth is zero and the average probability is $\bar{P} = \sin^2\theta$. For small mixing angles, $P_{2e} \simeq P_{\nu-e}$.

The range in which the resonance effect occurs in the Earth does not exceed one order in $E/\Delta m^2$, so that, in the case of three neutrinos and a mass hierarchy, the suppression factors for upper and lower resonances does not overlap.

For oscillations into sterile states, $\rho^{eff}(\nu_e - \nu_s) = \rho^{eff}(\nu_e - \nu_\mu)/2$ and, correspondingly, the resonance length of the $\nu_e \to \nu_s$ oscillations is greater by a factor of two

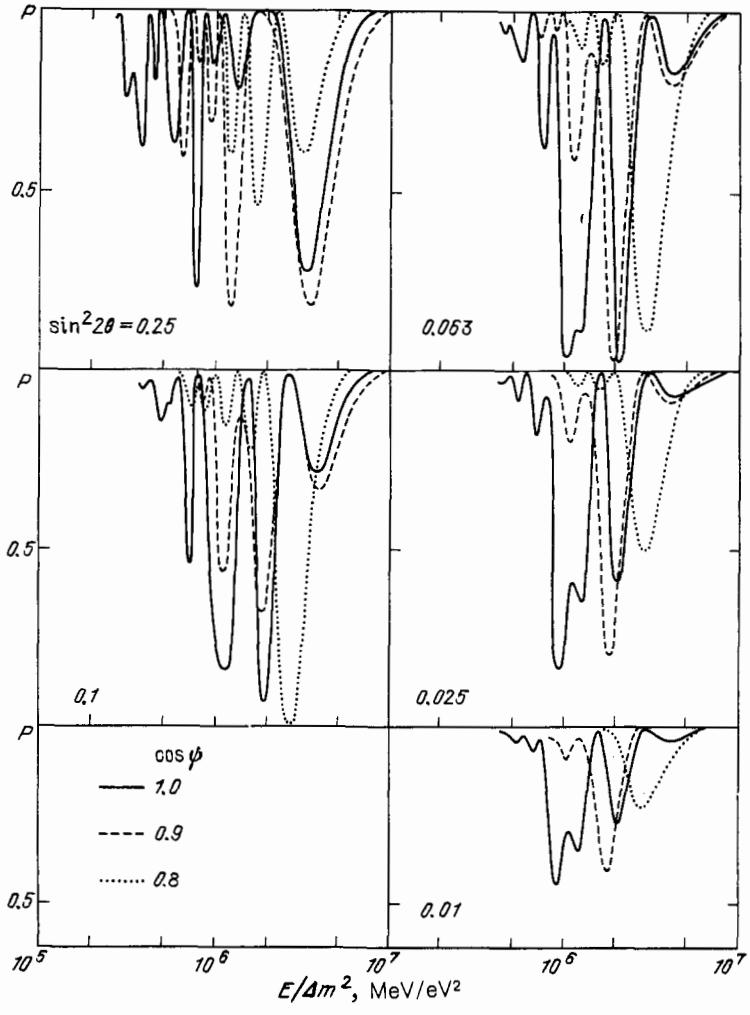

FIG. 20. Suppression factor for the Earth as a function of $E/\Delta m^2$ for different values of the mixing angle in vacuum and different zenith angles.

than that for the $\nu_e \to \nu_\mu$ oscillations. This means that the conditions for strong oscillatory transitions are satisfied less well for the $\nu_e \to \nu_s$ process. The suppression peaks are shifted relative to the $\nu_e \to \nu_\mu$ peaks by a factor of two, and the two peaks are appreciable only for large θ and $\cos\psi \simeq 1$.

5.3. Neutrino oscillations in matter and the spectroscopy of solar neutrinos

5.3.1. Solar neutrino fluxes in installations. Regeneration of ν_e in the Earth. The resultant oscillation effect produced along the path between the point at which the neutrinos are created and the point at which the neutrino detector is located consists of effects produced in the solar material itself and in the material of the Earth (at night, when the Sun is below the horizon). The latter effect produces diurnal and seasonal modulation of the neutrino flux.[16]

A noncoherent flux of neutrinos with definite masses (ν_1 and ν_2) is incident on the Earth's surface. Loss of coherence occurs because of the separation of the ν_1 and ν_2 wave packets in the Sun and along the path between the Sun and Earth, and also as a consequence of averaging at the point of neutrino generation. The fraction of the ν_2 in this flux is $k_2 = (\cos^2\theta - P_S/\cos 2\theta$, where P_S is the suppression factor in the Sun. The resultant suppression factor can be written as $P = k_2 P_{2e} + (1 - k_2) P_{1e}$ or

$$P = (P_S + P_{2e} - 2P_{2e}P_S - \sin^2\theta)(\cos\theta)^{-1}. \quad (5.9)$$

where P_{1e} and P_{2e} are the probabilities of transitions in the Earth. A large portion of the region of the strong effect in the Earth (Fig. 20) lies inside the region of maximum suppression on the Sun whenever $P_S = \sin^2\theta$. At the same time,

$$P = P_{2e} \quad (5.10)$$

i.e., the neutrino state at exit from the Sun is the same as ν_2. Outside the region of the strong effect in the Earth, we have $P = P_S$.

The ν_e flux is regenerated in the Earth.[16,29,31,48] Some of the ν_μ (or ν_τ, ν_s) formed as a result of the $\nu_e \to \nu_\mu$ transformation on the Sun return to the original ν_e state. The total suppression factor increases (see Fig. 18). Regeneration occurs at night, and its average effect is a maximum in the winter and a minimum in the summer.[47,48,49]

5.3.2. "Solutions" of the solar neutrino problem. The rate at which the ^{37}Ar atoms are created in the Cl-Ar experiment (Q_{Ar}^{exp}), averaged over 70 series of measurements,[50] is lower by a factor of 2–4 than the expected rate of production under the influence of the ν_e in the standard solar model:[51]

$$R_{Ar} = \frac{Q_{Ar}^{exp}}{Q_{Ar}^{SSM}} = \frac{1}{4} - \frac{1}{2}.$$

This discrepancy constitutes the solar neutrino problem, an dcan be explained in terms of resonance oscillations in the Sun and Earth. The suppression of the rate of production of ^{37}Ar as a result of oscillations is described by

$$R_{Ar}^{th}(\sin^2 2\theta,\ \Delta m^2) = \frac{1}{N}\int\limits_{E_{th}} dE\sigma_{Ar}(E)\sum_\alpha F_\alpha^0 P_\alpha(E,\ \Delta m^2,\ \sin^2 2\theta), \quad (5.11)$$

where

$$N = \int_{E_{th}} dE\sigma_{Ar}\sum_\alpha F_\alpha^0$$

α = Be, B, pp, pep, O, and N and σ_{Ar} is the cross section for the $\nu_e^{37}\mathrm{Cl} \to e^{-37}\mathrm{Ar}$ reaction. The quantity R_{Ar} is determined by multiplying the spectrum by the suppression factor P_α (suppression bath-tub). The relative position of F^0 and P_α on the E scale depends on Δm^2, so that, as Δm^2 decreases, the bath-tubs shift to the left relative to the spectrum. The size of the bath-tub for $\sin^2 2\theta \gtrsim 0.01$ is much larger than the observed part of the spectrum, and the suppression effect amounts to 10^{-2} over a wide range of energies (Figs. 17 and 18). This means that, for a given $\sin^2 2\theta$, we can choose a mutual disposition of F^0 and P_α (i.e., the magnitude of Δm^2) for which $R_{Ar}^{th} = 1/2$–$1/4$. The values of $\sin^2 2\theta$ and Δm^2, for which a 2-4-fold suppression of the rate of production of ^{37}Ar is observed, are referred to as "solutions" of the solar neutrino problem. The equation $R_{Ar}^{th}(\sin^2 2\theta,\ \Delta m^2) = a = \text{const}$ defines lines of equal suppression (isosnu line[15]) on the $\sin^2 2\theta$, Δm^2 plane[9,10,45] (Fig. 21). The solutions lie between the isosnu lines $a = 1/2$ and $a = 1/4$.

Depending on the neutrino oscillation regime and the nature of the distortion of the energy spectrum, it is possible to identify a number of types of "solution."

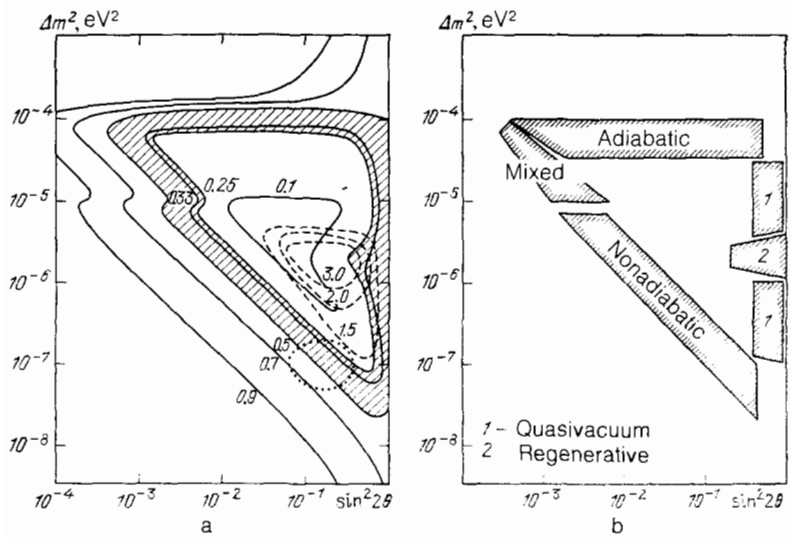

FIG. 21. a—Lines of equal suppression (isosnu lines) of the rate of production of ^{37}Ar in the Cl-Ar experiment on the Δm^2, $\sin^2 2\theta$ plane. The numbers shown against the curves are the values of the suppression factors. Broken lines bound the regions of strong diurnal modulation of Q_{Ar} [the numbers shown against the curves represent the ratio $\overline{Q}_{Ar}$(night)/$\overline{Q}_{Ar}$(day)]. The dotted curve defines the region in which appreciable diurnal modulation of Q_{Ge} is expected in the Ga-Ge experiment. b—Regions of different "solutions" of the solar neutrino problem.

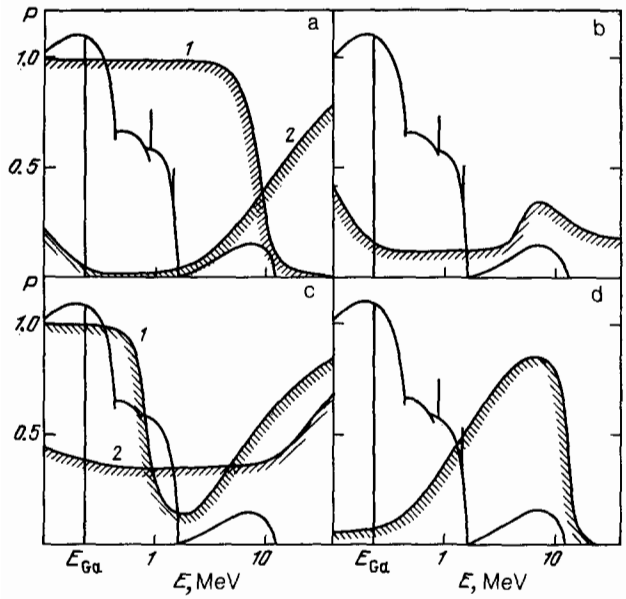

FIG. 22. Mutual disposition of suppression "bathtubs" and of the spectrum of solar neutrinos in different solutions (distortion of the ν_e-spectrum). a: 1—adiabatic "solution," 2—nonadiabatic "solution"; b: 1—mixed in the 2ν-case, 2—quasivacuum; c: regenerative; d—mixed in the 3ν-case.

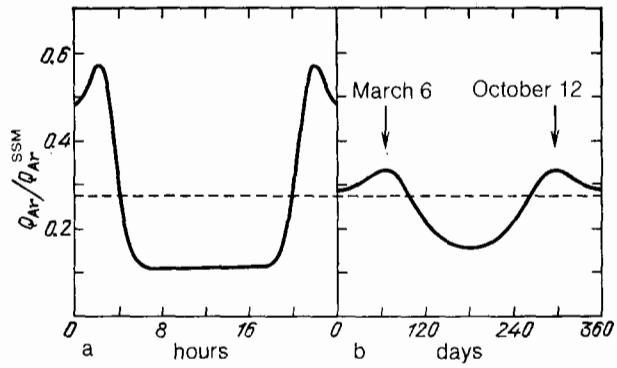

FIG. 23. Regeneration of the ν_e-flux of solar neutrinos in the Earth. The suppression factor for the rate of production of Ar in the Cl-Ar experiment, averaged over the year, is shown as a function of the time of day (a). The daily average is also shown as a function of time in the course of the year (b). For $\Delta m^2 = 1.5\cdot 10^{-6}$ eV^2, $\sin^2 2\theta = 0.4$.

A) Adiabatic solution.[9,10,15,12,23] $\Delta m^2 = 8\times 10^{-15}$–$12\times 10^{-5}$ eV^2, $\sin^2 2\theta = 0.003$–0.3 The neutrino spectrum lies on the left edge of the bath-tub (Fig. 22a), its high energy part is suppressed, the pp-neutrino flux varies very little, and neutrinos in the central part of the spectrum undergo intermediate suppression. Oscillations occur in the adiabatic regime.

B) Nonadiabatic solution.[9,10,15,17,18,19,24–26] $\Delta m^2 = 1.5\times 10^{-8}$–$4.5\times 10^{-8}$ eV^2/$\sin^2 2\theta$, $\sin^2 2\theta \simeq 0.004$–$0.4$. The spectrum lies on the right edge of the bath-tub (Fig. 22a); its low energy part is suppressed. The B, Be, etc., neutrinos that contribute to the production of ^{37}Ar propagate in the nonadiabatic state; the pp-neutrinos enter the region of maximum suppression and their flux is reduced by the factor $\sin^2\theta$. When $\sin^2 2\theta \simeq 0.3$, some of the pp-neutrinos are found in the region corresponding to the resonance effect in the Earth and experience diurnal and seasonal modulation.

C) "Mixed" solution. $\sin^2 2\theta \leqslant 0.004$, $\Delta m^2 = 7\times 10^{-6}$–$8\times 10^{-5}$ eV^2. For small mixing angles, the suppression bath-tubs are found to be so narrow that high-energy neutrinos lie on the nonadiabatic edge and the low-energy neutrinos on the adiabatic edge (Fig. 22b). The middle portion of the spectrum is most highly suppressed. The structure of the isosnu lines (Fig. 21) is due to the fact that the main contribution to Q_{Ar} is due to two types of neutrino, namely, boron and beryllium neutrinos ($E = 0.86$ MeV). The second peak at $\Delta m^2 \simeq 10^{-5}$ eV^2 corresponds to the suppression of resonance in the Sun for the Be neutrinos.

D) The "quasivacuum" solution. $\sin^2 2\theta = 3/4$–$8/9$, $\Delta m^2 = 3\times 10^{-5}$–$10^{-7}$ eV^2. The spectrum lies at the bottom of the bath-tub, which is raised to the height $P = 1/4$–$1/2$. The suppression is roughly the same for all parts of the spectrum, i.e., the result is the same as the average vacuum result.

E) "Regenerative"solution.[47,48] $\delta m^2 = 10^{-6}$–$5\cdot 10^{-6}$ eV^2, $\sin^2 2\theta > 0.1$. The spectrum of boron neutrinos lies in the region of the resonance effect in the Earth (Fig. 22c). The production of ^{37}Ar occurs at night. At the latitude of 42°, at which the Davis experiments were performed (and the Ga-Ge detectors will be located at roughly the same latitude), regeneration is mostly due to resonance in the mantle. The core of the Earth provides a small contribution. The maximum diurnal effect, averaged over the year, occurs at 02.00 and 22.00 hours (Fig. 23a); the maximum annual effect, averaged over the day, occurs at the beginning of March and in October (Fig. 23b). These results correspond to the maximum amount of matter traversed in the mantle along the neutrino path.[45] When $\Delta m^2 = 3\times 10^{-6}$ eV^2 and $\sin^2 2\theta = 0.3$–0.1, strong annual modulation is in conflict with the Davis data.[47,48]

The situation with three neutrinos (in the case of mass hierarchy) is conveniently analyzed using the two-neutrino Δm^2, $\sin^2 2\theta$ diagram[45] (Fig. 21). Each of the resonances is represented by a point on the diagram. Two resonances (l and h) can occur in the Sun and the solution in the 3ν case is determined by two points. Since the edges of the bath-tubs are slowly-varying functions of θ_i, the same Q_{Ar} suppression can be achieved for any pair of points lying on the corresponding lines h_i and l_i (Fig. 23): one lies on l_i and the other on h_i. By comparing the h_i, l_i lines with isosnu lines for the 2ν-solutions (Fig. 21), it is possible to show that:[45]

1) very approximately, a given suppression R_{Ar} is achieved in this case when the l- and h-resonances lie on the 2ν isosnu lines a_1 and a_2 satisfying the condition $a_1 a_2 = R_{Ar}$

2) when the required (experimental) suppression is R_{Ar}, at least one of the resonances must lie between the isosnu lines corresponding to R_{Ar} and $R_{Ar}^{1/2}$. This means that, in the 3ν case, the isosnu lines transform into isosnu *bands*

3) if one of the resonances lies on the $a \simeq 1$ isosnu line, the other must lie on the line $a = R_{Ar}^{exp}$: the 3ν-solution reduces to the 2ν-solution. These statements are valid provided the suppression of Q_{Ar} is not too strong. Moreover, they rely on the approximate factorization of the 3ν-probability, i.e., $P \simeq P^l P^h$ (see Sec. 5.1).

The three-neutrino oscillations yield two new types of solution.

A) *Mixed solution for* 3ν. The h-resonance lies on the adiabatic branch: $\Delta m^2 \simeq 0.8\times 10^{-4}$–$2\times 10^{-4}$ eV^{-2}, $\sin^2 2\theta = 10^{-4}$–10^{-1}; the l-resonance lies on the nonadiaba-

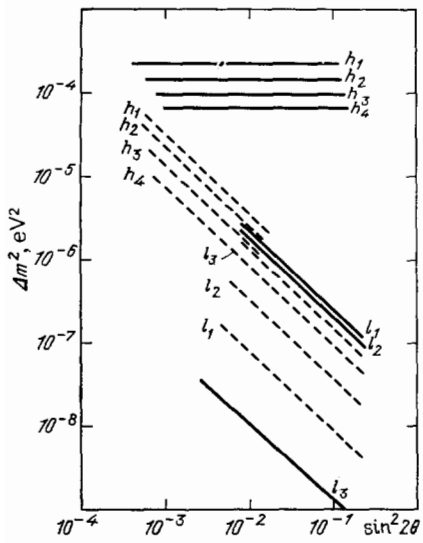

FIG. 24. "Solutions" in the case of three-neutrino oscillations. Solid lines with the same number define the position of the h- and l-resonances in the mixed solution; broken lines have the same significance in the nonadiabatic solutions.

tic branch: $\Delta m^2 = 10^{-9}/\sin^2 2\theta - 4\cdot 10^{-8}/\sin^2 2\theta$ eV^2, $\sin^2 2\theta = 0.01$–0.3 (Fig. 24). The P^l and P^h bath-tubs overlap slightly, and the resultant suppression has the form shown in Fig. 18b. High-energy neutrinos (^{8}B) then lie on the adiabatic edge of P^h and are transformed mostly into ν_τ, whereas low-energy neutrinos lie on the nonadiabatic edge of P^l and transform into ν_μ. The middle part of the spectrum (pep and ^{7}Be-neutrinos) is suppressed to a lesser extent (Fig. 22d).

B) *Nonadiabatic solution in the 3ν-case.* Both resonances now lie on the nonadiabatic branch (Fig. 23) and this corresponds to configuration a) (Fig. 18). The low-energy part of the spectrum is suppressed, but the suppression shape is more complicated than that in the 2ν-case. In particular, the pp-neutrino flux can be reduced to much greater extent than the neutrino flux at intermediate energies.

The effects observed in the case of 3ν-oscillations can be shown on the isosnu diagram m_2, m_3 for different values of the mixing angle.[39]

The results for oscillations into sterile states are practically the same as those obtained above for $\nu_e \leftrightarrow \nu_\mu$. There are two differences: the region of the adiabatic solution is shifted by a factor of 1.3 in Δm^2, and regeneration effects in the Earth are much less well defined.

We note that the solution of the solar neutrino problem with allowance for the effect of the medium can be obtained for small vacuum mixing angles, down to $\sin^2 2\theta = 10^{-3}$. This is significantly different from the solution based on vacuum oscillations, for which maximum or near-maximum degree of mixing is required.

5.3.3. Spectroscopy of solar neutrinos. The question we have to answer is: do resonance neutrino transformations occur in the Sun and in the Earth and, if they do, what is the magnitude of Δm^2 and of the mixing angles? The consequence of resonance oscillations is a definite distortion of the energy spectrum that depends on Δm^2 and θ. This means that the solution of the problem must rely on the neutrino spectroscopy of the Sun,[52] based on radiochemical experiments with different reaction thresholds, and direct measurements of the ν_e spectrum by electronic methods.

Apart from the chlorine experiment that we have already discussed, and which is sensitive mostly to the high-energy part of the spectrum, the most important experiments with solar neutrinos have been the following.

A) Gallium experiment.[53,55] The low threshold for the $\nu^{71}\mathrm{Ga} \to e^{71}\mathrm{Ge}$ reaction ($E_{th} = 0.235$ MeV) means that the pp-neutrinos can be recorded (the SSM contribution of the ν_{pp} to Q_{Ge} is about 80%). The isosnu lines $R_{Ge} = Q_{Ge}/Q_{Ge}^{SSM}$ with $R_{Ge} < 0.5$ are similar in shape to the isosnu lines for Cl-Ar, but are shifted downward relative to the latter (in Δm^2) by the factor $\overline{E}_B/\overline{E}_{pp} \simeq 30$ (Refs. 9 and 38). When $R_{Ge} > 0.5$, the $R_{Ge}(\Delta m^2, \sin^2 2\theta) = \text{const}$ lines have a more complex structure because Q_{Ge} includes the contribution of neutrinos from a larger number of reactions than for Q_{Ar}. For given $R_{Ar} = 1/2$–$1/4$, the suppression of the rate of production of ^{71}Ge can range from 0.97 in the adiabatic solution to 0.05 in the nonadiabatic solution (Fig. 25a). Similar limits for R_{Ge} yield the mixed 3ν-solution. Diurnal and annual modulation due to the effect of the Earth are expected in the nonadiabatic and quasivacuum solutions.

B) Scattering by electrons[57] and deuterons.[58] Direct electronic methods have high experimental thresholds ($E_{th} = 5$–10 MeV) and are sensitive to boron neutrinos alone. Studies of $\nu_e e$ and $\nu_e d$ scattering reveal the presence of a distortion of the spectrum which, in the case of resonance oscillations, is determined[9,10,15] by the suppression factor $P(E)$ (Figs. 17, 22). By recording the time at which each ν-interaction occurs, it is possible to search for diurnal modulation of the ν_e flux.[16] Lines of equal suppression of the total number of events are close to the isosnu lines in the Cl-Ar experiment.[48] Neutrino-deuteron scattering (other nuclei are also being discussed[59]) can be used to determine the ratio of the number of events due to neutral currents [which are not sensitive to $\nu_e \leftrightarrow \nu_\mu(\nu_\tau)$ oscillations] and charged

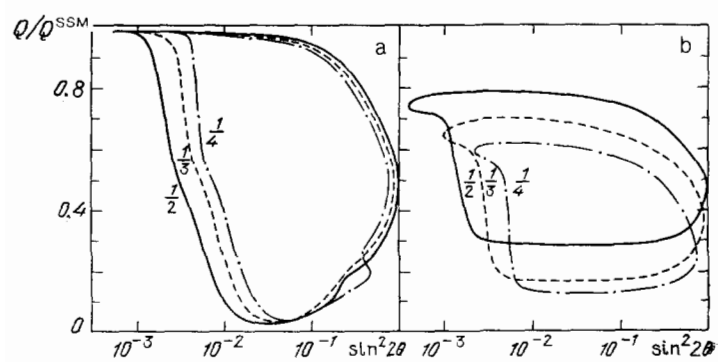

FIG. 25. Suppression factors for the production rate. a: ^{71}Ge in the Ga-Ge experiment, b: ^{7}Be in the Li-Be experiment as functions of $\sin^2 2\theta$ for different magnitudes of suppression of Q_{Ar} (indicated by the numbers shown against the figures).

TABLE I.

Solution	Ga–Ge, R_{Ga}	Li, R_{Li}	Suppressed in the spectrum	Modulation	NC/CC- effect
Adiabatic	$\geqslant 0.9$	0.6—0.8	High E	Absent	Present for flavor oscillations
Nonadiabatic	0.03—0.1	0.1—0.3	Low E	Diurnal annual Q_{Ge}	
Mixed	0.1—0.9	0.1—0.8	Intermediate E	Absent	
Regeneration	$\leqslant 0.2$	0.4	High and low	Diurnal annual Q_{Ar}	
Pseudovacuum	$\sim 1/3$	$\sim 1/3$	Equal suppression	Absent	
Nonadiabatic 3ν	$\leqslant 0.1$	0.1—0.3	Low	Absent	
Mixed 3ν	0.03—0.9	0.1—0.8	High and low E	Absent	
Low solar temperature	0.7	0.7	High E	Absent	Absent
Vacuum oscillations (average)	1/3	1/3	All equally	Absent	
Spin precession in magnetic fields	0.3—0.5	0.3—0.5	Low E	Semiannual 11-year Q_{Ar}	Absent
$\nu_e \to \nu\psi$ decay	0.1	0.2	Low E	Absent	

currents, and hence to obtain information on flavor oscillations.

C) Lithium experiment [50,52,56] ($\nu^7\text{Li} \to e^7\text{Be}$). the threshold for this reaction is $E_{th} = 0.861$ MeV and the experiment is sensitive to the middle part of the spectrum for low temperatures at the center of the Sun. The predictions for most of the solutions are intermediate between Q_{Ar} and Q_{Ge} (Fig. 25b). The only exception is presented by mixed solutions, in which Q_{Be} may be found to be weakly (3ν) or strongly (2ν) suppressed (in contrast to Q_{Ar} and Q_{Ge}).

Additional information will be provided by the molybdenum experiment,[60] in progress now, and the planned Br-Kr experiment.[61]

Table I lists the effects expected in the above experiments for different "solutions."

5.3.4. Solution of the solar neutrino problem. The low rate of production of ^{37}Ar in the Davis experiment can be explained by astrophysical factors, i.e., the fact that the standard solar model is either incorrect or incomplete, and by the properties of the neutrinos themselves, namely, decay, vacuum oscillations, and transitions to right-hand sterile states due to spin precession in the magnetic field. The question is: how to establish the true reason for the observed deficit of electron neutrinos and can we distinguish resonance oscillations from other effects?

A) Most astrophysical mechanisms for the suppression of the neutrino flux ultimately rely on a reduction in the temperature T_c at the center of the Sun. The flux of boron neutrinos is proportional to T_c^{20} and a 5% reduction in T_c is sufficient to explain the Davis data. The reasons for the low temperature may include low density of heavy elements,[62] the presence of wimps (weakly interacting massive particles[63]) at the center of the Sun (both factors tend to increase thermal conductivity), periodic mixing of the medium[64] and other effects. A 5% reduction in T_c has little effect on the pp-neutrino flux ($F_{pp} \sim T_c^4$) and, correspondingly, the prediction for Q_{Ge} in the Gallium experiment remains almost intact. This situation ($R_{Ar} \sim 1/2$–$1/4$ and $R_{Ge} \sim 1$) is realized in the adiabatic and mixed solutions (see Table I). These two cases can be separated by measuring the spectrum of boron neutrinos. Astrophysical factors modify the ratio of the total fluxes of neutrinos from different reactions, but they do not affect the *shape* of the spectrum, which is determined by the elementary process of β-decay. Resonance oscillations on the other hand, do alter the shape of the spectrum. In the adiabatic solution, the high-energy part of the spectrum is suppressed but, in the mixed solution, the low-energy region is suppressed. Moreover, the presence of flavor oscillations can be established by examining neutrino-electron scattering and the ratio of neutral to charged currents on deuterons. In all other solutions, the prediction is that there should be an appreciable or strong suppression of Q_{Ge}, and this cannot be reproduced by changing the model of the Sun.[31]

More or less the same situation occurs in the other mechanism for reducing the boron neutrino flux, i.e., exclusion of the beryllium branch by increasing the concentration of ^{3}He or reducing the concentration of ^{4}He.

It is important to note that virtually all the astrophysical methods of explaining the Davis experiment encounter considerable difficulties.

The effects of oscillations in matter are not very dependent on the chosen solar model. The left-hand edge of the bath-tubs is determined by the central density ρ_c, and a variation of this quantity between 100 and 200 g/cm^3 leads to a shift of the edge and, hence, of the isosnu lines in the adiabatic solution by a factor of 1.5. The right-hand edge depends on the single parameter $\rho(d\tau/dr)^{-1} = h$, which is known very accurately.[16] A change in ρ_c and h does not produce a large change in Δm^2.

The Davis result can, of course, be explained in terms of a combination of different factors. If $T_0 < T < T_c^{SSM}$, where T_c^{SSM} is the central temperature in the standard solar model and T_0 is the temperature at which a threefold suppression of Q_{Ar} is achieved, then some of the effect is explained by a reduced temperature, and oscillatory suppression should be weaker. The solutions should then lie on isosnu lines with $a > 1/2$. Stronger oscillatory suppression is necessary if $T > T_c^{SSM}$. The solutions shift to the inner isosnu lines ($a < 1/4$).

B) The average effect of vacuum oscillations will be observed on the Earth[1,2,65] for $\Delta m^2 = 10^{-2}$–10^{-3} eV^2,

10^{-9}–10^{-11} eV^2, and $\Delta m^2 = 10^{-2}$–10^{-11} eV^2. The maximum suppression factor $P = 1/n$ (n is the number of maximally mixed components) is the same for all parts of the spectrum. In contrast, in the quasivacuum solution, the suppression is different for different parts of the spectrum, and modulation of part of the spectrum (ν_{pp} or ν_B) by the material of the Earth is predicted. When $\Delta m^2 \sim 10^{-12}$ eV^2, the vacuum oscillations are not averaged for the high-energy part of the spectrum, and the suppression factor is

$$P \approx 1 - \sin^2 \frac{\pi}{2} \cdot \frac{E_0 (\Delta m^2)}{E}.$$

Averaging does occur at lower energies (ν_{pp}).

C) If the neutrino has a magnetic moment $\mu_\nu \simeq 10^{-10}$ μ_B, where μ_B is the Bohr magneton, spin precession in the magnetic field of the Sun may produce a transition of ν_e into right-hand states, whose weak interactions are suppressed.[66,67] Semiannual variations in the neutrino flux, due to the inclination of the Earth's orbit to the plane of the solar equator, are predicted.[67] The maximum suppression of Q_{Ar} occurs in March and September during the years of solar activity. An anticorrelation with the 11-year cycle is expected. In the case of resonance oscillations, variations are either absent or annual in character (the maximum suppression of Q_{Ar} is expected in the summer). A magnetic moment of 10^{-10} μ_B can be verified for the ν_e by laboratory experiments.

D) We cannot exclude the possibility that the neutrinos decay along their path toward the Earth, and a light or massless scalar particle is emitted:[17] $\nu_e \to \nu' + \varphi$ (Ref. 68). The necessary reduction in the rate Q_{Ar} is achieved if neutrinos with energies $E_0 \simeq 10$ MeV have lifetimes of about 500 s. The suppression factor $P \simeq \exp(-E_0/E)$ is the same as the suppression factor in the nonadiabatic solution for small mixing angles. Decay can be distinguished from resonance oscillations in flavor by measuring the ratio NC/CC in ν-scattering by deuterons and electrons. In the nonadiabatic solution with $\sin^2 2\theta \simeq 0.1$–$0.01$, the prediction is of a diurnal modulation of the pp-neutrino flux and, consequently, of the rate of production Q_{Ge}. For smaller values of $\sin^2 2\theta$, the pp-neutrino spectrum is found to lie on the adiabatic edge of the bath-tub and its suppression is reduced: $Q_{Ge}^{osc} > Q_{Ge}^{decay}$.

The problem of the solar neutrinos is not confined to the suppression of the rate of production of ^{37}Ar alone. Other processes under discussion include possibility correlation between the Davis data and solar flares,[69] anticorrelations with the 11-year cycle of solar activity,[69,71] and periodicity of the ν_e-flux itself.[71,72] These effects do not fit into the predictions of the standard solar model. On the other hand, some of them can be explained by resonance oscillations. The question is whether solar neutrinos are responsible for the effect observed in the Davis experiment. If they are not, a suppression of Q_{Ar} (ν_e) by a factor of more than 2–4 would be necessary. This degree of suppression can, in fact, be produced by resonance oscillations. Another possibility is that future experiments may show that the ν_e fluxes agree with the predictions of the standard model. Allowance for resonance oscillations would then enable us to exclude an extensive range of oscillatory parameters, namely, $\Delta m^2 = 10^{-9}$–10^{-4} eV^2 and $\sin^2 2\theta \gtrsim 10^{-3}$.

We now summarize the experimental data that would unambiguously indicate the presence of oscillations.

1) Suppression of the high-energy part of the spectrum of boron neutrinos.

2) Distortion of the pp-neutrino spectrum. A strong argument in favor of resonance oscillations would be a low rate of production of ^{71}Ge: $Q_{Ge}^{exp} \lesssim 0.5 Q_{Ge}^{SSM}$ in the Gallium experiment.

3) Diurnal and annual variations of the ν-flux.

4) Different effects in neutral and charged currents.

5.4. Other applications of resonance oscillations

5.4.1. Atmospheric neutrinos. Resonance oscillations in the material of the Earth can distort the spectrum of atmospheric neutrinos.[16] The flux F_α^0 of neutrinos of type $\alpha (\alpha = e,u)$, crossing the Earth at zenith angle ψ, will be suppressed by the factor $F(E) = P_{\alpha\text{-}\alpha}(E/\Delta m^2, \sin^2 2\theta, \cos\psi) F^0$, where the factor $P_{\alpha\text{-}\alpha}$ was discussed in Section 5.2 (Fig. 20) and $F^0(E)$ is a smooth function. The oscillations then produce a valley in the spectrum, whose form is complicated and depends on the distribution of the medium along the neutrino path. According to Sec. 5.2, this valley occupies not more than an order of magnitude in energy and its position is determined by Δm^2, i.e., $E \simeq 10^3$–10^4 GeV ($\Delta m^2/1$ eV^2). The effect is expected for oscillations of $\overset{(-)}{\nu}_e$ ($\overset{(-)}{\nu}_\mu$) into $\overset{(-)}{\nu}_\tau$ or $\overset{(-)}{\nu}_s$. In the case of $\overset{(-)}{\nu}_e \leftrightarrow \overset{(-)}{\nu}_\mu$, the effect is modified by the fact that the initial flux contains both oscillatory components: $R = F(\nu_e)/F(\nu_\mu) = 0.15$–$0.20$. The change in the fluxes is then given by $F/F^0 = P + R^\delta (1 - p)$, where $\delta = +1 (-1)$ for $\nu_e (\nu_\mu)$. Since $R < 1$, the ν_μ ($\bar{\nu}_\mu$) flux is reduced, and the largest effect is thast the $\nu_e (\bar{\nu}_\mu)$ flux increases (by a factor of not more than $R^{-1} \simeq 4$–6).

The possible experimental consequences of resonance oscillations are as follows. 1) The appearance of a structure on the very smooth neutrino energy spectrum. 2) A difference between F/F^0 and unity, where F^0 is the calculated flux. 3) A change in the ratio of neutrino to antineutrino fluxes $F(\nu)/F(\bar{\nu})$ and in the ratio of neutrino fluxes with different flavors, $F(\nu_e)/F(\nu_\mu)$, as compared with the predictions when oscillations are not taken into account. 4) A change in the dependence of these ratios on the angle of incidence of the neutrinos. 5) A change in the ratio of the neutrino fluxes recorded by installations in the upper and lower hemispheres of the Earth, F_u/F_l, as compared with the predictions.

In actual experiments, there is a number of factors that mask oscillatory effects.[16,78] They include: 1) The energy and the direction of arrival of the neutrinos are subject to experimental uncertainty. Actually, an integration is carried out over very wide ranges of E and ψ. 2) The neutrino and anti-neutrino signals are added together in installations in which the sign of the lepton charge is not determined. The resonance transformation occurs only for ν or $\bar{\nu}$, so that the suppression factor increases on summation: $P(\nu + \bar{\nu}) = P(\nu) + \beta[1 - P(\nu)](1 + \tilde{R})^{-1}$, where $\beta = \tilde{R}$ (or 1) if the resonance lies in the $\nu(\bar{\nu})$ channel and $\tilde{R} = F(\bar{\nu})/F(\nu) = 0.5$–$0.6$. Consequently, the maximum reduction in flux does not exceed 0.3–0.6.

In existing underground installations, the main contribution to the number of recorded muons from the lower hemisphere is due to neutrinos with energies 10–100 GeV. Neutrino detectors located deep under water are sensitive to

the same energy range or, more precisely, to $E_\nu \gtrsim 100$ GeV. However, when $E_\nu > 100$ GeV, the resonance values $\Delta m^2 \gtrsim 0.03$ eV^2 ($\sin^2 2\theta \gtrsim 0.1$) lie in the region that has already been excluded by laboratory experiments.

In this connection, the most interesting studies would seem to be those concerned with the interactions of neutrinos with energies E_ν between 0.1 and a few GeV, using large Cherenkov water detectors. The IMB collaboration (USA)[79] has measured the ratio F_1/F_u for $\nu_\mu + \bar{\nu}_\mu$ fluxes with energies $E_\nu > 450$ MeV. The ratio is in agreement with the expected value (to within experimental uncertainty), so that, taking into account the resonance oscillations, it has been possible to exclude a large range of values of Δm^2 near $1.1 \cdot 10^{-4}$ eV or $\sin^2 2\theta \gtrsim 0.1$. These values of θ and Δm^2 lie in the region of the adiabatic solution for the solar neutrinos (Fig. 21).

5.4.2. Resonance oscillations of neutrinos from gravitational collapses. A powerful and very short ($\Delta t \leqslant 20$ s) pulse of neutrino radiation should be generated during a gravitational collapse.[84,85] This pulse carries most of the gravitational energy released in the event ($\mathscr{E}_\nu \simeq 5 \cdot 10^{53}$–$10^{54}$ erg) and could be recorded on the Earth[86] if the collapse were to occur in our galaxy.[18)] The problem is similar to the solar problem: having been created in the central regionof the star, the neutrinos cross layers of matter with an enormous density drop, and may experience very strong resonance transformations.

In the case of a collapse, these transformations have two aspects. First, there is a change in the neutrino flux and, hence, in the neutrino signal on the Earth, and this must be taken into account in the interpretation of observational data. Second, since the neutrinos play an important part in the evolution of the star, resonance oscillations may influence the dynamics of collapse.

A collapsing star shows a number of peculiarities as compared with the Sun.[11,16]

A) The density distribution varies during the ν-burst. Before the collapse and at its very beginning, the form of $\rho(r)$ is typical for white dwarfs with central density $\rho_c = 3 \cdot 10^8$–$3 \cdot 10^9$ g/cm^3 and linear dimensions $3 \cdot 10^3$–$3 \cdot 10^5$ km. This core may be surrounded by a tenuous H-He shell with density $\rho = 10^{-8}$–10^{-9} g/cm^3 and radius $100 R_\odot$–$10^4 R_\odot$. The thickness of the medium in the shell is $d \simeq 10^7$ g/cm$^3 \ll m_N / G_F$, and its influence on the oscillations is negligible. The profile shown in Fig. 26 arises as a result of the hydrodynamic stage of the collapse, during which the central region of the core is rapidly compressed. The central region is not transparent to the neutrinos. The radius of the neutrinosphere is $R_\nu = 10$–20 km during collapse to a neutron star, and $R_\nu = 20$–50 km during collapse directly to a black hole. The densities in the neutrinosphere are, correspondingly, $\rho_\nu = 10^{13}$–10^{14} g/cm^3 and $\rho_\nu = 10^{12}$–10^{13} g/cm^3. Accretion of the outer layers of the core leads to a reduction in the mass of the material above the neutrinosphere and to a steeper distribution $\rho(r)$.

B) Because of neutronization, the effective densities $\rho^{e\mu}$ and ρ^{es} for $\nu_e \to \nu_\mu$ and $\nu_e \to \nu_s$ channels are very different from ρ and from each other (Fig. 26): $\rho_{e\mu} = \rho Y_e = \rho(1+\theta_n)^{-1}$ and $\rho^{es} = \rho[Y_p - (Y_n/2)] = \rho[1 - (\theta_n/2)](1+\theta_n)^{-1}$, where $\theta_n \equiv n_n/n_p$ increases from 1 on the periphery to 30–100 in the neutrinosphere. When $\rho \simeq 10^{10}$ g/cm^3, $\theta_n = 2$ above the neutrinosphere, and ρ^{es} vanishes. If $\Delta m^2 < 0$ (ν_e consists mostly of the lighter component), then when $\rho < 10^{10}$ g/cm^3 the resonance condition is satisfied for the neutrinos, and when $\rho > 10^{10}$ g/cm^3 for the antineutrinos. The roles of ν and $\bar{\nu}$ are interchanged if $\Delta m^2 > 0$.

For the $\nu_e - \nu_\mu$ and $\bar{\nu}_e - \bar{\nu}_s$ channels, the situation is similar to the solar situation: the neutrinos propagate from the region with higher effective density to the region with lower density. The suppression factors as functions of $E/\Delta m^2$ have the bathtub shape. Their left-hand edges are determined by the appearance of resonance at maximum density, and the right-hand edges by the departure from adiabaticity in the outer layers. The height of the bottom is $\sin^2 2\theta/4$. As θ decreases, the bathtubs become narrower, and the right-hand edges move toward the region of lower $E/\Delta m^2$. Since $\rho^{es}(r)$ is a nonmonotonic function, the neutrinos cross two resonance layers in the case of $\nu_e - \nu_s$ oscillations. The condition for an appreciable oscillatory transition is a strong departure from adiabaticity in the inner resonance layer

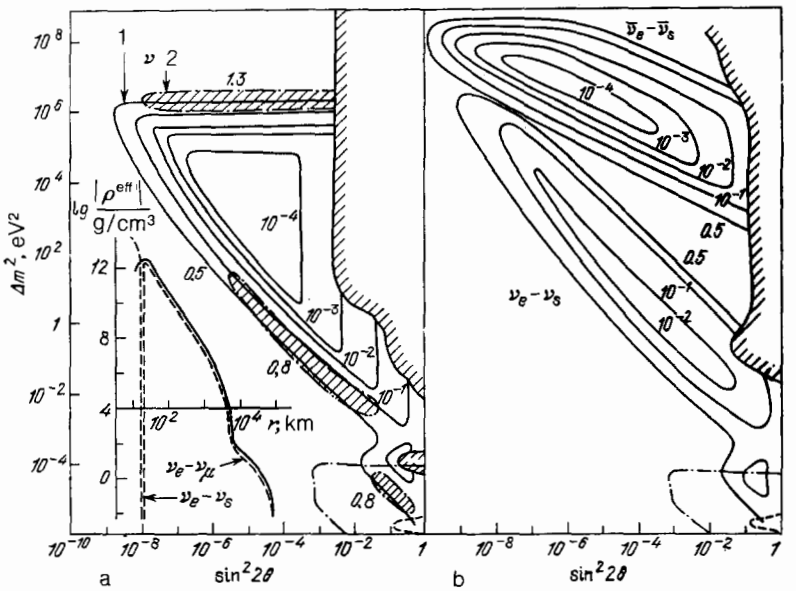

FIG. 26. Lines of equal suppression of the total energy of a ν_e ($\bar{\nu}_e$) burst from a collapsing star, and the effective density distributions: a—ν_e-ν_μ oscillations, b—ν_e-ν_s oscillations. The figure also shows the region of the strong resonance effect in the Sun (dot-dash lines), in the Earth (dashed line), and the laboratory limits (dashed region).

while, in the outer layer, the adiabatic condition is satisfied (or slightly violated). Consequently, both edges of the suppression bathtubs for the $\nu_e - \nu_s$ channels are determined by the adiabatic condition and, as θ decreases, they are both shifted toward lower $E/\Delta m^2$.

C) Central regions of the star, $r < R_\nu$, are opaque to the neutrinos. Inelastic collisions lead to the averaging of the oscillatory result: $F(\nu_e) = F(\nu_s)$ (see Sec. 4.4). The averaging effect is reduced with reducing mixing angle and density ρ_R as compared with ρ_ν, i.e., as the resonance layer shifts to the periphery. Inelastic interactions determine the upper boundary of the strong effect region on the Δm^2, $\sin^2 2\theta$ diagram.

D) Electrons in central regions are found to be ultrarelativistic (see Sec. 4.5).

E) Comparable fluxes of ν_e, ν_μ, ν_τ, and of their antiparticles are produced during the neutrino opaqueness stage. The spectra have the Planck shape, with an additional cutoff at high energies. Because the inelastic interactions of ν_e and ν_μ (ν_τ) are different, the neutrinosphere lies deeper, and has higher temperatures, for ν_μ than for ν_e. The ν_μ spectrum is shifted relative to the ν_e spectrum, with $\overline{E}(\nu_\mu) \simeq 2\overline{E}(\nu_e)$. The total ν_e and ν_τ luminosities are roughly the same. It is clear that the ν_μ and ν_τ spectra are the same, and there are no observable consequences of the $\mu\tau$-resonance.

F) Spin precession in strong magnetic fields may lead to appreciable sterile neutrino fluxes, and this may modify the observed consequences of $\overset{(-)}{\nu}_e \leftrightarrow \overset{(-)}{\nu}_s$ oscillations.

G) The parameters of collapsing stars are not known accurately, and may vary from star to star. Here it is important to note that the boundaries of the region of the strong effect and the lines of equal suppression are actually determined by the central (maximum) densities and by the derivative $d \ln \rho / dr$. A change in the stellar model and in the energies of the emitted neutrinos leads only to a redefinition of the parameters Δm^2 and $\sin^2 2\theta$, but the oscillation effects themselves remain in force.

5.4.3. Effects of resonance oscillations. Oscillations change the shape of the energy spectrum and the total energy $\mathscr{E}_\nu$ of neutrinos of a given type. The suppression factor for $\mathscr{E}_{\nu_e}$ is

$$R_{\nu_e}(\Delta m^2,\ \sin^2 2\theta) = \mathscr{E}_0^{-1} \int dE\, E \sum_\alpha P_{\alpha \to e}(\Delta m^2,\ \sin^2 2\theta)\, F^0_{\nu_\alpha}(E), \qquad (5.12)$$

where $F^0_{\nu_\alpha}$ and $\mathscr{E}_0$ are, respectively, the ν_α flux and ν_e energy without oscillations, respectively. The sum is evaluated over all the types of neutrino that are created.

The following observable effects are possible.

A) Suppression of the ν_e peak due to neutronization.[11,27] During the neutrino transparency stage, there are no appreciable ν_μ, ν_τ (or ν_s) structures, and only the single component $P_{e \to e} F^0_{\nu_e}(E)$ need be taken into account in (5.12). The lines of equal suppression $R_{\nu_e}(\Delta m^2, \sin^2 2\theta) = \text{const}$ are shown in Fig. 26a. Suppression should become weaker during the opaqueness stage.

B) $\overset{(-)}{\nu}_e$ and $\overset{(-)}{\nu}_\mu \left(\overset{(-)}{\nu}_\tau \right)$ spectrum exchange.[11,16] The ν_e flux leaving the star is $F_{\nu_e} = F^0_{\nu_e} P_{e \to e} + F^0_{\nu_\mu}(1 - P_{e \to e})$. When the entire energy range of the ν_e and ν_μ falls on the bottom of the suppression bathtub, ν_e are transformed into ν_μ and ν_μ into ν_e to the same extent, so that ν_e and ν_μ exchange their spectra. The ν_e spectrum becomes harder, $\overline{E}(\nu_e) \simeq 2E_0(\nu_e) = 2E(\bar{\nu}_e)$, and the number of ν_e events in the apparatus increases, although the total energy of the ν-burst is not appreciably changed. When the spectrum of the neutrinos falls on the edge of the bathtub, the exchange between its ν_e and ν_μ components is asymmetric. On the right (nonadiabatic) edge, more ν_e neutrinos are transformed into ν_μ than vice versa, and the ν_e luminosity is reduced. On the left (adiabatic) edge, the transformation of the ν_μ into ν_e dominates the reverse process, and the ν_e signal is enhanced. In the limiting case of a rectangular bathtub, the ν_e spectrum at exit is either the intersection or the envelope of the original ν_e and ν_μ spectra. The lines of equal suppression (amplification) of the ν-burst energy are shown in Fig. 26a. When $\Delta m^2 > 0$, analogous effects occur in the $\bar{\nu}_e$-channel but, in this case, it is important to take into account the laboratory restrictions on the ν_e mass: $m_\nu \lesssim 20$–30 eV. It is quite probable that the two resonances in the $\nu_e - \nu_\mu - \nu_\tau$ system fall into the strong effect region on the Δm^2, $\sin^2 2\theta$ diagram. When the 3ν-oscillations are taken into account, the ν_e-flux at exit from the star is

$$F(\nu_e) = \sum_{\alpha = e,\, \mu,\, \tau} F^0(\nu_\alpha)\, P_{\alpha \to e} = F^0(\nu_e)\, P_{e \to e} + F^0(\nu_\mu)(1 - P_{e \to e}),$$

where $F^0(\nu_\alpha)$ are the initial fluxes (ν_α) and $P_{\alpha \to e}$ are the probabilities of $\nu_\alpha \to \nu_e$ transformations. We have taken into account the fact that $F^0(\nu_\mu) = F^0(\nu_\tau)$ and the normalization condition $\Sigma_\alpha P_{\alpha \to e} = 1$. The problem has thus been reduced to a two-particle problem, but $P_{e \to e}$ is now calculated with allowance for two resonances: $P = P^l P^h + K$ (see Sec. 4.2). Correspondingly, the edges of the complete suppression bathtub and, hence, the distortion of the neutrino spectrum may turn out to be more complicated than in the 2ν case.

C) Strong suppression of the ν_e (or $\bar{\nu}_e$) flux due to oscillations into sterile states. For values of Δm^2, $\sin^2 2\theta$ for which averaging due to inelastic collisions is small, the $\nu_e \leftrightarrow \nu_s$ oscillations lead to a strong suppression of the ν_e signal. The shape of the lines of equal suppression of the energy of the ν-burst (Fig. 26b) reflects the position of the edges of the suppression bathtub along the $E/\Delta m^2$ axis. The upper branches of the contours are determined by the maximum effective density ρ^{es} and by the condition of strong departure from adiabaticity in the inner resonance layer. The lower branches correspond to weak departure from adiabaticity in the outer resonance layer. For the $\bar{\nu}_e \to \bar{\nu}_s$ oscillations ($\Delta m^2 < 0$), the shape of the upper branches depends on averaging effects due to inelastic collisions.

When the ν_e (or $\bar{\nu}_e$) spectrum falls on the bottom of the bathtub, all its segments are suppressed equally, and one of the manifestations of resonance oscillations is that the observed energy of the $\nu_e(\bar{\nu}_e)$ burst ($\mathscr{E} \simeq F\overline{E}_\nu$) is small in comparison with the energy estimated from the temperature of the neutrino radiation: $\mathscr{E} = 4\pi R_\nu^2 (7/16)\sigma T_\nu^4$, where $kT_\nu = (2/7)\overline{E}_\nu$ and R_ν is the radius of the neutrinosphere. When the spectrum lies on the edge of the bathtub, its shape is expected to be distorted.

According to (26b), oscillations into sterile neutrinos

lead to a strong (up to several orders of magnitude) suppression of the ν_e or $\bar{\nu}_e$ flux in a wide range of Δm^2, $\sin^2 2\theta$. The very fact that the ν-signal from the gravitational collapse will have been observed will enable us to exclude a large range of values of Δm^2, $\sin^2 2\theta$. This is critical for models with pseudo-Dirac neutrinos, models based on the L-R symmetry, and so on.

D) Time-dependence of the effects. Because of accretion of the outer layers on the core, the density distribution $\rho(r)$ becomes steeper, the adiabatic condition is not as well satisfied, and the lines of equal suppression shift toward larger Δm^2. (We note, however, that there is another possible regime in which the adiabaticity region expands for large values of mixing angles and Δm^2 that correspond to resonance in the outer layers.) As a result of these changes, the neutrino spectrum that lies inside the strong effect region may be found to be partly or completely removed from this region, or vice versa. Apart from the suppression (increase) of total luminosity, this will lead to a truncation of the ν_e or $\bar{\nu}_e$ pulse, a delay of the ν_e or $\bar{\nu}_e$ pulse, a lack of correspondence between the signal strength due to neutronization and the subsequent ν_e-signal during the opaqueness stage, a time-dependent mean neutrino energy, and so on.

Comparison of the ν_e and $\bar{\nu}_e$ signals is an important experimental method of searching for resonance effects. For given Δm^2 and $\sin^2 2\theta$, all the above effects occur either for the neutrino or the antineutrino. At the same time, the ν_e and $\bar{\nu}_e$ fluxes (with the exception of the contribution due to neutronization) and the total intensities of the ν_e and $\bar{\nu}_e$ pulses are roughly equal in the absence of oscillations. This means that a significant difference between the observed ν_e and $\bar{\nu}_e$ signals would be an indication of the existence of resonance oscillations. In principle, the ν_e and $\bar{\nu}_e$ signals can be reconstructed using 1) the data from scintillation systems designed to record $\bar{\nu}_e p \to n e^+$ events (the detection of the neutron would distinguish this from $\nu e \to \nu e$ scattering), 2) the data produced by Cherenkov water counters capable of resolving the isotropic signal corresponding to $\bar{\nu}_e p \to n e^+$ reactions from the directional signal due to $\overset{(-)}{\nu} e \to \overset{(-)}{\nu} e$ interactions,[87] and 3) the data from radiochemical detectors of solar neutrinos that are sensitive only to ν_e.

E) Resonance oscillations in the material of the Earth can also modify the neutrino signal from a collapsing star. Since the duration of the burst is $\lesssim 20$ s, the effect is determined by the instantaneous density distribution along the path of the neutrino and, consequently, is different for installations located at different points on the Earth.[11,16] In accordance with Fig. 26, it may then happen that the regions of the strong resonance effect in the Earth and Sun do not overlap; on the other hand, they may do so. In the former case, the $\overset{(-)}{\nu}_e - \overset{(-)}{\nu}_s$ oscillations in the Earth lead to a suppression of the ν_e ($\bar{\nu}_e$) signal; the ν_e-ν_μ oscillations reduce the ν_e-signal if the suppression peak lies on the ν_e-spectrum, and amplify it if the peak overlaps the ν_μ-spectrum. In the second case, the effect in the Earth has the character of a regeneration of the neutrinos of the original type. The largest ν_e-signal will be produced by a system that is maximally shielded by the Earth.

5.4.4. Effects in collapsing stars and the problem of solar neutrinos. Despite the fact that the density range in a collapsing star covers completely the density range in the Sun, the regions of strong oscillatory transformations do not overlap to any considerable extent. [The overlap is confined to the region of the adiabatic and quasivacuum "solution" (Fig. 26).] This is so because the core of a collapsing star is a compact object with $R \ll R_\odot$, and the density gradient is much greater than in the Sun. This means that the departure from adiabaticity is greater for the same density: the adiabatic limit shifts toward larger θ and Δm^2. The strong effect on the Sun need not actually be accompanied by any change in the ν-signal from collapse. If, on the other hand, Δm^2 and $\sin^2 2\theta$ lie in the crossing region, the following effects are expected (Fig. 26b): 1) suppression of the peak due to neutronization up to 0.1 [$\nu_e \to \nu_\mu (\nu_\tau)$ oscillations]. 2) Asymmetric spectrum exchange $\overset{(-)}{\nu}_e \leftrightarrow \overset{(-)}{\nu}_\mu (\overset{(-)}{\nu}_\tau)$, with the result that the ν_e ($\bar{\nu}_e$) signal is reduced. 3) If the adiabatic solution $\nu_e \to \nu_\mu$ with $\Delta m^2 = 10^{-4}$ eV^2 is valid for the Sun, it is quite possible that Δm^2 for $\nu_e \to \nu_\mu$ is much greater than 10^{-4} eV^2. Complete exchange of the ν_e and ν_τ spectra then occurs in the collapsing star, and the suppression of the neutronization peak is greater. 4) If the adiabatic $\overset{(-)}{\nu}_e \leftrightarrow \overset{(-)}{\nu}_s$ oscillations occur in the Sun, the suppression of the ν_e ($\bar{\nu}_e$)-signal during collapse may reach 0.1.

Studies of the neutrino signal from stellar collapses may therefore confirm the oscillatory solution of the solar neutrino problem or it will enable us to exclude a particular range of values of Δm^2 and $\sin^2 2\theta$. In either case, an important argument will emerge for the validity of a particular "solution."

6. CONCLUSION

If the neutrinos are massive, it is quite probable that they mix. If they mix, they should oscillate. If oscillations do occur in matter, then interactions between neutrinos will modify the oscillation picture.

In wide ranges of neutrino parameter values, the material of the Sun, the Earth, and collapsing stars amplifies these oscillation effects, leading to significant changes in the properties of the ν-beams, even for very small mixing angles.

Nonzero neutrino masses and mixing are the only assumptions. The effects have actually been verified for systems analogous to mixed neutrinos.

The resonance intervals of Δm^2 and $\sin^2 2\theta$ include values lying well beyond the sensitivity of laboratory experiments. It follows that the search for the effect of resonance oscillations is a unique method of measuring the mass and mixing of neutrinos.

Solar neutrino oscillations are, clearly, the most interesting application. The Cl-Ar data can serve as an indication of the existence of resonance oscillations which then provide a natural explanation of the Davis data. New effects have been predicted and will be examined in experiments now in preparation. Complete solar neutrino spectroscopy may well provide a very precise determination of the difference between the squares of the masses and of the mixing angles of the neutrinos.

Solar neutrinos illustrate all the basic states of ν-oscillations: constant density regime, adiabatic regime, departure from adiabaticity in the resonance layer, and density jump.

Other applications (ν-bursts from gravitational col-

lapses, atmospheric neutrinos, and so on) are of interest in themselves, but they can also provide additional elucidation of the solar neutrino problem.

The authors are deeply indebted to G. T. Zatsepin for numerous discussions and support for this research from its inception. The authors gratefully acknowledge useful discussions with J. N. Bahcall, V. S. Berezinskiĭ, L. Wolfenstein, V. L. Ginzburg, Ya.B. Zel'dovich, A. Yu. Ignatiev, B. Kayser, E. M. Kolb, P. Krystev, V. A. Kuz'min, P. Langacker, V. A. Matveev, A. Messiah, D. K. Nadezhin, V. A. Rubakov, Ya. A. Smorodinskiĭ, A. N. Tavkhelidze, V. A. Tsarev, V. A. Chechin, A. E. Chudakov, and M. E. Shaposhnikov. We wish to note the important contributions of S. T. Petcov, R. Davis Jr., N. Cabbibo, and L. B. Okun' to the acceptance of the idea of resonance oscillations.

[1)]In addition to these neutrinos, there may well be the so-called sterile neutrinos ν_s that do not exhibit the usual weak interaction.

[2)]This example was described in our previous paper.[27] The actual model was demonstrated by S. Weinberg at the Rochester Conference on High-Energy Physics at Berkeley, USA (July 1986).

[3)]ν-states that appear in weak charged currents together with particular leptons will be referred to as e, μ, τ-states with definite flavors.

[4)]In the Weinberg-Glashow-Salam theory, there are no nondiagonal neutral currents, and they will not be considered here (see, however, Ref. 4).

[5)]In (2.19), $\overline{H}$ corresponds to $2M$ and H corresponds to m in Refs. 9 and 10.

[6)]The exception is the parametric resonance, in which ρ and, consequently, $\dot{\theta}_m/\dot{\varphi}$ are the periodic functions[34] ($\dot{\theta}_m\dot{\varphi} \sim \cos\varphi'$).

[7)]In addition, each packet spreads out because of its finite energy width. In the most important positions, this effect turns out to be less significant than the separation effect, and will not be considered from now on.

[8)]For simplicity, CP-violation effects will be neglected and $\hat{S}$ will be assumed to be real.

[9)]In the lowest-order perturbation theory, $H_\mu(\rho)$ and $H_\tau(\rho)$ are parallel, so that there are only two resonances.[39]

[10)]We assume, for simplicity, that the neutrino energy does not change in the collision.

[11)]The relevant criterion here may be: maximum effect in the case of vacuum oscillations. For two neutrinos $\overline{P}_{vac}^{max} = 1/2$, so that transformations in the medium are regarded as strong when $\overline{P} < 1/2$.

[12)]The quantity σ should be estimated at the proton energy of about 20 keV and is of the order of the mean energy of particles entering nuclear reactions. The minimum transferred momentum is $q_{min} \sim 1/\overline{r}$, where $\overline{r}$ is the mean distance between particles.

[13)]By analogy with quarks, we take it that mixing between generations 1 and 3 is less than mixing between 1 and 2: $s_\varphi < s_\omega$, i.e., P^h is narrower than P^l.

[14)]The possibility of a strong resonance effect in the Earth was first noted in Ref. 20.

[15)]The SNU (Solar Neutrino Unit) is a measure of the rate of production of daughter atoms in radiochemical experiments (Refs. 50 and 51).

[16)]Analysis of the 5-min solar oscillations, which can be used to determine the density profile up to $R \simeq 0.2R_\odot$, confirms the standard model.

[17)]The decays of the neutrino into a majoron or familon have been discussed in this connection. The detection of the ν-signal from the gravitational collapse of a star would exclude this possibility.

[18)]A collapse in the Magellanic Cloud galaxy that is closest to us is also at the limit of the possibilities of existing underground installations.

[1]B. Pontecorvo, Zh. Eksp. Teor. Fiz. **33**, 549 (1957) [Sov. Phys. JETP **6**, 429 (1958)]; **34**, 247 (1958) [**7**, 172 (1958)].
[2]S. M. Bilen'kiĭ and B. M. Pontecorvo, Usp. Fiz. Nauk **123**, 181 (1977) [Sov. Phys. Usp. **20**, 776 (1977)].
[3]V. N. Gribov and B. Pontecorvo, Phys. Lett. **28**, 493 (1969).
[4]L. Wolfenstein, Phys. Rev. D **17**, 2369 (1978); **20**, 2634 (1979).
[5]V. Barger *et al.*, *ibid.* **22**, 2718 (1980).
[6]S. Pakvasa, DUMAND-80, Hawaii Univ., USA, 1981, Vol. 2, p. 457.
[7]H. J. Haubold, Astrophys. Space Sci. **82**, 457 (1982).
[8]P. V. Ramana Murthy, Ed., Proc. Eighteenth Intern. Conf. on Cosmic Rays, Nat. Sci. Docum. Centre, Bangalor, India, 1983, Vol. 7, p. 125.
[9]S. P. Mikheyev and A. Yu. Smirnov, Talk given at Tenth Intern. Conf. on Weak Interactions, Savonlinna, Finland, 1985; Yad. Fiz. **42**, 1441 (1985) [Sov. J. Nucl. Phys. **42**, 913 (1985)].
[10]S. P. Mikheyev and A.Yu. Smirnov, Nuovo Cimento C **9**, 17 (1986).
[11]S. P. Mikheev and A.Yu. Smirnov, Zh. Eksp. Teor. Fiz. **91**, 7 (1986) [Sov. Phys. JETP **64**, 4 (1986)].
[12]H. Bethe, Phys. Rev. Lett. **56**, 1305 (1986).
[13]N. Cabibbo, Summary Talk given at 10th Intern. Conf. on Weak Interactions, Savonlinna, Finland, 1985.
[14]P. Langacker, Private Communication, January 1986 (see Ref. 77).
[15]a) S. P. Rosen, Proc. Sixth Moriond Workshop on Massive Neutrinos in Astrophysics and in Particle Physics, ed. by O. Fackler and J. Tran Thanh Van, Tignes, Savoie, France, January 25–February 1, 1986, p. 1. b) S. P. Rosen and J. M. Gelb, Phys. Rev. D **34**, 969 (1986).
[16]S. P. Mikheyev and A. Smirnov, see Ref. 15a, p. 355.
[17]W. Hampel, Preprint Max Planck Institute, Heidelberg, January 1986.
[18]M. Spiro, see Ref. 15a, p. 129. J. Bouches *et al.*, Z. Phys. C **32**, 499 (1986).
[19]A. Messiah, see Ref. 15a, p. 373; Preprint PhT/86-46, Saclay, 1986.
[20]V. K. Ermilova, V. A. Tsarev, and V. A. Chechin, Pis'ma Zh. Eksp. Teor. Fiz. **43**, 353 (1986) [JETP Lett. **43**, 453 (1986)]; Preprint FIAN SSSR No. 45 [in Russian], Moscow, 1986.
[21]S. P. Mikheev and A.Yu. Smirnov, Proc. Intern. Seminar "Quarks-86" [in Russian], Institute of Nuclear Research, Academy of Sciences of the USSR, Tbilisi, 1986, p. 277.
[22]S. P. Mikheyev and A.Yu. Smirnov, Proc. Seventh Workshop on Grand Unification, ed. by J. Arafune, Togama, Japan, April 16–18, 1986.
[23]V. Barger, R. J. N. Phillips, and K. Whisnant, Phys. Rev. D **34**, 980 (1986).
[24]W. C. Haxton, Phys. Rev. Lett. **57**, 1271 (1986).
[25]S. J. Parke, *ibid.* p. 1275.
[26]E. W. Kolb, M. S. Turner, and T. P. Walker, Phys. Lett. B **175**, 478 (1986).
[27]S. P. Mikheyev and A.Yu. Smirnov, Proc. Twelfth Intern. Conf. on Neutrino Physics and Astrophysics, ed. by T. Kitagaki, Sendai, Japan, 3–8 June, 1986, p. 177.
[28]L. Wolfenstein, *ibid.* p. 1.
[29]M. Cribier, W. Hampel, J. Rich, and D. Vignaud, Phys. Lett. B **182**, 89 (1986).
[30]S. P. Mikheyev and A.Yu. Smirnov, Proc. Intern. Symposium on Weak and Electromagnetic Interactions in Nuclei, ed. by H. V. Kapdor and J. Metzinger, Springer Verlag, 1986, p. 710.
[31]W. Hampel, *ibid.* p. 718.
[32]L. B. Okun', Yad. Fiz. **41**, 1272 (1985) [Sov. J. Nucl. Phys. **41**, 812 (1985)]. Preprint ITEF-195 [in Russian], Moscow, 1984.
[33]S. P. Mikheev and A.Yu. Smirnov, Zh. Eksp. Teor. Fiz. **92**, 404 (1987) [Sov. Phys. JETP **65**, 230 (1987)].
[34]V. K. Ermilova, V. A. Tsarev, and V. A. Chechin, Kratk. Soobshch. Fiz. No. 5, p. 26 (1986) [Sov. Phys. Lebedev Inst. Rep. No. 5 (1986)].
[35]A. Dar, A. Mann, and Y. Melina, Preprint Technion-PH-26-2, 1986.
[36]L. Landau, Phys. Z. Sowjetunion **2**, 46 (1932).
[37]C. Zener, Proc. R. Soc. London Ser. A **137**, 696 (1932).
[38]S. J. Parke and T. P. Walker, Phys. Rev. Lett. **57**, 2322 (1986).
[39]T. K. Kuo and J. Pantaleone, *ibid.* 1805; Preprint PURD-TH-86-20, 1986.
[40]S. Toshev, Phys. Lett. B **185**, 177 (1987).
[41]L. M. Sehgal, *ibid.* **162**, 370 (1985).
[42]S. T. Petcov and S. Toshev, Preprint INPNE, Sofia, 1987.
[43]A.Yu. Smirnov, Yad. Fiz. **46**, 1152 (1987) [Sov. J. Nucl. Phys. **46**, 672 (1987)].
[44]A.Yu. Smirnov, Seventh Moriond Workshop on Search for New and Exotic Phenomena, Les-Arc, Savoie, France, January 24–31, 1987.
[45]S. P. Mikheyev and A.Yu. Smirnov, *ibid.*
[46]S. Toshev, Phys. Lett. B **180**, 255 (1986).
[47]A. J. Baltz and J. Weneser, Phys. Rev. D **35**, 528 (1987).
[48]H. Gribier, J. Rich, M. Stripo, D. Vignaud, W. Hampel, and B. T. Cleveland, Preprint DPhPE87-01, Saclay, January 1987.
[49]A. Dar. A. Mann, Y. Melina, and D. Zajfman, Preprint TECHNION-PH-86-30.
[50]J. N. Bahcall, B. T. Cleveland, R. Davis Jr., and J. K. Rowley, Astrophys. J. **292**, L79 (1985); J. N. Bahcall, Phys. Lett. **13**, 332 (1964); J. K. Rowley, B. T. Cleveland, and R. Davis Jr., AIP Conf. Proc., 1985, Vol. 126, p. 1.
[51]J. N. Bahcall *et al.*, Rev. Mod. Phys. **54**, 767 (1982); J. N. Bahcall and B. R. Holstein, Phys. Rev. C **33**, 2121 (1986).
[52]V. A. Kuzmin and G. T. Zatsepin, Proc. Ninth Intern. Conf. on Cosmic Rays, ed. by A. C. Strickland, Inst. Phys. and Phys. Soc., 1965, Vol. 2, p. 1023.
[53]V. A. Kuzmin, Phys. Lett. **17**, 27 (1965).
[54]I. R. Barabanov *et al.*, AIP Conf. Proc., 1985, Vol. 126, p. 175.
[55]T. Kirsten, see Ref. 15, p. 119.
[56]V. A. Kuzmin and G. T. Zatsepin, Proc. Intern. Conf. on Neutrino Physics and Astrophysics, Nauka, Moscow, 1969, Vol. 2, p. 156.

[57]M. Baldo-Ceolin, see Ref. 15a, p. 159; A. Suzuki, ICEPP Preprint UT-ICEPP-86-07, 1986.
[58]D. Sindair *et al.*, Nuovo Cimento C **9**, 308 (1986).
[59]R. S. Raghavan, S. Pakvasa, and B. A. Brown, Phys. Rev. Lett. **57**, 1801 (1986).
[60]W. C. Haxton, see Ref. 15a, p. 143.
[61]R. D. Scott, Nature **264**, 729 (1976).
[62]J. N. Bahcall *et al.*, Astron. Astrophys. **73**, 121 (1979).
[63]W. A. Fowler, Nature **238**, 24 (1972); D. N. Spergel and W. H. Press, Astrophys. J. **296**, 679 (1985); J. Faulkner and R. L. Gilliland, *ibid.* **299**, 994; J. Faulkner, see Ref. 44.
[64]F. W. Dilke and D. O. Gough, Nature **240**, 262.
[65]G. T. Zatsepin, Proc. Eighth Workshop on Weak Interactions, ed. by A. Morales, Javea, Spain, 1982, p. 129.
[66]A. Cisneros, Astrophys. Space Sci. **10**, 87 (1980).
[67]M. B. Voloshin and M. I. Vysotsky, IETP Preprint No. 1, Moscow, 1986; L. B. Okun, M. B. Voloshin, and M. I. Vysotsky, IETP Preprint No. 20, Moscow, 1986; M. B. Voloshin, M. I. Vysotskiĭ, and L. B. Okun', Zh. Eksp. Teor. Fiz. **91**, 754 (1986) [Sov. Phys. JETP **64**, 446 (1986)].
[68]J. N. Bahcall, S. T. Petcov, S. Toshev, and J. W. F. Valle, Phys. Lett. **181**, 369 (1986).
[69]G. A. Bazilevskaya, Yu. I. Stozhkov, and T. N. Charakhch'yan, Pis'ma Zh. Eksp. Teor. Fiz. **35**, 273 (1982) [JETP Lett. **35**, 341 (1982)].
[70]K. Sakurai, Nature **278**, 146 (1979).
[71]A. Subramanian, Curr. Sci. **48**, 705 (1979).
[72]V. N. Gavrin, Yu. S. Kopysov, and N. T. Makeev, Pis'ma Zh. Eksp. Teor. Fiz. **35**, 491 (1985) [JETP Lett. **35**, 608 (1985)].
[73]M. Gell-Mann, P. Ramond, and R. Slansky, in: Supergravity, ed. by P. van Nieuwehuisen and D. Z. Freedman, North-Holland, Amsterdam, 1979; T. Yanagida, in: Proc. Workshop on Unified Theory and Baryon Number of Universe, KFK, Japan, 1979.
[74]R. D. Peccei, see Ref. 30, p. 891.
[75]A. Masiero, D. V. Nanopoulos, and A. I. Sanda, Phys. Rev. Lett. **57**, 663 (1986).
[76]K. Kang and M. Shin, Phys. Lett. B **185**, 163 (1987); J.W. F. Valle, *ibid.* **186**, 73.
[77]P. Langacker, S. T. Petcov, G. Steigman, and S. Toshev, Nucl. Phys. B **282**, 549 (1987).
[78]E. D. Carlson, Phys. Rev. D **34**, 1454 (1986).
[79]J. Lo Secco, Phys. Rev. Lett. **57**, 652 (1986); Phys. Lett. B **184**, 305 (1987).
[80]S. Toshev, Preprint INRNF No. 56, Sofia, February, 1987.
[81]F. J. Botella, C. S. Lim, and W. J. Marciano, Phys. Rev. D **35**, 896 (1987).
[82]C. W. Kim and W. K. Sze, *ibid.*, p. 1404.
[83]C. W. Kim, S. Nussinov, and W. K. Sze, Phys. Lett. B **184**, 403 (1987).
[84]Ya. B. Zel'dovich and O. Kh. Guseinov, Dokl. Akad. Nauk SSSR **162**, 791 (1965) [Sov. Phys. Dokl. **10**, 524 (1965)].
[85]V. S. Imshennik and D. K. Nadezhin, Preprints ITEF-91, ITEF-98 [in Russian], Moscow, 1980.
[86]G. V. Domogatsky and G. T. Zatsepin, Proc. Tenth Intern. Conf. on Cosmic Rays, London, September 1965, Vol. 2, p. 1032.
[87]T. P. Walker and D. N. Schramm, Fermilab-Pub-86/133A, 1986.

Translated by S. Chomet